TECHNISCHE UNIVERSITÄT MÜNCHEN

Klinikum rechts der Isar, Fakultät für Medizin

Frauenklinik und Poliklinik

Feng Yang

Clinical Relevance of the Tissue Protease KLK4 for Triple-negative Breast Cancer

Vollständiger Abdruck der von der Fakultät für Medizin

der Technischen Universität München zur Erlangung des akademischen Grades eines

Doktors der Medizin (Dr. med.)

genehmigten Dissertation.

Vorsitzender: Univ.-Prof. Dr. Ernst J. Rummeny

Prüfer der Dissertation:

1. Univ.-Prof. Dr. Manfred Schmitt (schriftliche Beurteilung)
   apl. Prof. Dr. Viktor Magdolen (mündliche Prüfung)
2. Univ.-Prof. Dr. Marion B. Kiechle

Die Dissertation wurde am 07.04.2015 bei der Technischen Universität München eingereicht und durch die Fakultät für Medizin am 14.12.2016 angenommen.

Table of Contents

1. Introduction 1
   1.1 Breast cancer 1
   1.2 Triple-negative breast cancer (TNBC) 4
   1.3 Biomarkers in breast cancer 5
   1.4 Kallikrein-related peptidases (KLKs) 6
   1.4.1 KLKs in normal and diseased tissues 8
   1.4.2 KLKs in carcinoma tissues 10
   1.4.3 KLKs as biomarkers in hormone-related cancers 13
   1.5 Kallikrein-related peptidase 4 (KLK4) 20
2. Aim of the study 23
3. Materials 24
   3.1 Triple-negative breast cancer patients 24
   3.2 Reagents and materials 27
   3.3 Cells and cell culture 30
   3.4 Antibody directed to rec-KLK4 31
4. Techniques and methods 33
   4.1 Cell microarrays (CMA) and cytospins 33
   4.2 Flow cytometry experiments (FCs) 36
   4.3 Confocal laser scanning microscopy (CLSM) 37
   4.4 Quantitative polymerase chain reaction (qPCR) 38
   4.5 Western blotting (WB) 41
   4.6 Immunohistochemistry (IHC) 47
   4.7 Digitization of histological images and quantification of immunostaining 53
   4.8 Statistical analyses 55
5. Results 56
   5.1 Cell microarrays (CMAs) for KLK4 assessment 56
   5.2 Cytospins for KLK4 assessment 58
   5.3 Flow cytometry for KLK4 assessment 66
   5.4 CLSM for KLK4 assessment 70
   5.5 Assessment of KLK4 mRNA expression by qPCR 73
   5.6 Assessment of KLK4 protein expression by western blotting 74

5.7 Assessment of KLK4 protein expression and localization in different TMAs by IHC 79
5.8 Statistical analysis of KLK4 expression in the triple-negative breast cancer collective 85
6. Discussion 94
7. Summary 99
8. Appendix 100
9. List of own publications 106
10. Acknowledgements 106
11. References 108

Tables and figures

Table 1. Distinct subtypes of breast cancer based on intrinsic gene subset 3
Table 2. Level-of-Evidence framework 5
Table 3. KLKs as breast cancer biomarkers (mRNA and/or protein level) 19
Table 4. Clinical and pathological characteristics of the TNBC breast cancer collective (n=188) 25
Table 5. Reagents and materials used in the experiments 27
Table 6. List of cell lines used in the studies 30
Table 7. Contents of culture medium 31
Table 8. Antibody directed to KLK4 used in this study 33
Table 9. FACS staining protocol 37
Table 10. Prepare the cDNA synthesis reaction in a microcentrifuge tube 39
Table 11. Total volume of each RT reaction 20 ul 40
Table 12. Amplification cycles 40
Table 13. RIPA (Radio Immuno Precipitation Assay) lysis buffer for 5ml 42
Table 14. Sheet for Protein Assay (96-well plate) 44
Table 15. Sample buffer (5 x Laemmli) for cell migration 45
Table 16. Separating, stacking, and electrophoresis buffer 45
Table 17. Semi-dry buffer for blotting and prestaining buffer (Ponceau S) 46
Table 18. Loading controls and cellular fractionation markers and stripping buffer used in the study 47
Table 19. KLK4 immunoscores based on Remmele score 55
Table 20. Fixative variables tested in the present study 59
Table 21. Permeabilization variables tested in the present study 61
Table 22. Staining variables tested in the present study 63
Table 23. Summarized intensities of staining with variables tested in the present study 65
Table 24. Quantification of cellular fractions, whole cell lysates, and dialyzed culture media. 75
Table 25. Manual and automatic scoring values of KLK4 immunostaining of TNBC TMA specimens 86
Table 26. KLK4 staining scoring values: Spearman correlations (rho) 86
Table 27. Association of clinical/histomorphologic factors with KLK4 immunoscores 87
Table 28. Uni- and multivariate Cox regression analysis for time-to-progression in TNBC patients 89
Table 29. Uni- and multivariate Cox regression analysis for overall survival (OS) in TNBC patients 90
Table 30. Summary of cell lines and techniques used to investigate cellular KLK4 expression 95
Table 31. Summary of cell lines and techniques used to investigate localization of cellular KLK4 96

Figure 1. Schematic representation of the exon and intron gene sequence of KLKs 7
Figure 2. Schematic representation of the protein sequence of KLKs 7
Figure 3. Comparative mRNA and protein expression of KLKs in normal female breast tissues 16
Figure 4. Comparative mRNA and protein expression of KLKs in breast cancer tissues 17
Figure 5. Crystal structure of KLK4 and schematic representation of its gene and protein structure) 21
Figure 6. Schematic representation of the major structure of recombinant KLK4 32
Figure 7. Schematic workflow for adherent tissue culture cells (user protocol of S-PEK) 43

Figure 8. LSAB method 50
Figure 9. Zytomed HRP One-Step Polymer system..... 52
Figure 10. Procedure of automated image analysis with Definiens Developer XD software 54
Figure 11. Relative KLK4 staining intensity in OV-MZ-6 cells transfected with different KLKs..... 57
Figure 12. Relative KLK4 staining intensity in different tumor cells and blood cells..... 58
Figure 13. CMA clots vs cytospins consisting of MDA-MB-231 cells 59
Figure 14. Cytospins stainining. LSAB method..... 60
Figure 15. Cell cytospins stained with pAb587..... 62
Figure 16. OV-MZ-6 KLK4 cytospins, tested with KLK4 antibody pAb587. 64
Figure 17. OVMZ-6 RSV-KLK4 stained for KLK4 with pAb587 (3.5 µg/mL)..... 65
Figure 18. OV-MZ-6 pRc RSV KLK4 cytospins stained with KLK4 antibody pAb587 66
Figure 19. Living and 4 % PFA-fixed OV-MZ-6 pRc RSV KLK4 cells..... 68
Figure 20. Fluorescence mean channel values of OV-MZ-6 pRc RSV KLK4 cells..... 69
Figure 21. Mean fluorescence values 70
Figure 22. CLSM image for cytospin..... 70
Figure 23. CLSM image for KLK4 staining. 72
Figure 24. CLSM image for PC-3 pRc RSV KLK4 cells. 73
Figure 25. Relative KLK4 mRNA expression in cell lines 74
Figure 26. Different amounts of recombinant KLK4..... 76
Figure 27. Blocked with 5% skimmed milk and 5% BSA 77
Figure 28. Different cell lysates and rec-KLK4 immunoprecipitated with pAb587 78
Figure 29. Cell fractions immunoprecipitated with pAb587..... 79
Figure 30. Prostate tissue stained for KLK4 employing pAb587+/- pretreatment..... 81
Figure 31. Prostate tissue stained for KLK4 (pAb587, 3.5 µg/mL) 81
Figure 32. TMAs were stained with pAb587 employing the Ventana ultraView® method 84
Figure 33. Expression of KLK4 antigen in breast cancer tissues..... 85
Figure 34. Kaplan-Meier curves (TTP) concerning KLK4 protein expression in TNBC..... 92
Figure 35. Kaplan-Meier curves (OS) concerning KLK4 protein expression in TNBC .. 错误！未定义书签。
Figure 36. OV-MZ-6 cell line transfected with different KLKs (cell microarray) 103
Figure 37. 31 different cell types as part of a cell microarray, stained with pAb587 to KLK4 104

1. Introduction

1.1 Breast cancer

Breast cancer is the most common cancer affecting women both in the developed and developing world, being the second leading cause of cancer deaths in women after lung cancer, with a mortality rate of > 500,000 cases per year. In 2012, among women, there were about 1.67 million new cases diagnosed and 522,000 deaths from breast cancer around the world recorded[1]. Although the high mortality rate has decreased in the past two decades as a result of increased awareness, earlier detection, improved treatment options and reduction of estrogen therapy after menopause[2], according to World Health Organization (WHO) estimates, in Germany, still about 91.6 in 100,000 women per year are aquiring breast cancer which accounts for 16.8 % of female deaths caused by malignancies.

Studies have identified various risk factors for developing breast cancer, including advanced age (> 60), early menarche (first menstruation < 12 years), late menopause (> 50 years), first pregnancy after 30 years, personal or family history, nullipara, obesity, alcohol abuse, etc. Besides these, genetic mutations (e.g. BRCA1/2) and postmenopausal hormone-replacement therapy are also known to increase the risk of developing breast cancer[2].

After the onset of the breast cancer disease, about 90 % of patients are expected to survive at least 5 years after the primary surgery. The recent introduction of the concept of sentinel lymph node biopsy is meant to reduce the need of full axillary lymph node dissection[3, 4]. Radiation therapy is usually performed after breast-conserving therapy, it may reduce disease recurrence and prevent early death[5]. Systemic cancers therapy works through the circulatory system and affects not only the tumor tissue but all parts of the human body. Neoadjuvant chemotherapy

given prior to surgery is designed to shrink the tumor size and to increase the possiblity for breast-conserving surgery[6]. Adjuvant systematic therapy is given to erase remaining but undetected or disseminated tumor cells after surgery.

Yet, these treatment options are not always effective since breast cancer cannot be considered as a uniform, homogeneous malignant disease. Instead, histological and genomic analyses have shown that breast cancer represents a group of very heterogeneous diseases which differ by multiple morphological features, clinical behavior, and response to therapy[7, 8].

The traditional classification of breast cancer depends on its histological features including TNM staging, tumor grading, and histological subtypes (AJCC, see appendix 11.1). The TNM-staging system classifies turmors on the basis of primary tumor size (T), regional lymph node involvement (N), and incidence of distant metastasis (M)[9]. In Europe, the Nottingham grading system is in use as well, which is based on tubule, nuclear grading, and mitotic rate[10]. The majority of breast cancers are derived from the epithelium lining the ducts or lobules, including in situ tumors whose proliferation is limited to the epithelial tissue without other cell extravasation. About 80 % of breast tumors derive from ductal epithelial cells, whereas a large part of the remaining 20 % have their origin in the lobular epithelia. Very rare are distinct subtypes including medullary, papillary, mucinous, or neuroendocrine carcinoma.

Besides that, some potential biological markers were exploited to identify various molecular subtypes, including estrogen receptors (ER), progesterone receptors (PR), and the human epidermal growth factor receptor 2 (HER2). Based on these investigations, five distinct subtypes of breast cancer were classified using a set of genes which is called "intrinsic gene subset" of breast cancer: Luminal A, Luminal B, normal breast-like, HER2-type, and basal-like breast cancer[7, 11].

Table 1. Distinct subtypes of breast cancer based on intrinsic gene subset

Subtypes	ER, PR, HER2 status	Cell of origin
Luminal A	ER+or PR+or both+, Her2-	Luminal epithelial cell
Luminal B	ER+or PR+o rboth+, Her2+	Luminal epithelial cell
Claudin-low	ER-, PR-, Her2-	Stem cell
HER2+	ER-, PR-, Her2+	Late luminal progenitor
Normal breast- like	Not fill into these categories	Luminal epithelial cell
Basal-like	ER-, PR-, Her2-/+	Basal/myoepithelial/bipotent progenitor

Today, to a large extent, treatment of breast cancer adheres to these histoclinial prognostic or predictive biomarkers. Different systemic therapies, such as endocrine immunotherapy with SERMs (selective estrogen receptor modulators) or aromatase inhibitors, are based on tumor-associated biomarkers[12]. SERMs (such as tamoxifen) serve as partial antagonists for ER, since they can interfere with growth stimulation by preventing estrogen from binding to ER[13]. Aromatase inhibitors (e.g. anastrozole, exemestane, letrozole) is another type of medication by inhibiting generation of estrogen[14]. Among all of these cases, around 15~30 % of breast cancers overexpress HER2. The HER2 oncogene encodes a transmembrane tyrosine kinase receptor, belonging to the epidermal growth factor receptor family. The immunized monoclonal antibody trastuzumab (Herceptin®) specifically targets the extracellular domain of the HER2 protein, and together with standard adjuvant chemotherapy, can reduce the risk of disease recurrence and death of breast cancer patients by 52 % and 33 %, respectively, in comparison to adjuvant chemotherapy strategies alone[15]. Lapatinib (Tykerb®), a tyrosine kinase inhibitor, is another medication to treat HER2+ breast cancer[16].

Still, to date, there are not enough well-established factors for standard classification into more elaborate breast cancer subtypes. Major challenge is to find appropriate biomarkers indictative of heterogeneity of this disease. In the ideal situation, the optimal therapy should be tailored treatment of each individual patient, probably based on specific diagnostic tests. Thus, "trial and error" or “one size fits all” concepts will be absolete in the future[17]. At present, the heterogeneity

of breast cancer but the lack of suitable tumor biological diagnostic, prognostic, or predictive markers does not allow to develop comprehensive individualized treatment strategies.

1.2 Triple-negative breast cancer (TNBC)

The terms “basal-like cancer” and “triple-negative breast cancer” have been interchanged and misused for a long time period. There are two different types of epithelial cells in the breast gland: luminal cells originating from a differentiated luminal precursor cell which can express ER, PR, and cytokeratins 8/18, and basal cells originating from basal/myoepithelial cells which are positive for cytokeratins 5/6, 14, and 17, for vimentin, and p-cadherin[18, 19]. On the basis of that, breast cancer was classified into five intrinsic subtypes based on microarray studies: Luminal A, Luminal B, normal breast-like, HER2+, and basal-like breast cancer (Table 1). Among them, basal-like tumors have a large molecular overlap with triple-negative cancers[20].

Triple-negative breast cancer (TNBC) is defined by absence of the estrogen receptor (ER), progesterone receptor (PR), and human epidermal growth factor receptor 2 (HER2/neu). It may include basal-like cancers, claudin-low cancers, and normal breast-like tumors. Basal-like cancer is more like a genotype where genetic microarray, classification based on many variables is more appropriate for better classification than IHC markers [11]. In spite of that, considering the use of RNA from formalin-fixed paraffin-embedded tissue is not convincing and these IHC stainings can be routinely available in most pathology departments, the "triple-negative breast cancer" is mainly used as a surrogate marker for basal-like breast cancer[21].

TNBC is a very aggressive subgroup of breast cancer accounting for up to 17 % of all breast cancer cases[22, 23]. Compared with other breast cancer subgroups, TNBC is equipped with higher nuclear grade, abundant necrotic background, lymphocytes infiltrated, and many evidence of syncytial clusters[24]. Clinically, such breast cancers are more frequently found in younger women (<50 years) and commonly associated with a more aggressive behavior, larger tumor

size, increased risk of brain metastases, and disease recurrence within the first three years after primary surgery plus shorter survival following the first metastatic event[11, 23, 25–27].

Due to the lack of specific molecular targets, TNBC is insensitive to treatment with endocrine therapies or HER2-directed therapy. At present, poly-chemotherapy consisting of plantinum- or anthracycline-based therapies is the standard therapy for patients suffering from TNBC. Although other ongoing clinical trials, including poly (ADP-ribose) polymerase (PARP) inhibitors involved in repairing single-strand breaks in DNA (iniparib, olaparib and veliparib), antiangiogenic agents against vascular endothelial growth factor (bevacizumab and sunitinib), and epidermal growth factor receptor blockers (cetuximab and erlotinib), showed considerable promise[28, 29], up to now, none of targeted approaches besides systemic chemotherapy is remarkablely effective for TNBC patients. Research needs to be intensified to explore additional biomarkers which can specificly address prognostic and predictive features of this breast cancer subgroup.

1.3 Biomarkers in breast cancer

The American Society of Clinical Oncology (ASCO) breast cancer guidelines, first published in 1996, aims to assist physicians in clinical decision making. The past 2007 update of the ASCO breast cancer guidelines for the use of tumor markers in breast cancer [30] reviewed thirteen tumor markers with reference to Level-of-evidence-classification.

Table 2. Level-of-Evidence framework

Level-of-Evidence (LOE) framework	
LOE 1	single, high-powered, prospective, randomized controlled trials specifically designed to test the utility of the marker or meta-analyses of well-designed studies
LOE 2	prospective therapeutic trials in which marker utility is a secary study objective
LOE 3	evidence from large but retrospective studies

As a result, CA 15-3 and CA 27.29, carcinoembryonic antigen (CEA), steroid hormone receptors and HER2, urokinase plasminogen activator (uPA), plasminogen activator inhibitor 1 (PAI-1), and certain multiparameter gene expression assays showed evidence of clinical utility for breast cancer and were recommended for use in practice. At that time, other categories like DNA/ploidy by flow cytometry, p53, cathepsin D, cyclin E, proteomics, certain multiparameter assays, detection of bone marrow micrometastases, and circulating tumor cells demonstrated insufficient evidence to support routine clinical use.

ER, PR, and HER2 should be routinely measured on every primary invasive breast cancer in order to guide selection of systemic breast cancer treatment. uPA/PAI-1 reached LOE-I, serving as prognostic factors and predicting response to systemic adjuvant therapy in many patients [30, 31, 32].

To summarize, besides these biomarkers mentioned above, more meaningful parameters including the tumor's gene and protein-expression profile which can characterize individual breast cancers, especially for some specific subgroups like TNBC, need to be explored and validated. Qualified biomarkers should be used to identify the type of the cancer (diagnostic), to determine the course of disease (prognostic), and to predict response to cancer treatment (predictive). Besides that, they should be used to detect the state of disease (monitoring), and to optimize systemic treatment[33, 34].

1.4 Kallikrein-related peptidases (KLKs)

Human kallikrein-related peptidases (KLKs) encompass a family of 15 highly conserved serine proteases with similar structures and comparable functional properties. Tissue kallikrein (KLK1) was initially identified in pancreatic (*kallikreas* in Greek) extracts in the 1930s, which is secreted by the liver into the blood circulation. It exhibits substantial kininogenase activity [35].

Concerning the significant homology between the family members, but lacking kinogenase activity, the remaining 14 KLKs (KLK2-15) were named as kallikrein-related peptidases [36].

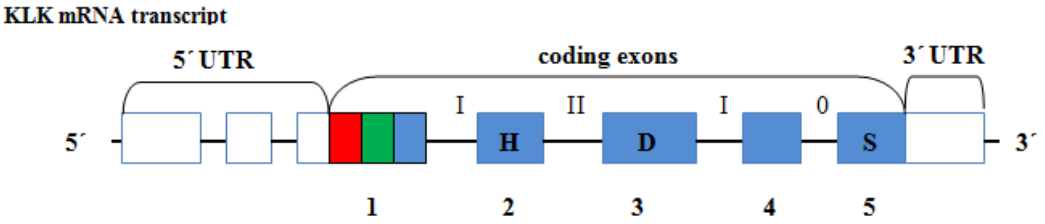

Figure 1. Schematic representation of the exon and intron gene sequence of KLKs

Localized on a chromosomal locus 19q13.3-4, all of the 15 KLK genes share between 40–80 % sequence similarity at the nucleotide and amino-acid level[37–39]. All human KLK genes are composed of 5 coding exons and 4 intervening introns with lengths ranging from 4-10 kb. Coding exon lengths are similar, but intron lengths are variable among KLK genes with a conserved phase pattern (I, II, I, 0). The active-site catalytic residues are highly conserved with the histidine (H) codon near the end of coding-exon 2, aspartic acid (D) codon in the middle of coding exon 3, and serine (S) codon near the start of coding exon 5. Unlike the "classical" KLK genes (KLK1, 2, 3), The majority of the 12 KLKs (KLK4-15) have one or two non-coding exons in the 5 ´-untranslated region (UTR). The 3 ´UTR typically varies in length [40]. So far, more than 70 alternatively spliced mRNA transcripts have been discovered among members of the kallikrein family. Each KLK gene can generate at least two transcripts that can encode structurally and functionally unique proteins. Most of KLK alternative splicing is featured by exon skipping, exon extension/truncation, and intron retention within the 5 ´UTR[38].

Figure 2. Schematic representation of the protein sequence of KLKs

All currently known 15 KLKs are single-chain secreted serine proteases and encoded as inactive precursors or zymogens which sterically mask the active site and thereby inhibit substrate binding. Structurely, the pre-pro-peptide usually contains a 16 to 30 amino acids long pre-peptide that functions as a signal peptide to direct newly synthesized KLKs into the endoplasmatic reticulum for secretion, followed by a pro-peptide of four to nine amino acids, that renders them as inactive precursors (zymogen) and containing a catalytic domain, which comprises the active center of the mature protein[41]. Targeted proteolysis of the pro-preptide will convert the KLKs-zymogen into the active KLKs-enzyme via diverse mechanisms. At first, pre-pro-KLKs are proteolytically converted into enzymatically inactive pro-KLKs via removal of an amino-terminal signal peptide to enter into the secretory pathway. Subsequently, pro-KLKs are activated extracellularly into mature peptidases by specific proteolytic cleavage of their amino-terminal propeptide. Mature KLK proteins have fully conserved amino acids around these catalytic residues, the invariant His57, Asp102, Ser195 catalytic triad, characteristic for serine proteases. Most of the KLKs denote a trypsin-like activity, while KLK3, KLK7, and KLK9 are chymotrypsin-like presences[42].

1.4.1 KLKs in normal and diseased tissues

KLKs are are found to be expressed at various levels in diverse kinds of tissues both at the mRNA and protein level. The diverse expression, secretion, and function of KLK family members indicate their potential role in important biological and pathological processes. In fact, due to this presence in diverse tissues and their serine protease activity, evidence is supported that KLKs might be involved in a wide range of complex proteolytic cascades, e.g. by activating each other or affecting signaling transduction pathways involving kinases, phosphatases, and other proteases, and thus to regulate physiological and pathological processes like cell growth,

digestion, fibrinolysis, coagulation, complement activation, wound healing, angiogenesis, and apoptosis [43].

To date, several biological roles have been attributed to human KLKs. For instance, the physiological role of KLK1 includes a variety of functions ranging from regulation of blood pressure to processing of growth factors. KLK1 is involved in cleavage of low-molecular-weight kininogen to release bradykinin and mediates various processes such as regulation of blood pressure, smooth muscle contraction, vascular permeability, and inflammatory cascades. In addition to its kininogenase activity, KLK1 is also implicated in the processing of growth factors and peptide hormones of the pancreas and other tissues[44]. Unlike KLK1, KLK2 and KLK3 (PSA) possess relatively low kininogenase activity. Both KLK2 and KLK3 can hydrolyze seminal vesicle protein, seminogelin I and II and fibronectin, which contribute to seminal plasma clot liquefaction and thus enhanced sperm motility. KLK3 cleaves at different sites and higher efficiency than KLK2[45–47]. Potential substrates like the peptide hormones and insulin-like growth factor binding protein-3 (IGFBP-3) have been identified as targets for KLK2 and KLK3. KLK3 has also been found in women's nipple aspirate fluid, breast cancer cyst fluid, amniotic fluid, milk of lactating women, and breast cancer tissues[48, 49]. The KLK4 protein is involved in tooth development via enamel matrix protein degradation[50]. KLK5 is proposed to not only degrade intercellular structures to facilitate cell shedding or desquamation during the terminal stages of epidermis turnover, but also to cleave extracellular matrix molecules (such as collagen types I–IV, fibronectin, and laminin) and cell adhesion molecules to contribute to cancer invasion, metastasis, and angiogenesis[51, 52]. Furthermore, KLK6 is assumed to participate in the deposition of amyloid plaques in Alzheimer ́s disease[53]. Accumulating data suggests that KLK7 is involved in skin desquamation during epidermal homeostasis[54–56]. Furthermore, KLK3, 5, 6, 13, and 14 were found to cleave constituents of the extracellular matrix and the basement

membrane, promoting tumor tissue remodeling, malignant transformation, and tumor cell growth[57].

KLKs may also be involved in other pathways including the plasminogen activation system[58, 59], matrix metalloproteinases (MMPs)[60], and proteinase-activated receptors (PARs)[61] to mediate physiological or pathological functions (see chapter 1.4.2). Evidence suggests that certain KLKs may autoactivate themselves or potentially activate other KLKs and pro-KLK proteins can function as substrates for activated KLKs, thereby forming a complex network of intracellular and extracellular proteolytic cascade pathways[43, 62], effecting cell morphology, cell mobility, cell proliferation, and cell invasion. Nevertheless, the physiologic roles of many of the KLKs have not been fully elucidated. In vivo targets of many KLKs still remain ill-defined.

1.4.2 KLKs in carcinoma tissues

Through the activation of growth factors, plasminogen, MMPs, and PAR-related cascades (protease-activated receptor), as well as the auto/cross-activation network, KLKs directly or indirectly impact upon growth factors, cell adhesion molecules, cell surface receptors, and extracellular matrix proteins, hereby facilitating tumorigenesis, degradation of the ECM, and inducing EMT-like changes in cancer cells, further stimulating tumor growth, angiogenesis, and distant metastasis.

Tumor growth, as the initial phase of tumor progression, is also effected by KLKs through regulation of diverse signaling cascade pathways including the insulin-like growth factor (IGF) axis and PARs mitogenetic family.

The IGF axis is considered to be a crucial modulator of mitogenic and anti-apoptotic nature for promotion of tumor cell growth. KLK2[63], KLK3[64], KLK4[65], KLK11[66], and KLK14[67] have

been reported to reduce insulin-like growth factor binding proteins (IGFBP), which may not only eliminate the tumor-suppressive functions of IGFBPs but may also cause the release of IGFs, resulting in increased availability of IGFs and their interaction with receptors (IGFRs) [68]. Hence, KLKs may promote the mitogenic and anti-apoptotic process through the stimulation of the IGF axis[69].

Protease-activated receptors (PAR1-4), as members of the G protein-coupled receptor (GPCR) subfamily, can be activated by serine protease medicated cleavage within the extracellular N-terminus which in turn reveals a tethered ligand that binds to the extracellular receptor domain to initiate cell signaling. Recently, several members of the KLK family have been shown to initiate trans-plasma membrane signal transduction via PARs. KLK2 can regulate extracellular signal-regulated kinase (ERK) signaling to activate the expression of PAR1, and thus stimulate the proliferation of prostate cancer cells[61]. KLK5, 6, 14 have been demonstrated to stimulate ERK1/2 kinase phosphorylation through activation of PAR-2 signaling and KLK14 can promote tumorigenesis by activating PAR-2, e.g. in colon cancer[70, 71]. KLK4 has been reported to mediate both PAR1- and PAR2- signaling in PC3 cells[72]. KLK4 may initiate tumor–stroma interactions through activation of PAR-1 in the surrounding stroma, triggering the release of interleukin-6 (IL-6) that facilites the growth and proliferation of prostate cancer cells through ERK- and STAT3-signaling[73].

Degradation of extracellular matrix (ECM) is an essential part of tumor progression, facilitating tumor cell invasion into surrounding tissues, their escape into the blood circulation and finally, formation of distant metastases. MMPs, plasmin, and cathepsins are mainly responsible for cancer-related ECM degradation[74]. KLKs have been found to cleave structural compounds of the subendothelial basement membrane and extracellular matrix directly[75], but are also indirectly instrumental in degradation of this target though the activation of the

plasminogen activation system or by activation of matrix metalloproteinases (MMPs)[59, 76, 77]. KLK2 and KLK4 can active pro-uPA which is thereby transformed into uPA to bind to its transmembrane receptor (uPAR), resulting in the activation of plasmin and MMPs from their precursors plasminogen and proMMPs, respectively[58, 59]. KLK2 also can target and hereby inactive plasminogen inhibitor type-1 (PAI-1) by cleavage at peptide position Arg346-Met347 to form a KLK2-PAI-1 complex[78]. Alternatively, in addition to directly cleave the uPAR receptor to activate the uPA-uPAR cascade, other KLKs (5,6,13) can degrade extracellular fibronectin, laminin, and collagen, which also can activate MMPs or affect the uPA-uPAR interaction[51–52, 79]. Additionally, KLKs have been postulated to be involved in "activation cascades" with other KLKs and endopeptidases, demonstrating the potential for extensive KLK activation cascades[80]. Considering that enzymatic cascades promote amplification of the starting stimuli, the activation of the above mentioned proteolytic cascades can trigger massive ECM remodeling.

Epithelial-mesenchymal transition (EMT), as a key point for cancer progression, represents a cellular process which describes the transformation of epithelial cells into spindle-shaped mesenchymal-like cells, accompanied by loss of cell-cell adhesion, hereby enhancing tumor cell growth and invasiveness[81]. KLK1 is proposed to promote prostate cancer cells invasion and migration through a PAR1-related pathway[82]. Moreover, PSA/KLK3- and KLK4- transfected prostate cancer cells have been shown to enhance migration capacity and spindle-shaped morphology of tumor cells because of loss of E-cadherin and upregulation of vimentin[83]. KLK3 triggers release of latent TGF-β, which facilitates EMT-like changes, and thus promotes EMT[84]. Upregulation of KLK4 expression can affect both pro-PSA and pro-uPA, leading to increased migration of prostate cancer cells[59]. By contrast, KLK6 plays a protective role during tumor progression, most likely affected by inhibition of EMT[85]. Apart from these KLK family

members, KLK7 can also induce EMT-like changes, leading to enhancing the mobility and invasiveness of prostate carcinoma cells[86].

Angiogenesis is crucial for survival and growth of tumor cells, invasion of tumor cells into surrounding tissues, and for the spread and formation of distant metastases. PSA/KLK3 may activate the pro-angiogenic factor TGF-β and thus stimulate angiogenesis directly[87]. KLK1 has been reported to support angiogenesis through the release of bradykinin from kininogen[88]. Conversely, angiogenesis can be prevented by action of PSA/KLK3, KLK5, KLK6, or KLK13 through releasing biologically active angiostatin-like fragments from plasminogen, which strongly inhibits endothelial cell angiogenesis[89, 51, 62, 90]. Recent studies revealed that KLK12 might regulate some angiogenesis-promoting growth factors: vascular endothelial growth factor (VEGF), TGF-β1, and fibroblast growth factor-2 (FGF-2) by cleavage of various matricellular proteins[91].

Metastasis, as a complex pathological progress, is regulated by a multitude of factors. KLKs present at the metastatic site may control tumor cell invasion by degradation of ECM barriers, which is necessary for tumor cells to detach, invade, and metastasize. KLKs may induce PAR signaling with a stimulatory or preventive effect on tumor cell invasion[92–93]. KLK3 releases latent TGF-β[84], thus promoting EMT, but regulates bone remodeling and formation of bone metastasis[87, 94]. Upregulation of KLK4 expression promotes migration of prostate cancer cells and attachement to bone-matrix proteins[95].

1.4.3 KLKs as biomarkers in hormone-related cancers

KLKs are very well known for their implication in different pathological stages of cancer, either by promoting or inhibiting carcinogenesis by their regulative role in tumor progression, invasiveness, and metastasis. In past years, KLKs emerged as biomarkers for several types of

cancer, primarily in hormone-related malignancies. In order to exemplify the effect of different KLKs on cancer progression, the currently known clinical relevance of KLK expression in endocrine-related prostate, ovary, or breast cancer has been documented.

Prostate cancer

KLK2 has been reported to enhance the diagnostic specificity in distinguishing prostate cancer cases from benign cases[96] and to predict outcome of prostate cancer patients affiliated with rapid disease progression and biochemical relapse after local therapy[97]. Up to now, PSA/KLK3 was considered as useful tumor marker for prostate cancer screening, diagnosis, prognosis, and monitoring, although it is not a prostate cancer-specific marker to be expressed in a wide range of other human tissues. Clinically, PSA/KLK3 is mainly applied for screening of the male population for incidence of prostate cancer and for monitoring of treatment success in prostate cancer patients[98]. Elevation of PSA/KLK3 levels is also known to indicate the presence of residual tumor mass and disease recurrence in prostate cancer patients[99]. KLK4 is reported to be significantly overexpressed in prostate cancer tissue, compared with benign prostate epithelium[100, 101]. KLK4-transfected prostate cancer cells (PC-3 and DU145) have been associated with augmented cell proliferation and colony formation, implicating that KLK4 is involved in tumor cell proliferation and metastatic capacity of prostate cancer cells[95, 100]. By contrast, KLK5 expression was found to be correlated with less-advanced prostate cancer disease stages and low Gleason scores, predicting a favorable prognosis for prostate cancer patients[102]. Like KLK5, lower KLK11 mRNA levels were reported to be correlated with advanced tumor stages and less-differentiated malignancies, implicating a favorable prognostic value of KLK11 for prostate cancer patients[103, 104]. Besides that, increased KLK14 expression is associated with advanced stage of the cancer disease, high tumor grade, high Gleason score, and an elevated risk for biochemical relapse, which indicates the unfavorable prognostic nature of KLK11 in prostate

cancer patients[105]. Likewise, up-regulated KLK15 mRNA levels have been associated with an aggressive phenotype and an unfavorable prognosis of the prostate cancer patients[106].

Ovarian cancer

KLK4 is not expressed in the normal ovary but highly expressed in ovarian carcinoma tissues, both at the mRNA and/or protein level[38, 107]. KLK4 expression in ovarian cancer is associated with advanced stage, higher tumor grade, and short survival[98, 108, 109–110]. Increased KLK4 has the potential value to predict resistance to paclitaxel-based chemotherapy in patients suffering from ovarian cancer, suggesting that KLK4 is a predictive marker for chemoresistance in several advanced stage ovarian cancers[101]. Increased KLK5 is also associated with an unfavorable prognosis of ovarian cancer patients[111, 112]. KLK6 was shown to act as an unfavorable prognostic biomarker in ovarian cancer. The combination of KLK6 and KLK10 was demonstrated to serve as a tool to improve the diagnostic sensitivity and specificity of ovarian cancer detection to enhance the power of CA125 as a marker for early diagnosis of ovarian cancer[113–116]. Furthermore, elevated KLK6 and KLK10 concentrations are significantly correlated with an aggressive phenotype, decreased survival, and poor response to chemotherapy as well[98, 110, 117–119]. Gene expression analyses have revealed KLK7 mRNA levels to be correlated with an unfavorable prognosis of ovarian cancer patients presenting with advanced-stage tumors and resistance to treatment and thus limited survival probability[98, 110, 120–121]. Conversely, KLK8 mRNA expression analysis in ovarian carcinomas has been shown to predict favorable prognosis of ovarian cancer patients since elevated KLK8 mRNA expression levels correlate with early stage, low nuclear grade, and favorable survival of ovarian cancer patients[112, 122–124]. Like KLK8, KLK9 expression levels were also found to be significantly elevated in ovarian cancer patients with early-stage disease and favorable disease-free and overall survival[125]. Enhanced KLK10 gene expression, compared to benign and normal ovarian tissues, also serves as a potential

diagnostic biomarker to detect ovarian cancer, an increase in tumor-associated KLK8 mRNA revealed a correlation with with advanced disease stages and residual tumor mass[114, 126]. Elevated KLK11 expression in ovarian tumors was reported to be significantly associated with increased disease-free and overall survival[127]. Additionally, KLK13 mRNA levels in invasive epithelial ovarian carcinoma were found to be correlated with poor clinical outcome and reduced disease-free suvival[128]. On the other hand, elevated KLK14 mRNA expression is associated with a favorable prognosis of ovarian cancer patients since higher KLK14 mRNA expression levels have been correlated with less-advanced disease, reduced CA-125 blood concentration and improved survival[129]. KLK15 mRNA levels have been shown to be correlated with unfavorable clinical outcome of ovarian cancer patients [130].

Breast cancer

Expression levels of all of the fifteen KLKs, except for KLK10,12, and 15, have been identified in normal female breast tissues at the mRNA and protein level. KLK mRNAs: low to moderate: (KLK2-5, 9, 12 and 13), high (KLK1, 6-8, 10, 11 and 14). Protein level: low to moderate (KLK1-2, 4-8 and 13-15), high (KLK9 and 11), no expression (KLK10 and 12). Depending on the individuals, KLK3 can be expressed or absent in the female breast[131, 132].

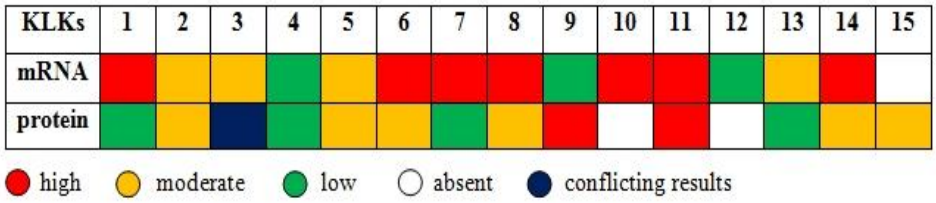

Figure 3. Comparative mRNA and protein expression of KLKs in normal female breast tissues

Compared to expression levels in normal breast tissue, several KLK genes except KLK4, 6, and 13-15 are down-regulated in breast cancer tissues and/or cell lines at the mRNA level[98, 131, 133-135].

KLK13 mRNA is expressed in breast cancer tissue but has not been compared with KLK13 mRNA expression in normal breast tissue. KLK6 gene was known to be down-regulated in metastatic breast cancer but upregulated in primary breast cancer[136]. However, an in-silico analysis provides evidence that KLK6 is downregulated in breast cancer[137]. Opposite results have also been reported regarding the gene expression of KLK14 in malignant samples compared to benign ones, depending on the study[138–140]. At the protein expression level, data are available for six KLKs when tumor tissue was compared to normal breast tissue. KLK4 mRNA and protein expression was shown to be elevated compared to normal breast tissue. For KLK6 and 14 both increases and decreases at the protein level have been reported[132]. KLK3 is decreased or can even be absent in breast cancer tissue. Other KLKs such as KLK2, 7–9, 11–13 and 15, have not been assessed for protein expression in breast cancer tumor tissue yet[131–132, 141].

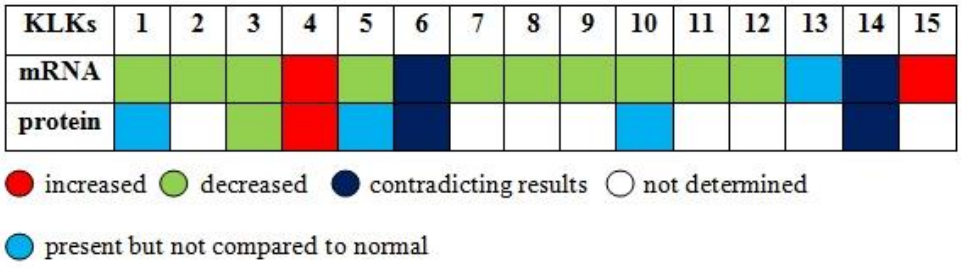

Figure 4. Comparative mRNA and protein expression of KLKs in breast cancer tissues

Some members of the KLK family, PSA/KLK3, KLK5, 10, and 14, are considered candidates for breast cancer risk assessment. PSA present in the blood circulation has been reported to be of use to differentiate breast cancer patients from individuals with benign breast disease[142]. In addition to that, PSA protein expression is down-regulated in nipple aspirate fluids (NAF) of breast cancer patients compared to normal breast fluid[49, 141]. It has been proposed that high concentrations of PSA in NAF or in serum is inversely related to breast cancer risk, aiding in early detection of breast cancer[141]. In addition, KLK5[143], KLK10 [144], and KLK14[145] serum levels have also been reported to be elevated in tumor diseases of breast cancer patients compared with serum of

healthy volunteers, implicating that these KLK family might be potential breast cancer diagnostic biomarkers.

Other KLKs are considered as potential prognostic or predictive cancer biomarkers in breast cancer. The mRNA expression levels of KLK1, 4, 5, 7, 10, and 14 are associated with adverse clinical outcome of breast cancer patients. In contrast, KLK3, 9, 12, 13, and 15 may function as indicators of favorable breast cancer outcome[38, 98, 110, 147].

In in vitro assays, a KLK1 inhibitor was shown to suppress invasion of MDA-MB-231 breast cancer cells, indicating that KLK1 might enhance breast cancer cell invasiveness[148]. High PSA/KLK3 levels have been related to a favorable prognosis with better disease-free survival (DFS) and overall survival (OS)[149] which might increase the chance of breast cancer patients to benefit from endocrine therapy[150]. Significantly increased gene expression levels of KLK4 were reported for breast carcinomas compared to benign ones[151]. Elevated KLK4 expression levels were detected in the stromal microenvironment and have been associated with advanced tumor grade, aggressive tumor behavior, and reduced progesterone receptor expression, and with poor prognosis, highlighting its significance for monitoring the clinical outcome of breast cancer patients[134, 151]. In breast cancer, KLK5 mRNA expression levels have been reported to be down-regulated compared to normal tissue counterparts[152]. KLK5 protein expression levels determined by ELISA in the serum of cancer patients have been elevated compared to sera of healthy volunteers[143]. Increased KLK5 expression was found to indicate shorter DFS and OS of breast cancer patients[153, 154]. KLK6 has been demonstrated to serve as a tumor suppressor in breast cancer. KLK6 might reduce the production of vimentin and restoration of cytokeratin 8 and 19, and therefore also be associated with inhibition of epithelial-to-mesenchymal transition and restrain proliferation of tumor cells[89]. In breast cancer, KLK7 is often co-expressed with KLK5 expression. Its mRNA expression levels are down-regulated in breast carcinomas[155] and

have been repeatedly associated with shorter survival of the breast cancer patients[156, 157], indicating that KLK7 expression may be a useful marker to predict unfavorable prognosis in breast cancer patients. Multivariate analysis revealed that KLK9 expression is correlated with small tumor size, early tumor stage, and with increased disease-free and overall survival[158]. KLK10 has been proposed as a tumor suppressor gene and as a potential diagnostic and predictive breast cancer biomarker[159]. The loss of KLK10 by exon 3 methylation is associated with an elevated risk for disease recurrence and shorter survival time[160]. Furthermore, elevated KLK10 expression levels may predict resistance to tamoxifen therapy[161]. Enhanced KLK13 mRNA expression is significantly associated with increased disease-free and overall survival, suggesting favorable outcome of breast cancer patients[162]. By contrast, in breast cancer, KLK14 has been identified as an unfavorable prognostic marker, patients with high KLK14 mRNA values are associated with advanced disease stage and increased risk of metastasis and early death[163]. Elevated KLK14 protein levels are more likely to be associated with an aggressive tumor phenotype of the mammary gland[139]. Otherwise, KLK15 gene expression has been correlated with a favorable prognosis of breast cancer patients[164].

Table 3. KLKs as breast cancer biomarkers (mRNA and/or protein level) ND= Not defined

KLKs	Expression in breast tumors	Clinical application	References
KLK1	↓	↑ Invasiveness	Wolf WC, 2001
KLK2	↓	Not defined	Shaw JL, 2007
KLK3	↓	Diagnostic marker	Black MH, 2000 Sauter ER, 2004; Yu H, 1998; Foekens JA, 1999
		↑ Survival	
		Response to tamoxifen	
KLK4	↑	↑ Tumor grade	Mangé A, 2008; Papachristopoulou G, 2009
		↓ Progesterone receptor	
KLK5	↑ In serum	Diagnostic marker	Yousef GM, 2002; Talieri M, 2011
	↓	↓ Survival	
KLK6	↓ In metastatic tissue	↓ Proliferation	Anisowicz A, 1996; Yousef GM, 2004; Pampalakis G, 2009
	↑In primary tumors		

KLK7	↓	↑ Stage	Li X, 2009; Talieri M,2004; Holzscheiter L, 2006
		↓ Survival	
KLK8	↓	Not defined	Yousef GM, 2004
KLK9	↓ Expression	↓ Stage, ↑ Survival	Yousef GM, 2003
KLK10	↑ In serum	Marker of diagnosis	Ewan King L, 2007 Luo LY,2002; Yousef GM, 2005; Kioulafa M, 2009
	↓ Expression in tumor	Resistance to tamoxifen	
	↓ Expression ↑methylation	↓ Survival	
KLK11	↓	↑ Proogression	Sano A, 2007
KLK12	↓	Not defined	Yousef GM, 2000
KLK13	↓	↑ Survival	Chang A, 2002;
KLK14	↑ In serum	Marker of diagnosis	Borgoño CA, 2003 Yousef GM, 2002; Fritzsche F, 2006; Papachristopoulou G, 2011
	↓	↑ Grade, ↑ Size ↑ Stage, ↓ Survival	
KLK15	↓	↑ Survival	Yousef GM, 2002

In these cancers, KLKs, as a tissue-and clinical-associated proteolytic system, can be seen as a rich source of diagnostic, prognostic, or therapy-response cancer biomarkers, allowing early diagnosis, molecular classification, and prognosis of human malignancies as well as prediction of response to cancer treatment. In breast cancers, differing from other KLKs, only KLK4 is of clinical relevance, both at the mRNA and protein level, which implicates that it may play a unique and essential role in the development of breast cancer. Yet, until now, no validated data are available regarding the prognostic and/or predictive value of KLK4 in breast cancer. More detailed studies about KLK4 expression at the gene or protein level are thus of strong clinical need.

1.5 Kallikrein-related peptidase 4 (KLK4)

KLK4, otherwise known as ARM1, EMSP, EMSP1, KLK-L1, MGC116827, MGC116828, Prostase, PRSS17, and PSTS, has been detected in prostate, breast, and ovarian cancer tissues. Although KLK4 was originally described as a protease with prostate-restricted expression[165], the major physiological function of KLK4 was ascribed to dental enamel biomineralization by

degrading matrix proteins in the enamel matrix of developing teeth[166]. KLK4 protein is also expressed in normal breast ductal epithelium and is overexpressed in breast cancer tumor tissue[167]. Due to its abnormal elevated expression at the mRNA and protein level in breast cancer, KLK4 is considered as a potential diagnostic and/or predictive biomarker for patients afflicted with breast cancer and even as a target for selective cancer therapy[134, 151].

The KLK4 gene consists of five exons and four intervening introns, among which three alternative transcription start sites (TSSs) have been predicted or identified. At least 9 alternative KLK4 transcripts have been found, including variants with TSS deletion (TSS1 and TSS2), exon deletion (exon 4), intron insertion (intron II or III), and combinations thereof[168, 169].

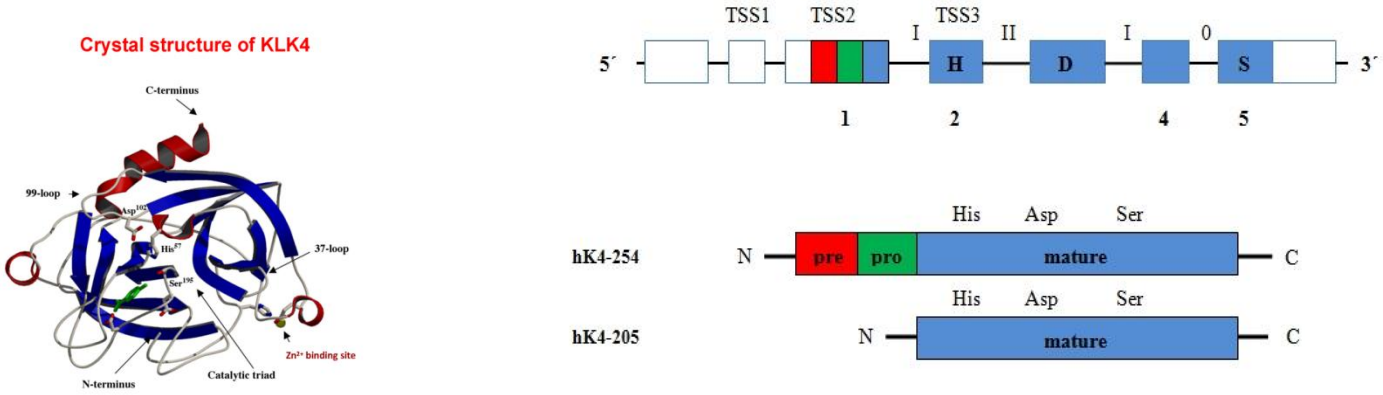

Figure 5. Crystal structure of KLK4 (left) and schematic representation of its gene and protein structure (right)

Like other KLKs, the conserved catalytic triad His57, Asp102, Ser195, typical for serine proteases, is essential for its proteolytic activity. Among various variants, only two KLK4 transcripts, full-length KLK4 (hK4-254) transcript and the exon 1 deleted form (5′-truncated hK4-205) encode for an active serine protease. Other KLK4 transcripts with splice variations

between exons 2 and 5 exhibit a frame shift in the coding region and thus do not have the essential serine and/or aspartic acid residues of the catalytic triad[170–171].

Interestingly, most KLK proteins are found in the cytoplasm of luminal secretory cells of normal epithelial cells or in the cytoplasm of malignant human epithelial cells. KLK4 is located in the nucleus too, which is different from other KLKs. The sequence encoding the signal peptide is retained in most of the KLKs, indicating that most KLK protein variants are likely to be secreted and thus to be present in biological fluids. In case of KLK4, however, full-length KLK4 gene encodes a 254-amino-acid pre-pro-peptide (hK4-254). After synthesis, the signal peptide is detached and the KLK4 zymogen is subsequently secreted and then activated to generate the mature active KLK4 enzyme, whereas the exon1 deleted form encodes an N-terminally truncated 205-amino acid KLK4 protein (hK4-205). This 5′-truncated hK4-205 initiated from the ATG2 (TSS3) in exon 2, lacking the pre-signal peptide and pro-region, is unlikely to be secreted and then activated extracellularly. All these suggest that these two isoforms might have a differential cellular localization and endowed with different functional roles.

Higher expression levels of the exon 1 deleted KLK4-205 transcript and lower expression levels of full-length KLK4-254 were reported[172–174]. Full-length KLK4-254 was found to be localized to the cytoplasm, although N-terminal truncated KLK4-205 was predominantly localized to the nucleus[174, 175]. KLK4-254 but not N-terminal truncated KLK4-205 is detected at a higher level in malignant prostate cells than in benign prostate cells, which implicates that full-length KLK4-254 may serve as a candidate diagnostic marker for prostate cancer. By contrast, only truncated KLK4 transcripts were found to be regulated by androgens in LNCaP cells[175]. To date, uncertainties about which of these KLK4 isoforms are secreted and where they are precisely localized in tumor cells are matter of discussion[176, 177].

KLK4 has been reported to degrate IGFBPs to increase IGF release which promotes tumor cell growth[65]. Also, KLK4 converts the urokinase-type plasminogen activator proenzyme (pro-uPA) into active HMW-uPA, thus facilitating extracellular matrix remodeling, EMT changes, tumor invasion, and metastasis[59, 179]. In addition, PAR-1 and PAR-2, members of the protease-activated receptor family of G-protein-coupled receptors, have been shown to be receptive for KLK4[61, 72]. KLK4 stimulates the proteolytic cleavage of PAR-1 in the surrounding stroma where the induction of interleukin-6 and other cytokines ultimately leads to the initiation of tumor–stroma interactions and stimulation of cancer cells invasion[73].

Even to date, the precise physiological role of KLK4 in breast cancer is still not clearly defined, although KLK4 expression has been investigated in breast cancer cells or tissue collectives by use of various methods[134, 151, 175, 180–182], including traditional immunohistochemistry. Therefore, further investigation for discovering the appropriate immunohistochemical tools is required to characterize KLK4 expression and to explore the potential function of KLK4 in human breast malignancies.

2. Aim of the study

Recent discoveries in breast cancer genomics and protomics have led to refined classification of the disease, to identification of cancer biomarkers associated with pathological features, and improved prediction of clinical outcomes and responses to cancer therapy. With respect to that, triple-negative breast cancer, an aggressive form of breast cancer, should draw more attention due to the absence of effective therapeutic targets and its aggressive behavior. As a member of the cancer biomarker family, KLK4 emerges as a novel highly clinically relevant biomarker in breast cancer.

Although previous research has demonstrated the diagnostic, predictive, or prognostic value of KLK4 in breast cancer in this disease, a thorough assessment of its expression, by immunohistochemistry has not been done yet. No standard operation procedures have been established yet for identification of KLK4 in breast cancer, also not for the aggressive triple-negative subgroup. The quantitative evaluation of KLK4 expression by immunohistochemisty through well-established standard operating procedures (SOPs), as well as the subsequent analysis of relation to the course of the disease and and clinical outcome are still absent.

Aims of the thesis therefore are: (1) Exploration of the expression and localization of KLK4 in cancer cells. (2) Production, testing, and set-up of SOPs for immunohistochemical localization and quantification of KLK4 in breast cancer tissues, especially in triple-negative breast cancer tissues. (3) Exploration and validation of the clinical relevance of KLK4 protein expression to predict outcome in triple-negative breast cancer patients.

3. Materials

3.1 Triple-negative breast cancer patients

257 primary breast cancer tissues of triple-negative breast cancer patients have been collected at the Frauen Klinik, Klinikum rechts der Isar, Technische Universität München, Germany between 1988 and 2013. Tissues were stored in liquid nitrogen after inspection by the pathologist. Standard surgical procedures, including breast conservation surgery and mastectomy, were performed after patients have gave written informed consent. Tumor samples were routinely assessed for steroid hormone receptor (ER and PR) and HER2 expression. the Institute of Pathology, Helmholtz Zentrum, München. Clinical follow-up data were available for 188 patients (age 27 to 85 years, median age of 57). The high proportion of patients at younger age

(32.4 % <50 years) and those with pre-menopausal status (27.7 %) is consistent with data reported previously[23]. Histological and morphological features were documented including histological subtype, TNM-stage, nuclear grade, and lymph node status. Of the 188 patients, the majority (79.3 %) suffered from invasive ductal carcinoma subtype. Rare subtypes included medullary, lobulary, and other subtypes. Tumors were staged according to the TNM staging system (AJCC, see appendix, Table 11.1) and graded according to the Nottingham grading system (See appendix, Table11.2). In our cohort, these breast cancers were more frequently found along with high grade (G3, 83.5 %), higher incidence of metastasis (29.8 %), and disease recurrence (18.1 %), which is comparable to data published previously[24]. 69 patients (36.7 %) died during the time of observation, 77 patients (41.0 %) progressed. The median time of follow-up of the patients was 57 and 37 months for overall survival (OS) and time to tumor progression (TTP), respectively. 118 (62.8 %) patients received anthracycline/cyclophosphamide-based chemotherapy, 30 (16.0 %) endocrine therapy, 137 (72.9 %) radiotherapy, 6 (3.2 %) were given immunotherapy. In addition, 20 patients received neoadjuvant therapy before primary surgery. Of particular, 148 (78.7 %) and 30 (16.0 %) patients were found to have low to moderate lymphocyte invasion, while 52 (27.7 %) have abundant necrotic background, which is in accordance with previous findings[24]. Relevant data on clinical and histomorphologic parameters of the patients are shown in Table 4.

Table 4. Clinical and pathological characteristics of the TNBC breast cancer collective (n=188)

Clinicopathological parameters	**n (%)**
Age (years)	
<50	61 (32.4)
⩾50	127 (67.6)
Median / range	57 / 27-85
Menopausal status	
pre-menopausal	52 (27.7)
peri-menopausal	7 (3.7)

post-menopausal	127 (67.6)
unknown	2 (1.1)
Histological subtype	
invasive ductal	149 (79.3)
medullary	18 (9.6)
lobular	9 (4.8)
other	12 (6.4)
Tumor size	
pT1	62 (33.0)
pT2	87 (46.3)
pT3	15 (8.0)
pT4	22 (11.7)
unknown	2 (1.1)
Nodal status	
pN0	87 (46.3)
pN1	69 (36.7)
pN2	19 (10.1)
pN3	7 (3.7)
unknown	6 (3.2)
Metastasis	
No	127 (67.6)
Yes	56 (29.8)
unknown	5 (2.7)
Histological grade	
G1	2 (1.1)
G2	22 (11.7)
G3	157 (83.5)
unknown	7 (3.7)
Treatment of primary tumor	
Breast-conservation	109 (58.0)
Mastectomy	73 (38.8)
unknown	6 (3.2)
Disease recurrence	
No	149 (79.3)
Yes	34 (18.1)
unknown	5 (2.7)
Neoadjuvant therapy	
No	163 (86.7)
Yes	20 (10.6)
unknown	5 (2.7)
Adjuvant treatment	
Chemotherapy	118 (62.8)
Endocrine therapy	30 (16.0)
Immunotherapy	6 (3.2)
Radiotherapy	137 (72.9)
Lymphocytic infiltrate (TMAs)	

None	7 (3.7)
Minimal	148 (78.7)
Moderate	30 (16.0)
Extensive	0 (0)
unknown	3 (0)
Necrosis (TMAs)	
None	136 (72.3)
Present	52 (27.7)

3.2 Reagents and materials

Table 5. Reagents and materials used in the experiments

Cell culture	
Albumin Bovine Fraction V	#160069 MP biomedicals, LLC
BLAUBRAND® counting chambers	Blau Brand, Germany
Centrifuge	Rotina 48R, Andreas Hettich, Tuttlingen, Germany
CO_2-Incubator	HERA Cell, Kendro, Langenselbold, Germany
Cell culture microscope	CK30, Olympus, Japan
DMEM (Dulbecco ś modified Eagle's medium) + Glutamax™	#61965-026, Gibco, Invitrogen, Paisley, UK
RPMI (Roswell Park Memorial Institute) 1640 medium+ Glutamax™	#11835-10, Gibco, Invitrogen, Paisley,UK
DMSO	#317275, Merck Chemicals, Darmstadt, Germany
EDTA (ethylenediaminetetraacetic acid) 1 % (w/v)	#L2113, Biochrom AG, Berlin, Germany
Fetal Bovine Serum (FBS)	#10270-106, Invitrogen, Carlsbad, CA, USA
Geneticin (G418)	#11811-031, Gibco, Invitrogen, Paisley, UK
HEPES (4-(2-hydroxyethyl)-1-piperazineethanesulfonic acid)	#15630-080, Gibco, Invitrogen, Darmstadt, Germany
CO_2-Incubator	Heraeus Function Line Serie 7000
Laminar flow cabinet	M1199, Hera Safe, Heraeus, Hanau, Germany
L-arginine	#A8094, Sigma, Munich, Germany
L-asparagine	#A7094, Sigma, Munich, Germany
Microscope slides cover slips	#005540 Menzel-Gläser, Braunschweig, Germany
RNase A	#12091021, Invitrogen, Carlsbad, CA, USA
Saponin	#S-1252, Sigma, St. Louis, USA
Na_2CO_3 (sodium carbonate)	#S-7795, Sigma-Aldrich, Steinheim, Germany
NH_4Cl (ammonium chloride)	#A-9434, Sigma-Aldrich, Steinheim, Germany
PBS/1 % BSA /0.1 % saponin	200 ml PBS 0.1 M, 2.0 g BSA, 0.05 g saponin
Triton X-100	#9002-93-1, Sigma, Munich, Germany
Trypan Blue	#T-8154, Sigma, Munich, Germany
Antibodies	
Alexa Fluor ®488 goat anti-rabbit IgG (H+L)	#A-11008, 2 mg/ml Invitrogen GmbH, Darmstadt, Germany
Rabbit anti-mouse IgG (Isotype)	#Z 0259, purified Ig fraction of rabbit antiserum, protein concentration 3.5g/l, DAKO, Denmark
Rabbit anti-mouse IgG, HRP-conjugated	#315-035-045, Dianova, Hamburg, Germany
Goat anti-rabbit IgG, HRP-conjugated	#111-035-003 (WB), Jackson ImmunoResearch
Mouse anti-GAPDH	#MAB374, Chemicon, Billerica, MA, USA

Rabbit anti-histone H3 antibody, polyclonal	#441190G, Invitrogen, Camarillo, CA, USA
Mouse anti-cytokeratin (CAM5.2)	#349205, BD biosciences, San Jose, CA, USA
Cytospin	
Cytospin centrifuge	Shandon 2 centrifuge, Thermo Fisher Scientific Inc., USA
Cytospin chamber slides	#59910051, Thermo Fisher Scientific Inc., USA
Cytospin chamber filter cards	#5991022, Shandon filter cards, Thermo Fisher Scientific Inc., USA
Cytospin plastic disposable sample chambers	#5991040, Thermo Fisher Scientific Inc., USA
Cytospin stainless steel clip	Thermo Fisher Scientific Inc., USA
Fluorescent staining	
DAPI	#10236276001, Roche, Mannheim, Germany
PI (propidium iodide)	#P3566, Invitrogen, Germany
BODIPY®650/665 phalloidin	B12382,330u, Invitrogen, Eugene, Oregon, USA
Wheat germ Agglutinin, Alexa Fluor ®647 conjugate	W32466, Invitrogen, Eugene, Oregon, USA
Cytofluorometry	
FACS Flow Sheath Fluid	BD Biosciences, Franklin Lakes, NJ, USA
Polystyrene-tubes (conical bottom, 4.5 mL)	Greiner Bio-One, Frickenhausen, Germany
FACSCalibur Sort Cytofluorometer with CellQuest software	BD Biosciences, Franklin Lakes, NJ, USA
CLSM	
Confocal Laser Scanning Microscope (CLSM) LSM700 from Carl Zeiss	Zeiss, Jena, Germany
ZEN2011	Software package for LSM700
Sarstedt chamber slides (8 well)	#946140802, 8 well non-pyrogenic, Sarstedt, Nümbrecht, Germany
DNA/RNA technology	
TRIzol® Reagent, ready-to-use	#15596-026, Invitrogen, Darmstadt, Germany
AffinityScript QPCR cDNA synthesis Kit	#600559, Invitrogen GmbH, Darmstadt, Germany
Brilliant II QPCR Master Mix with High ROX	#600805-12, Agilent Technologies, Böblingen,Germany
TaqMan® gene expression assay HS00191772 ready-to-use mastermix (20x)	#4453320, Applied Biosystems Deutschland GmbH, Darmstadt, Germany
Human HPRT1 (hypoxanthine guanine phosphoribosyl transferase 1) HS01003267 ready-to-use mastermix (20x)	#4310890E, Applied Biosystems, Darmstadt, Germany
Thermal cycler	Biorad, Munich, Germany
Mx3005P quantitative PCR	Agilent Technologies, Böblingen, Germany
Nanodrop	Thermo Scientific, Peqlab, Erlangen, Germany
Protein assay	
Nunc-Immuno-F96 Maxisorp	Thermo-Fisher, Nunc GmbH & Co. KG, Wiesbaden, Germany
SLT Spectra Elisa Reader, Software easy WIN fitting E 5.0 a	SLT, Crailsheim, Germany
Protein determination, SDS-Gel electrophoresis, Western blot-analysis	
Acrylamide/bisacrylamide (29:1)	Roth, Karlsruhe, Germany
Ammoniumpersulfate (APS)	Amresco, Solon, USA
Tween-20	#P2287, Fluka, Sigma, Munich, Germany
Ponceau S staining solution	Sigma-Aldrich, St. Louis, MO, USA
ProteoExtract® subcellular proteome extraction kit (S-PEK)	#539790, MERCK, Darmstadt, Germany
ECL Western Blotting Detection Reagent	#RPN2106, Amersham Biosciences, Little Chalfont, UK
BCA Protein Assay Kit	#23221, Pierce, Rockford, IL, USA
Protease inhibitor cocktail tablets complete	#11836145001, Roche, Mannheim, Germany
Protease Inhibiter Cocktail tablets complete, EDTA-free	#11873580001, Roche, Mannheim, Germany
PVDF membrane	#66547, PALL, Dreieich, Germany
PageRuler Prestained Protein Ladder	# 26616, Fisher Scientific, Schwerte, Germany

SDS	#2326.1, Carl Roth, Karlsruhe, Germany
Bromophenol blue	#1117460005, Merck Chemicals, Darmstadt, Germany
β-Mercaptoethanol	#444203, Merck Chemicals, Darmstadt, Germany
Glycerol	#G5516-100ML, Sigma, Munich, Germany
Acetic acid	#695092, Sigma, Munich, Germany
Ethanol	In-house
TEMED	#A1148,0100, Applichem, Omnilab, Munich, Germany
Skimmed milk	#70166, Fluka, Sigma, Munich, Germany
Whatman blotting paper	#3030672; Biometra, Goettingen, Germany
10 x TBS (Tris-buffered saline, pH 7.6)	60.5 g Trizma base, 90 g NaCl (in 1 L H_2O_{dist})
Thermomixer 5436, centrifuge 5417C	Eppendorf, Hamburg, Germany
Electrophoresis device	Blue Power 500, 3000, SERVA Electrophoresis GmbH, Heidelberg, Germany
Spectra/Por®molecular porous regenerated cellulose dialysis membrane and accessories	# 132650, Carl Roth, Karsruhe, Germany
Immunohistochemistry, immunocytochemistry	
Antibody diluent	#S2022, Dako, Glostrup, Denmark
Antibody diluent	#ZUC025-500, Zytomed Systems, Berlin, Germany
Bovine Serum Albumin (BSA)	#A-3912, Sigma, St. Louis, USA
Buffered paraformaldehyde solution 8 %	8 g paraformaldehyde was dissolved in 85 ml 0.1 M phosphate buffer in a fume hood on the heating plate (50-70 °C). 2N NaOH (2-3 drops) added to dissolve the turbidity, then adjusted with 2N HCl to pH 7.4. Adjust with 0.1 M phosphate buffer to 100 ml
Citric acid monohydrate	C1909 Sigma, St. Louis, USA
Citrate buffer	1 L H_2O_{dist}; 2.1 g citric acid monohydrate, adjusted with sodium hydroxide to pH 6
Coverslips	R. Langenbrinck, Teningen, Germany
DAB substrate kit (DAB high substrate buffer & liquid DAB chromogen)	#DAB 5000 plus, Zytomed Systems, Berlin, Germany
Ethanol	In-house ethanol provided by Department of Pathology, Technical University of Munich
Formalin	in-house formalin provided by Department of Pathology, Technical University of Munich
Goat serum (normal)	#X0907, Dako, Glostrup, Denmark
HCl (hydrogen chloride)	#3957.2, Carl Roth, Karlsruhe, Germany
Hematoxylin	Mayer ś acid hematoxylin
Hydrogen peroxide 3 % H_2O_2 (v/v)	45 mL H_2O_{dist}, 5 mL 30 % H_2O_2
Hydrogen peroxide 30 % (H_2O_2)	1.07210.0250, Merck, Darmstadt, Germany
Isopropanol	In-house isopropanol provided by Department of Pathology, Technical University of Munich
Light microscope	Axioskop, Carl Zeiss, Jena, Germany
LSAB DAB kit	#K5003, Dako, Glostrup, Denmark
Manual tissue microarray instrument	Alpha Metrix Biotech GmbH, Rödermark, Germany
Microscope slides	SuperFrost Plus, # 03-0060, R. Langenbrinck, Teningen, Germany
Microscope software	AxioVision Rel.4.6.3 (04-2007), Carl Zeiss, Jena, Germany
Microtome (electronic, rotary)	Microm HM 335E, Microm GmbH, Walldorf, Germany
Paraffin	In-house paraffin provided by Department of Pathology, Technical University of Munich
Paraformaldehyde	#31628.01 Serva Electrophoresis, Heidelberg, Germany
PBS/1 % BSA	20 ml PBS 0.1M, 0.2 g BSA
PBS/1 % BSA /0.1 % saponin	200 mL PBS 0.1M, 2.0 g BSA, 0.05 g saponin
Pertex (mounting medium)	PER3000, Medite, Burgdorf, Germany
Phosphate buffer	100 mL (0.1M) Na_2HPO_4 solution, 0.1M NaH_2PO_4 solution adjusted to pH 7.4, filled with H_2O_{dist} to 200 ml
Pressure cooker	Ankoch-Automatik, WMF, Geislingen/ Steige, Germany

Saponin	#S-1252, Sigma, St. Louis, USA
Scanning software NDP2.0	#40885, NanoZoomer Virtual Microscopy, Hamamatsu Photonics, Hamamatsu, Japan
NaCl	1.06404, Merck, Darmstadt, Germany
Na_2HPO_4 2 H_2O (sodium phosphate dibasic dihydrate)	S-0876, Sigma-Aldrich, Steinheim, Germany
NaH_2PO_4 2 H_2O (sodium phosphate monobasic dihydrate)	#2370, Carl Roth, Karlsruhe, Germany
NaOH	S-0899, Sigma-Aldrich, Steinheim, Germany
Trizma Base	T1503, Sigma-Aldrich, Steinheim, Germany
Tris-buffered saline (TBS)	60.5 g Trizma Base, 1 L $H_2O_{dist,}$ 2N hydrogen chloride, 90 g sodium chloride. Adjust to pH 7.6 solution for use: add 900 mL H_2O_{dist} to 100 mL of this stock solution
Xylene	In-house xylene provided by Department of Pathology, Technical University of Munich
Zytochem plus HRP One-Step polymer anti-mouse/rabbit /rat	#ZUC053-100, Zytomed Systems, Berlin, Germany
Ventana Benchmark® XT	N750-BMKTX-FS, Ventana, Tucson, AZ

3.3 Cells and cell culture

(a) Breast adenocarcinoma cell lines MDA-MB-231, MCF-7, (b) Wild type ovarian cancer epithelial cell line OV-MZ-6-*wt* and its vector counterpart (OV-MZ-6 pRc RSV vector) plus OV-MZ-6-*wt* transfected with a vector overexpressing KLK4 (OV-MZ-6 pRc RSV KLK4), (c) prostate cancer cell line PC-3 which is known as a KLK4–negative cell line and its vector control cell line (PC-3 RSV) and KLK4 overexpressed cell lines (PC-3 pRc RSV KLK4). Among them, MDA-MB-231 as a representative of claudin-low cell lines is ER-,PR- and HER-2 negative, while MCF-7 as a representative of the luminal A cell line subtype is ER-positive[183–184].

Table 6. List of cell lines used in the studies

Cell line	Origin	Source/information
MCF7	Breast adenocarcinoma	ATCC-HTB-22, ATCC
MDA-MB-231	Breast adenocarcinoma	ATCC-HTB-26, ATCC
PC-3 RSV	Prostate cancer	Transfected with empty vector
PC-3 pRc RSV KLK4	Prostate cancer	Transfected with overexpressed KLK4
OV-MZ-6-*wt*	Epithelial ovarian cancer	V. Moebus, Frankfurt, Germany
OV-MZ-6 RSV	Epithelial ovarian cancer	Transfected with empty vector
OV-MZ-6 pRc RSV KLK4	Epithelial ovarian cancer	Transfected with overexpressed KLK4

MCF-7, MDA-MB-231, and OV-MZ-6 cells were cultivated in DMEM while PC-3 cells were maintained in RPMI 1640, both of which were supplemented with 10 % FCS, 0.2 %, arginine/asparagine, and 1 % HEPES. G418 (geneticin) was also used for resistance clone selection in transfected cell lines. All incubation steps are performed in a humidified 37 ℃, 5 % CO2 incubator. After thawing and properly passaging, 70 % confluency of adherent cells was used for in the experiments. Detachment of all was performed by PBS plus 0.05 % EDTA. The Neubauer hemocytometer was used to determine cell number, the percentage of cell viability was checked by the trypan blue exclusion.

Table 7. Contents of culture medium

Substance of content	Amount (ml)
DMEM Glutamax/ PRMI1640 Glutamax	500.0
FCS (10 %)	55.0
HEPES (1 M)	5.5
Arginine (0.55 mM) and asparagine (0.272 mM)	1.0
G418 for transfected cell lines	0.301 g in 10 ml PBS

3.4 Antibody directed to rec-KLK4

Recombinant KLK 4 was produced in-house as described previously[185]. Briefly, KLK4 gene was isolated from cancer cell line, and fusion genes were expressed in transformed *Escherichia coli*, induced with IPTG. Expressed proteins, harboring an N-terminal (His) 6-tag followed by an enterokinase (EK) cleavage site (DDDDK ↓), were purified via its histidine-tag by nickel-nitrilotriacetic acid agarose affinity chromatography under denaturing/slightly reducing conditions and refolded subsequently, using reduced and oxidized glutathione as redox reagents to promote protein renaturation. Recombinant KLK4 was kindly provided by Prof. Dr. Viktor Magdolen, Frauenklinik, Klinikum rechts der Isar, Technische Universität München.

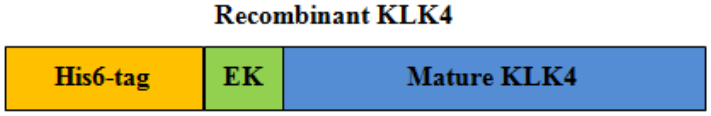

Figure 6. Schematic representation of the major structure of recombinant KLK4

Generation of polyclonal antibody #587 directed to rec-KLK4

The immunization procedure has been described elsewhere[185]. In brief, rabbits were immunized at the Department of Laboratory Medicine of the Radboud University, Nijmegen Medical Centre (Nijmegen, The Netherlands), by injection of purified and refolded recombinant (non-glycosylated) human KLK4 (rec-KLK4), carrying an N-terminal extension of 17 amino acids encompassing a histidine (His) 6-tag and an enterokinase (EK) cleavage site (DDDDK↓). Rabbits were immunized at first to the popliteal lymph glands and followed by subcutaneous injections[186]. In total, 12 booster vaccinations within 5 months after first immunization were administrated. Citrated plasma was generated from collected blood and stored at -20 ℃. Since previous research has shown that although purified polyclonal antibodies pAb 617A and C yield a very similar staining[185], pAb 617A and C are directed against different epitopes of KLK4: Fraction A(pAb 617A) contains monospecific, pAb directed against a surface-exposed loop (linear epitope 109-122) of KLK4, whereas fraction C (pAb 617C) is directed to the rest of the epitopes (rec-KLK4). No further purification was done to obtain different fractions of our antibody in the present study. Antibodies from the rabbits were purified by affinity chromatography through two consecutive procedures: (a) by a "negative" purification step using columns with immobilized peptides covering the N-terminal tag and non-KLK related sequences of the recombinant protein, (b) the effluent of the first column, which was depleted from antibodies directed to the non-KLK related sequences of rec-KLK, was applied to the sec column, coupled with the immunogen. The production of purification, pAb587, was employed in the present study.

"One-side ELISA" assay and western blot analyses demonstrated a very strong and specific reaction with the immunogen (rec-KLK4), and there was no crossreaction with tested other KLK

proteases (rec-KLK2, rec-KLK3, rec-KLK5-15), or other His- and/or EK-tagged proteins due to affinity purification[185].

Table 8. Antibody directed to KLK4 used in this study

Antibody	Source	Species	Immunogen	Purification
***# 587** anti-KLK4*	Prof. Dr. F- Sweep RUNMC (Nijmegen)	Rabbit	rec-KLK4	A: His & EK peptides B: rec KLK 4

4. Techniques and methods

4.1 Cell microarrays (CMA) and cytospins

Cell microarray preparation

Cell microarrays, from two panels of duplicates 31 cell lines and 14 different KLKs-transfected OV-MZ-6 cell lines, were constructed in-house. In brief, adherent cells (3×10^7) were detached and then fixed in 10 % buffered formalin for 30 min at 20 ℃. Subsequently, the cell sediment was solidified through incubation in Tris-HCl (pH 8.0, overnight at 4 ℃), consisting of thrombin (10 U/ml, 150 µL), casein (10 mg/ml, 750 µl), and fibrinogen (25 mg/ml, 600 µl). The fixed cells were immediately embedded in paraffin to form the donor block. Following that, using a manual tissue microarray instrument, three cylindrical tissue cores with a diameter of 1 mm were extracted from the donor block and transfered to a recipient paraffin block according to predefined coordinates. 2 µm-thick sections were cut from the CMA block and mounted onto microscope slides. Deparaffinization and rehydration of these sections were performed prior to permeabilization and immunohistochemical staining[187].

Basic protocol for cell microarray construction

- Detach and count cells, cell number to be adjusted to 3×10^7/ml.

- Fix in 10 % buffered formalin in TBS (30 min, 20 ℃)
- Incubate in a cocktail of Tris-HCl (0.04 M, pH 8.0) overnight at 4 ℃
- Paraffin-embeded to form the donor block
- Construct a recipient paraffin block based on pre-arranged map
- Cut and transfer sections to microscope slides
- Deparaffinize and rehydrate before use

Cytospin preparation

MDA-MB-231, MCF-7, OV-MZ-6-wt, OV-MZ-6 RSV, and OV-MZ-6 pRc RSV KLK4 cells were counted by use of a Neubauer hemocytometer and then adjusted to 300,000 cells/mL in PBS/1 % BSA. Aliquots of 200 µL were loaded into a cytospin sample chamber assembly and cytocentrifuged onto microscope slides for 5 min at 450 rpm. By use of centrifugal force (Shandon cytocentrifuge II), cells were deposited onto a predefined area of that slide. During centrifugation, excess residual fluid was absorbed into the sample chamber filter card.

In order to avoid drying of cells, cell fixation was performed immediately after centrifugation. Cells were fixed in phosphate-buffered PFA. After fixation, slides were washed in TBS and then airdried for 30 min. All slides were transferred into TBS to continue with later immunohistochemical staining[188].

Basic protocol for cytospin construction

- Detach and count cells, cell number to be adjusted to 3 x 10^5/ml
- Load 200 µl of cell suspension into each cuvette
- Cytospin at 450 rpm for 5 min at low speed
- Remove the slides, filter papers, and cuvette
- Proceed immediately with phosphate-buffered PFA fixation

- Wash slides in TBS to neutralize residual reactive aldehyde groups
- Store cytospins at -80 ℃

Permeabilization

Permeabilization with the natural detergent saponin 0.1-0.2 % (w/v) in PBS/1 % BSA for 30 min at RT or with the non-ionic detergent 0.05-0.1 % (w/v) Triton X-100 for 5-15 min at RT was optionaly performed on cell microarray sections and cytospins. Section slides without permeabilization were later compared to the ones exposed to these procedures. Permeablization was performed before immunohistochemistry staining procedures allowing access of antibodies to inner and subcellular organel compartments. Saponin is a relatively mild detergent that dissolves cholesterol in the plasma membrane, thereby big holes are formed in cell membranes allowing penetration of large molecules such as antibodies while internal membranes remain intact within the cytoplasm. By contrast, Triton X-100 efficiently dissolves cellular membranes without disturbing protein-protein interactions, but having a high risk of damaging the cell morphology. Established optimal conditions not only allow insertation of the antibodies into the cells, but also prevent damage of the cell morphological characteristics.

CMA and cytospin immunostaining for KLK4

Standard immunochemical staining protocols were adjusted to suit staining of CMAs and cytospins. OV-MZ6 pRc RSV KLK4 overexpressing cells were used as the positive control, cells with empty vector as the negative one. Omission of the primary antibody serves as a blank control. All slides were subjected to the same antigen retrieval and blocking procedures. Unspecific binding was blocked by PBS/0.1 % BSA for 30 min at RT. Antibody #587 was the primary antibody to visualize KLK4 expression. Different chromogen substrates were applied depending on the way of staining (LSAB or polymer). Before and after the incubation steps, the

sections were rinsed three times with PBS/0.1 % BSA. In the end, sections were sealed with Pertex mount coverslips and scanned with the Hamamatsu NDP-NanoZoomer virtual microscope. Detailed procedures see chapter "Immunochemistry staining (IHC)"

4.2 Flow cytometry experiments (FCs)

MDA-MB-231, MCF-7, and OV-MZ-6 RSV/KLK4 cells were grown to 70 % confluency and then detached with 0.05 % EDTA in PBS. Detached cells were immediately resuspended in cold PBS and then part of it counted in a Neubauer hemocytometer in the presence of Trypan blue to discriminate viable from dead cells. Optionally, cells (1 x 10^6/ml) were fixed with 4 % PFA for one hour at RT and then washed 3 times with TBS or left without fixation. For permeabilization, both viable and PFA-fixed cells were treated with 0.1-0.2 % saponin in PBS for 15-30 min or 0.05-0.1 % Triton-X-100 for 5/10/15 min at RT. Unspecific binding sites were blocked with PBS/ 1 % BSA for 30 min at RT. Primary antibody (pAb 587 to KLK4) was diluted 1:50,1:100,1:200 in PBS/1 % BSA and incubated together with the cells for 40 min at RT. An equivalent concentration of the isotype control antibody (#Z 0259 purified Ig fraction for rabbit antiserum, rabbit anti-mouse IgG, DAKO, Denmark) was tested in parallel. Cells were washed three times with PBS to discard excess antibodies. Secondary antibody conjugated with Alexa-488 (#A-11008 goat anti-rabbit IgG, Invitrogen GmbH, Darmstadt, Germany), (dilution 1:1,000 of the stock solution) was added to the cell and then the suspension incubated in the dark for 30 min at RT to prevent fluorescent conjugate from quenching. Propidium iodide was added for dead cell exclusion. Finally, 25 µl cell suspension was resuspended in 250 µL PBS/ 1 % BSA (1 x 10^5 cells /ml). Fluorescence staining was examined by use of a FACSCalibur flow cytometer. Data analyses were performed by the CellQuest software (Becton Dickinson, San Jos é, CA, USA).

Table 9. FACS staining protocol

Sample	Cell 10^7/ml	PBS/1 % BSA	1st Ab (dilution)	PBS/1 % BSA	2nd Ab (dilution)
Autofluorescence control	25 µl	225 µl	/	250 µl	/
Alexa 488 control	25 µl	225 µl	/	225 µl	25 µl (1:1000)
Dilution 1 (1st Ab/Isotype)	25 µl	223.75 µl	1.25ul (1:200)	225 µl	25 µl (1:1000)
Dilution 2 (1st Ab/Isotype)	25 µl	222.5 µl	2.5ul (1:100)	225 µl	25 µl (1:1000)
Dilution 3 (1st Ab/Isotype)	25 µl	220 µl	5ul (1:50)	225 µl	25 µl (1:1000)

4.3 Confocal laser scanning microscopy (CLSM)

Confocal laser scanning microscope is characterized by its point-by-point and optical sectioning image aquisition. In order to constantly acquire in-focus images, the diameter of pinhole aperture was moderated to obstruct light coming from object points outside the focal plane, acting like a spatial filter for the conjugated image plane. Images were acquired by light detector photomultipliers (PMT) and reconstructed with a computer, achieving interior cell structure image and three-dimensional reconstructions.

KLK4 overexpressing cell lines, OV-MZ-6 pRc RSV/KLK4 and PC-3 pRc RSV/KLK, were chosen to localize KLK4 expression at the subcellular level. OV-MZ-6 pRc RSV and PC-3 pRc RSV cell lines were used as a negative control. Besides these cell lines, MDA-MB-231 and MCF-7 were also tested by CLSM to visualize KLK4 expression in cellular compartments of breast cancer cells.

About 30,000 cells were detached and seeded into each well of a 8-well chamberslide and cultivated overnight (#946140802, non-pyrogenic, Sarstedt, Nümbrecht, Germany). Under the condition cell morphology was confirmed, detached cells (70 % confluency) were fixed with 4 % buffered PFA/PBS for 40 min at room temperature. 0.1 % saponin in PBS/1 % BSA was added for 30 min to allow cell permeablization. Unspecific binding sites were blocked with PBS/1 % BSA for 30 min. Subsequently, primary antibody pAb587 (stock concentration: 350 µg/ mL) was

diluted 1:100 in 1 % BSA/PBS and incubated with cells for 40 min at RT. After three washing steps with 1 % BSA/PBS, Alexa-488 labeled secary antibody (#A-11008; goat anti-rabbit IgG, 1:1000, stock: 2 mg/ mL) was added to wells for 30 min at RT in the dark. Besides that, the cell compartments were stained with different reference probes. The different organelle probes are displayed as different channels in the multicolor images in order to facilitate the annotation of the subcellular distribution. The following probes for diverse organelles were used as references: (a) DAPI (0.2 µg/ml, 10 min, Roche, Mannheim, Germany) or propidium iodide (1 µg/ml, 15 min, Invitrogen, Darmstadt, Germany) were applied for nuclear staining. (b) Phalloidin BODIPY650/665 (0.66 µM, Invitrogen, Eugene, Oregon, USA) as a marker of F-actin filaments to display the cytoplasm. Finally, after the washes, slides were rapidly subjected to confocal laser microscopy (LSM700, Carl Zeiss, Jena, Germany), and images processed by the software ZEN2011. See appendix 11.6.

4.4 Quantitative polymerase chain reaction (qPCR)

RNA extraction. MCF-7, MDA-MB-231, OV-MZ-6-wt, OV-MZ-6 pRc RSV vector/KLK4, PC-3 pRc RSV vector/KLK4 cells (1×10^7) were detached and harvested for mRNA preparation for RT-PCR assays. RNA isolation was performed under RNase-free conditions. Total RNA was isolated using *TRIzol® Reagent* (Invitrogen, Darmstadt, Germany) according to the manufacturer's instructions. Cell pellets were lysed by addition of 1 ml of *TRIzol® Reagent* and homogenized by pipetting the pellet up and down several times. Homogenized samples were incubated for 5 min at room temperature to permit complete dissociation of the nucleoprotein complex. Then 200 µl of chloroform per 1 ml *TRIzol® Reagent* was added to the homogenate and incubated 2-3 min at room temperature after mixing by vigorously shaking for 15 secs and centrifuged at 12,000 × g for 15 min at 4 ℃. The mixture then was separated into a lower red

phenol-chloroform phase, an interphase, and a colorless upper aqueous phase. The aqueous phase of the sample where RNA mainly remains was transferred to a new tube. Subsequently, 500 µl of 100 % isopropanol was added to the aqueous phase. Samples were incubated at room temperature for 10 min after vortexing at moderate speed for 5-10 sec and centrifuged at 12,000 ×g for 8 min at 4 ℃. The supernatant was discarded. As the next step, 1 ml of 75 % ethanol was added to wash the RNA pellet which was vortexed and then centrifuged at 12 000 ×g for 5 min at 4 ℃. Finally, RNA countering pellets were vacuum or air dried for 5–10 min. 30–50 µL RNase-free water was added to resuspend the RNA countering pellet. The quality and concentration of RNA was determined by measuring the A260/A280 nm quotient in a Nanodrop device (Thermo Scientific, Erlangen, Germany).

Reverse transcription. Approximately 1 µg of each RNA sample was reversely transcribed into complementary DNA using the AffinityScript QPCR cDNA Synthesis Kit (Invitrogen, Darmstadt, Germany), which is characterized by high efficiency conversion of RNA to cDNA. cDNA Synthesis Master Mix contains an optimized buffer for subsequent Q-PCR. Oligo (dT) and random primers allowed to use the best priming strategy for our target. Reverse transcriptase was provided, in combination with RNase block enzyme, to verify the absence of nuclease contaminants that may affect the cDNA synthesis. In our experiment, no-RT control for each RNA sample by omitting RT was performed which is expected to generate no signal in Q-PCR.

Table 10. Prepare the cDNA synthesis reaction in a microcentrifuge tube

Components	Per vial (20 ul)
Master mix	10 µl
Oligo (dT) primer	2 µl
Random primer	1 µl
Reverse transcriptase/RNase block enzyme	1 µl
RNA sample	0.3 pg~3 µg
RNase-free water	Adjust to a volume of 20 µl

Reverse transcription was performed in a total volume of 20 µL by the following procedure: the reaction mixture were incubated for 5 min at 25 ℃ to anneal primer, then samples were transferred into 95 ℃ for 5 min after heating at 42 ℃ for 45 min. For long-term storage, the PCR product was rapidly cooled down to 4 ℃. The cDNA was diluted 1:20 and stored at -20 ℃

RT-PCR-based amplification of DNA. RT-PCR was performed on the Mx3005P quantitative PCR instrument by using the Brilliant II QPCR Master Mix kit with High ROX (#600805-12, Agilent Technologies, Böblingen, Germany). Fluorescence from ROX dye does not change during the course of the PCR reaction but provides a stable baseline to which samples are normalized. The primers to detect the KLK4 gene were provided by Applied Biosystems (Darmstadt, Germany) and were TaqMan® Gene Expression Assay (HS00191772). Housekeeping gene hypoxanthine guanine phosphoribosyl transferase 1 (*HPRT1*-FAM, Hs01003267) were measured in the same cell samples. For each sample, KLK4 and the reference gene were run in triplicate. Negative controls with nuclease-free water and no-RT omitting RT were also performed on each plate.

Table 11. Total volume of each RT reaction 20 ul

Components	1x Master Mix for per well
Brilliant II QPCR Master mix	10 µl
Assay on demand primer	1 µl
cDNA	3 µl
RNase-free water	Adjust to a volume of 20 µl

The thermal cycle profile was started with pre-denaturation at 50 ℃ for 2 min, followed by 40 cycles of amplification with a 10 min denaturing cycle at 95 ℃, then followed by 15 sec of annealing and extension at 60 ℃ for 1 min, finally 5 min more for elongation was applied followed by a cooling procedure at 4 ℃.

Table 12. Amplification cycles

	Step	Duration	Temperature
	Initial denaturation	2 min	50.0 ℃
40 cycles	Denaturation	10 min	95.0 ℃
	Annealing	15 sec	95.0 ℃
	Elongation	1 min	60.0 ℃
	Final elongation	5 min	60.0 ℃
	Cooling down	infinite	4.0 ℃

Further calculations and statistical analyses were carried out using the Relative Quantitation (ΔΔCt) method[189]. Ct is defined as the cycle at which fluorescence is determined to be statistically significant above background. Calculations are based on the comparison of the distinct cycle determined by threshold values (Ct) at a constant level of fluorescence (difference between threshold values, **ΔCt**): $\mathbf{R = 2^{-[\Delta Ct\ sample\ -\ \Delta Ct\ control]} = 2^{-\Delta\Delta Ct}}$. Difference between cell lines is symbolized by the difference in their multiplication threshold values (**ΔΔCt**).

4.5 Western blotting (WB)

Sample preparation

Cell extracts (60 µg/lane), culture supernatants (30 µg/lane), cell fractions (30 µg/lane) as well as recombinant proteins (0.3-3µ/lane) were prepared prior to use.

Cell extracts. A modified RIPA buffer was used for cell extracts which will disrupt protein-protein interactions and may therefore be well suited for immunoprecipitation assays. Protease Inhibitor Cocktail tablets cOmplete (Roche, Mannheim, Germany) were added for inhibition of proteolytic action in the extraction solution, inhibiting a broad spectrum of serine and cysteine proteases. Since certain antibodies only recognize a protein in its native/non-denatured form, buffer without ionic (e.g. SDS, deoxycholate) and without non-ionic detergents (e.g. Triton X-100) were used under so called non-denaturing conditions.

Table 13. RIPA (Radio Immuno Precipitation Assay) lysis buffer for 5ml

Components (stock)	Work solution	5 ml
Triton X-100	1/100	50 µl
Sodium deoxycholate (5 %)	1/200	500 µl
Sodium chloride (5 M NaCl)	150 mM	150 µl
Sodium dodecyl sulphate (10 % SDS)	1/1000	50 µl
Tris-HCl pH 8.0 (1M)	50 mM	250 µl
Protease Inhibitor Cocktail /complete+EDTA (25x)	1/25	200 µl
Distilled water	/	3.8 ml

All lysis steps were performed on ice: ice-cold lysis buffer was added to dish-cultured cells (1 ml/per 10^7 cells) which were pre-washed with ice-cold PBS twice. The cells were then scraped off the dish using a cold plastic cell scraper. After sonication, 3 pulses for 10 sec at 35-40 % power, and centrifuge (30 min, 100,000g), the supernatant was transfered into a pre-cooled polypropylene tube and stored at -80 ℃ for further use.

Culture medium. Adherent cells were hungered for 24 h after 70 % confluency having reached. 10 ml of culture medium without serum or addictives was transfered into a new microfuge tube and immediately mixed with 400 µl protease inhibitor solution (stock: one tablet cOmplete, EDTA-free in 2 ml distilled water). The mixture was then transferred to a standard dialysis system, Spectra/Por®Molecularporous Regenerated cellulose dialysis (Carl Roth, Karsruhe, Germany), characterized by its "Molecular Weight Cut Off" (MWCO) which is defined by the molecular weight of the solution. The dialysis membrane with MWCO (4,000~6,000 Da) was chosen to remove salts and ions while most of the KLK4 (25~35 kDa) is retained. Tris-HCl buffer (5 mM, pH 8.0) was employed the dialysis buffer, with at least 100 times the sample volume (e.g. dialyze 10 ml of medium in 1 liter of dialysate). The whole dialysis procedure was performed in the dialysate overnight at 4 ℃ with a magnetic stir. Subsequently, 10 ml dialyzed medium was condensed to 1 ml by the use of the Speed-Vac system (Thermo Fisher Scientific).

Cell fractions. Adherent PC-3 pRc RSV KLK4 cells were extracted following the detailed instructions in the ProteoExtract® Subcellular Proteome Extraction Kit (S-PEK, Merck,

Darmstadt, Germany), which is designed for fast and reproducible extraction of subcellular proteins from adherent cells[190]. The S-PEK takes advantage of different solubilities of certain subcellular compartments in four selected reagents. The procedure is performed in the tissue culture dish without the need for cell removal. Cells or parts of the cells remain attached to the plate during sequential extraction of subcellular compartments, until the four appropriate extraction reagents are used. Thus, early destruction of the cellular structure by enzymatic or mechanical detachment of cells from the tissue culture plate and any mixing of different subcellular compartments is prevented.

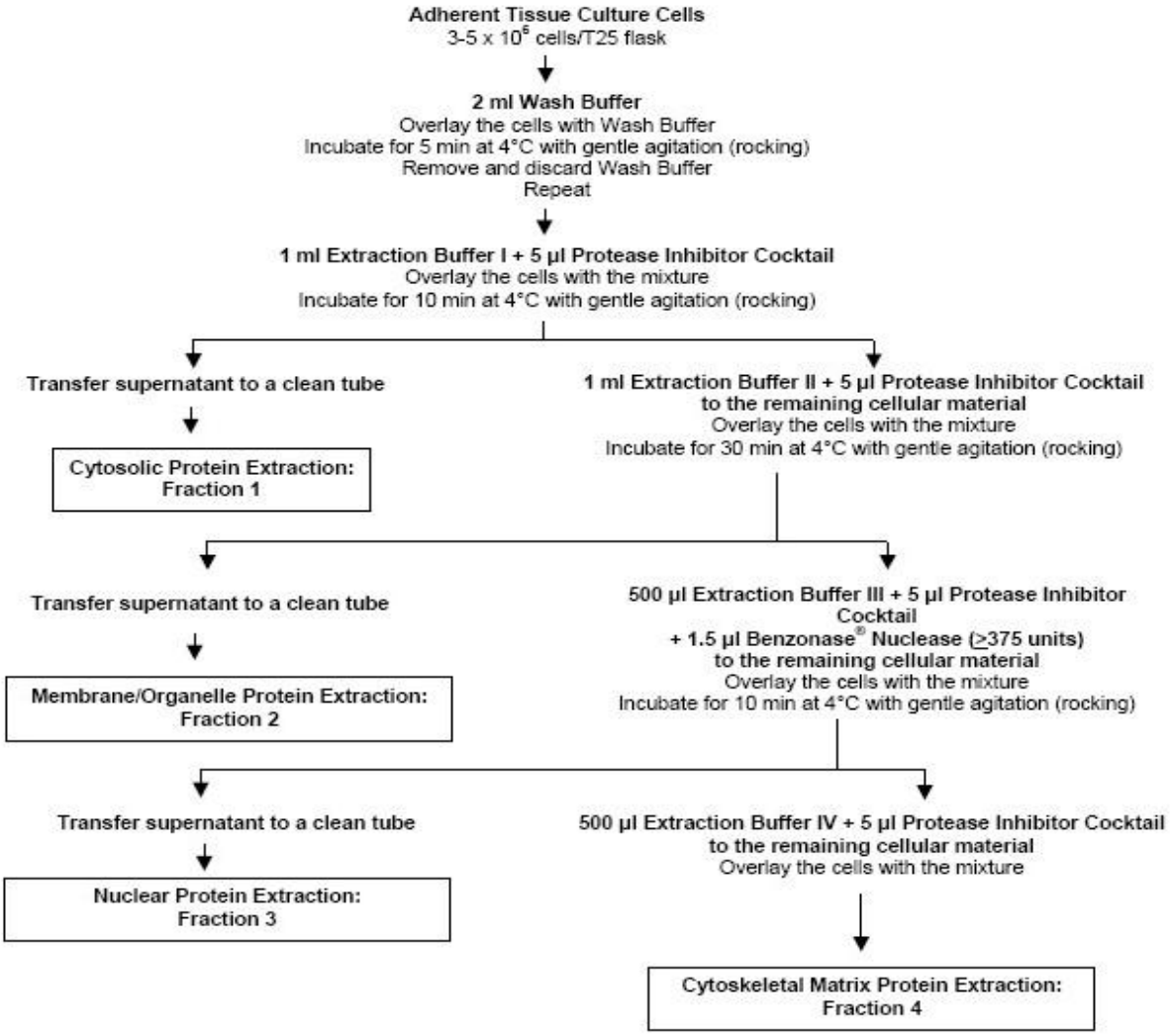

Figure 7. Schematic workflow for adherent tissue culture cells (user protocol of S-PEK)

Protein assay (quantification of protein concentration)

Proteins from cell fractions, whole extracts and culture medium was determined by use of the BCA protein assay test (BiCinchoninic Acid) kit manufactured by Pierce (#23221, Pierce, Rockford, IL, USA). This method relies on the formation of a Cu^{2+}-protein complex under alkaline conditions, followed by the reduction of Cu^{2+} to Cu^{+} (the biuret reaction). The amount of reduction is proportional to the amount of protein present. The highly sensitive and selective colorimetric detection of the cuprous cation (Cu^{+}) is performed using the BCA reagent (chelation of two molecules of BCA with one cuprous ion forms a purple-colored reaction product). The BCA assay is more sensitive and applicable than the Biuret or the Lowry procedures. Also it has less variability than the Bradford assay. After incubation for either 1 h at 37 ℃ or overnight at RT, absorbance of the produced colored complexes was determined at 562 nm using an ELISA reader (SLT Spectra, SLT Instruments, Germany). Protein concentrations were determined based on the standard concentrations curve of the reference protein (bovine serum albumin).

Table 14. Sheet for Protein Assay (96-well plate)

	1	**2**	**3**	**4**	**5**	**6**	**7**	**8**	**9**	**10**	**11**	**12**
A	A+B	Std3	Std7	K2	A4	B3	C2	D1	D5	E4		
B	A+B	Std3	Std7	K2	A4	B3	C2	D1	D5	E4		
C	Tbst	Std4	Std8	A1	A5	B4	C3	D2	E1	E5		
D	Tbst	Std4	Std8	A1	A5	B4	C3	D2	E1	E5		
E	Std1	Std5	Std9	A2	B1	B5	C4	D3	E2			
F	Std1	Std5	Std9	A2	B1	B5	C4	D3	E2			
G	Std2	Std6	K1	A3	B2	C1	C5	D4	E3			
H	Std2	Std6	K1	A3	B2	C1	C5	D4	E3			

Legend: All samples are duplicated (50 µl/well). **A+B (control)**: solution A +solution B from BCA kit (50:1);

Tbst: TBS+0.1 % Triton X-100+0.05 % Tween-20; **K1**:995 µl TBST+5 µl standards; **K2**:800 ul TBST+200 µl K1;

Std1: 10 µl BSA+490 µl TBST; **Std2**: 20 µl BSA+480 µl TBST; **Std3**: 30 µl BSA+470 µl TBST; **Std4**: 40 µl BSA+460 µl TBST; **Std5**: 50 µl BSA+450 µl TBST; **Std6**: 80 µl BSA+420 µl TBST; **Std7**: 120 ul BSA+380 µl TBST; **Std8**: 160 µl BSA+340 µl TBST**; Std9**: 200 µl BSA+300 µl TBST; **A**: MDA-MB-231 fractions, **B**: MCF-7 fractions, **C**: OV-MZ-6wt fractions, **D**: PC-3RSv fractions, **E:** PC-3 pRv KLK4 fractions**; Samples** 1:cytoplasm; 2: nucleus; 3: cytoskeleton; 4: culture medium; 5: whole cell lysate

Western blotting and immunodetection

SDS-PAGE samples are denatured by using a loading buffer containing the anionic denaturing detergent sodium dodecyl sulfate (SDS) and heating of the mixture at 95 ℃ for 5 min, +/- β-mercaptoethanol.

Table 15. Sample buffer (5 x Laemmli) for cell migration

Components	**20 ml**
1.5 M Tris-HCl, pH 6.8	4 ml
Glycerol (10 % (v/v))	10 ml
SDS (sodium dodecyl sulfate) 10 % (w/v)	2 g
1 % bromophenol blue	1 ml
β-mercaptoethanol (25 % (v/v))	5 ml

In the 5 x Laemmli buffer, SDS confers a negative charge to the polypeptides in proportion to their lengths, therefore, separation of polypeptides is determined by molecular weight but not by their electrical charge. Glycerol is added to increase the density of the sample to be easily loaded on the top of the stacking gel. Bromophenol blue is a small and anionic dye, which enables the visual control of molecular migration. β-mercaptoethanol is used to reduce disulphide bridges in proteins, allowing molecules to adopt an extended monomeric form. Non-reducing condition means migration buffer β-mercaptoethanol.

The 45 µl samples are immediately loaded into the slots of the stacking gel and separated by 12 % SDS-polyacrylamide gel electrophoresis at 100 V for 1 h. For assessment of the relative molecular mass of the separated proteins, a PageRuler Prestained Protein Ladder ranging from 11 to 170 kDa (# 26616, Fisher Thermo Scientific, Schwerte, Germany) was used.

Table 16. Separating, stacking, and electrophoresis buffer

Separating gels (1x 1.5 mm gel)		**Stacking gels**(1x 1.5 mm gel)		**Running buffer**	
Distilled water	4.2 ml	Distilled water	3.15 ml	Distilled water	to 1L
1.5 M Tris pH 8.8	2.5 ml	0.5 M Tris pH 6.8	1.25 ml	25 mM Tris base	3 g

10 % SDS	100 ul	10 % SDS	50 µl	10 % SDS	10 ml
40 % acrylamide	3.8 ml	40 % acrylamide	500 µl	1.44 % glycine	14.4 g
10 % APS 15 µl+TEMED 1.5 µl		10 % APS 25 ul+TEMED 5 µl		/	

Proteins, separated by SDS-PAGE, were transferred onto a polyvinylidene fluoride membrane (PVDF, PALL, Dreieich, Germany; 2 h at 75 mA/membrane), applying a sandwich semi-dry transfer apparatus (Whatman Biometra, Göttingen, Germany). The sandwich system refers to a system in which filter paper-gel-membrane-filter paper is saturated with buffer and is placed between the dry anode and cathode plates. After transfer, the membrane is pre-stained with 0.1 % Ponceau S (Sigma-Aldrich, St. Louis, MO, USA) to visualize and check the protein bands in the membrane, which is reversible to allow further immunological detection.

Table 17. Semi-dry buffer for blotting and prestaining buffer (Ponceau S)

Semi-dry buffer		**Prestaining buffer**	
Distilled water	800 ml	Distilled water	to 500 ml
50 mM Tris base	5.82 g	1 % acetic acid	5 ml
30 mM glycine	2.93 g	Ponceau S	0.5 g
0.4 % SDS	0.037 g		
add ethanol to 1L			

Subsequently, the membranes were blocked with 5 % skimmed milk powder (#70166, Fluka; Munich, Germany) or 5 % Ig-free BSA (fraction V, #A-3912, Sigma, Munich, Germany) in TBST buffer (pH 7.4, 60.5 g Trizma base, 90 g NaCl in 1 L H_2O_{dist}) for 1 h at room temprature or overnight at 4 °C. Subsequently, blots were incubated 2 h at room temprature with antibodies to GAPDH (mouse anti-GAPDH, 1:1000, #MAB374, Chemicon, Billerica, MA, USA), histone (rabbit anti-histone H3 antibody, 1:500, #441190G, Invitrogen, Camarillo, CA, USA), cytokeratin (mouse anti-cytokeratin (CAM5.2), 1:500, #349205, BD biosciences, San Jose, CA, USA) or KLK4 protein (pAb587, 1:1,000), diluted in blocking buffer, and then washed three

times (5 min ×3, RT) with changed TBST. Antigen-antibody complexes were visualized using the appropriate secary antibodies, such as goat-anti-rabbit-IgG-HRP (Jackson ImmunoResearch; #111-035-003, Dianova, Hamburg, Germany), or goat-anti-mouse-IgG-HRP (Dianova; #315-035-045, Hamburg, Germany), diluted 1:10,000 in blocking buffer for 1h at room temperature, followed by chemiluminescent reaction (ECL, Amersham Biosciences, Little Chalfont, UK). In order to confirm that the cell lysate was prepared appropriately, and no contamination between the respective cell fractions occured, the same blots were incubated with the following control antibodies (Table 18), after stripping the membranes with Bernatz buffer (1 % Tween-20, 1.5 % w/v glycine, 0.1 % w/v SDS; pH 2.2, 15 min, RT).

Table 18. Loading controls and cellular fractionation markers and stripping buffer used in the study

Target(kDa)	Antibodies	Dilution	Target
GAPDH (30-40)	Mouse anti-GAPDH (#MAB374, Chemicon)	1:1,000	Cytoplasm
Histone H3 (17)	Rabbit anti-Histone H3 (#441190G, Invitrogen)	1:500	Nucleus
Cytokeratin7/8 (48/52)	Mouse anti-cytokeratin (CAM 5.2) (#349205, BD)	1:500	Cytoskeleton

4.6 Immunohistochemistry (IHC)

Tissue microarrays (TMA). Tissue microarray were constructed from formalin-fixed tissues using previously established and validated techniques[191, 192]. For each TMA, hematoxylin and eosin staining (H&E) were performed by pathologists to identify tumor cell areas. Three different tissue cores biopsies (∅ 1 mm) were removed from selected areas of the donor block and positioned into empty cylindrical holes of the recipient block with the help of a MicroArrayer instrument (Alpha Metrix GmbH, Rödermark, Germany). Core biopsies of normal kidney, lung, and placenta tissue were used as reference tissues. Each sample spot can be precisely tracked according to the coordinate positions in the tissue microarray. For

immunostaining, 3 μm thick sections were cut from the tissue microarray blocks and transferred to electro-charged glass slides.

TMAs provide a high degree of standardization as all tissues are analyzed simultaneously with the same reagents and under the same conditions[193]. In our study, nine breast cancer TMAs were constructed for immunohistochemical staining, among which 257 human breast cancer tissue of the TNBC type were assembled based on a pre-arranged map, in order to evaluate the expression pattern of KLK4 in triple-negative breast cancers.

Full-face formalin-fixed paraffin-embedded tissue specimens. Tissue specimens from normal prostate, benign prostatic hyperplasia (BPH), and prostate cancer were routinely formalin-fixed and paraffin-embedded in the Institute of Pathology of the Technical University of Munich according to the in-house protocol[194]: The respective tissue specimens were examined and sectioned by pathologists, then fixed for 8 h in 3.7 % buffered formalin and dehydrated by passing them through the ascending row of alcohols using an automatic tissue processor: 70 % ethanol for one hour once, 96 % ethanol once for 45 min and once for one hour, isopropanol twice for one hour and once for 45 min, and finally xylene twice for one hour. Then, the samples were embedded in paraffin at 60 ℃ (twice for 15 min, once for 30 min and once for one hour). The 3 μm-thick sections were cut from paraffin blocks using a microtome and floated on a 38 ℃ warm distilled water bath. The tissue sections were transferred onto glass slides, and dried overnight at room temperature.

Immunohistochemistry (IHC) staining. Hematoxylin-eosin staining (HE-stain) for all tissue specimens is routinely performed by pathologists for histopathological examination. KLK4 immnohistochemical staining is performed on all tissue specimens, including TMAs and full-face tissue sections. For each staining procedure, negative control is required to be tested by

pure antibody diluent omitting primary antibody while prostate cancer tissue samples are used as positive control tissues.

Antigen retrieval. Antigen retrieval technique according to the HIER protocol (Heat-Induced Epitope Retrieval) was performed to reveal masked epitopes in paraffin sections. By that, formaldehyde-induced conformational changes of the target proteins were reduced by this heating procedure. Briefly, tissue sections cut from TMAs were placed in a plastic rack and then transferred to a household pressure cooker, filled to one-third with 10 mM citrate buffer, pH 6.0. The pressure cooker was brought to boiling point on a hot plate (4 min), cooled down (5 min) under running tap water, and then the slides washed twice in TBS[195].

Staining. Deparaffinization of the TMA sections was performed by passing FFPE tissue sections through xylene twice for 10 min at RT. Rehydration of the sections was achieved by passing them through a descending row of graded alcohols (100 % isopropanol twice, 96 % ethanol once followed by 70 % ethanol, for 5 min each). Finally, all slides were transferred into TBS with intervening buffer changes.

Streptavidin-biotin technology - LSAB method. The labeled streptavidin-biotin method (LSAB) is based on the strong affinity of avidin for the vitamin biotin. According to the LSAB kit manual, the following steps have to be observed: At first, endogenous peroxidase activity is to be quenched by incubating the sections with 3 % H_2O_2 (Merck, Darmstadt, Germany) for 20 min at RT in a humid staining chamber. Slides were rinsed with tap water for 5 min and then transferred into TBS for 5 min with intervening buffer changes. Afterwards, the endogenous avidin and biotin blocking solution was sequentially applied for 15 min at room temperature, with a 5 min washing step in between. After another washing step, the primary antibody diluted in antibody diluent (#S2022, Dako, Glostrup, Denmark) was applied to slides by using a pipette

and sections incubated for 2 h at RT or overnight at 4 ℃. Then, sections are washed with TBS with an intervening buffer change. Biotinylated antibody solution A and the HRP-labeled streptavidin complex solution B (#K5003, Dako, Glostrup, Denmark) were applied next to each section and incubated for 30 min each at room temperature, followed by a 5-min washing step with intervening buffer change. The chromogen substrate, 3,3 ´- diaminobenzidine (DAB) is then applied for 8 min at room temperature. After the final washing step, sections are counterstained with hematoxylin for 50 sec, then rinsed under running tap water shortly, and transferred into distilled water for 1 min. Finally, dehydration was performed by passing the slides through an ascending row of graded alcohols (70 % ethanol, 96 % ethanol, 100 % isopropanol twice and xylene twice, each for 5 min) and then the slides were immediately mounted with permanent Pertex mounting medium (PER3000, Medite, Burgdorf, Germany). For detailed procedures see " ***SOPs of KLK4 IHC/ICC staining with pAb587 using DAKO LSAB/DAB kit*** ".

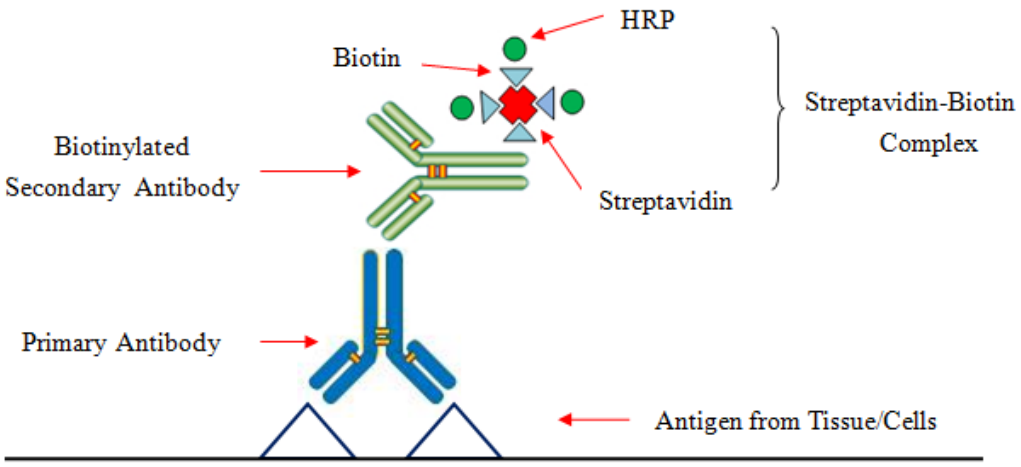

Figure 8. LSAB method. Streptavidin-biotin enzyme complex results in HRP-binding multiplier and signal amplification

Enzyme chain polymer-conjugated technology–Zytomed HRP One-Step Polymer system

Polymer-based immunohistochemical methods utilize a unique technology based on a polymer backbone to which multiple antibodies and enzyme molecules are conjugated. Endogenous peroxidase activity was blocked by pre-incubating the tissue sections with 3 % H_2O_2 (45 mL H_2Odist, 5 mL 30 % H_2O_2) for 20 min at RT, subsequent to a washing step in TBS for 5 min with an intervening buffer change. The primary antibody is then diluted in antibody diluent (#ZUC025-500, Zytomed Systems, Berlin, Germany) and applied to the sections for 2 h at RT or overnight at 4 ℃. After a 5 min washing step in TBS at RT including buffer change, a Zytomed plus One-Step polymer conjugated with horseradish peroxidase (HRP) was applied to the sections for 30 min. After an additional washing step, the DAB high substrate buffer and liquid DAB chromogen (#DAB 5000 plus, Zytomed Systems, Berlin, Germany) were mixed and applied to sections for 8 min at RT, which forms a dark brown product at the site of the enzyme reaction. The sections were counterstained with haematoxylin for 50 s, rinsed under tap water for 3 min, and then transferred to distilled water. Finally, the slides were passed through an ascending row of graded alcohols (70 % ethanol, 96 % ethanol, 100 % isopropanol twice and xylene twice, 5 min each) and mounted with Pertex mounting medium (PER3000, Medite, Burgdorf, Germany). Detailed procedures see "***SOPs of KLK4 IHC/ICC staining with pAb587 using Zytomed HRP one-step Polymer***".

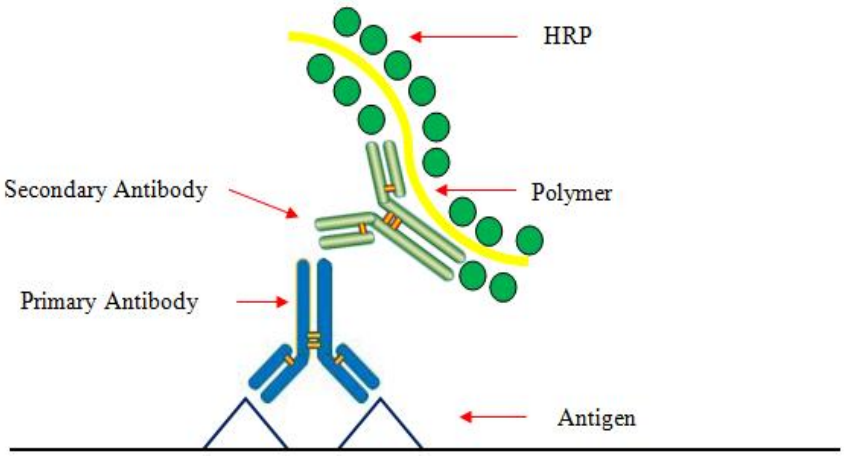

Figure 9. Zytomed HRP One-Step Polymer system. A dextran polymer chain attached with multiple HRP molecules achieves a greater signal and avoid unspecific binding

Automatic staining –Ventana Benchmark®XT system

In our study, automatic staining was applied using the Ventana Benchmark® XT system, which is a fully automated system and allows multiple IHC staining with various procedures including different pre-treatments, different primary antibodies, and different concentrations of them in one run. Therefore, different variables, including incubation time or temperature, can be compared simultaneously to establish optimal staining conditions. This method improves staining consistency and avoids or eliminates potential staining artifacts and mistakes compared with manual or semi-automated staining procedures. The automatic-stained slides should be assessed within two days of staining, but can be stored for up to two years at room temperature. For specific procedures see "***SOPs of KLK4 automatic staining using Ventana system ultraView®"***

The Ventana Benchmark® XT system is routinely used for immunohistochemical staining at the Department of Pathology of the Helmholtz Zentrum Munich. Its several modules, including air vortex mixers, liquid coverslip, slide heater pad, and the barcode system, present as a "closed" system, in which the variables for a specific staining protocol should not be modified, except for the primary antibody.

Yet, manual immunohistochemical SOPs cannot be directly translated to Ventana SOPs. Similar to manual staining SOPs, both LSAB and Polymer methods can be used with the Ventana system, called Ventana iVIEW® and ultraVIEW®. In our case, since the manual polymer staining system gave a crisp image compared with the LSAB method, the Ventana ultraVIEW® system was chosen to optimize the final automatical staining procedure. All tissue/cell specimens

assessd by the manual staining method, were re-tested, optimized, and eventually stained with the Ventana Benchmark® XT system, ensuring that all stainings were simultaneously performed under identical staining conditions.

4.7 Digitization of histological images and quantification of immunostaining

Slide scanning. All stained tissue specimens, including TMAs and full-face tissue sections, were scanned at high resolution and stored as high-definition and quality digital images, employing the Hamamatsu Nanozoomer HAT slide scanner which is based on line-scanning technology (#40885, NanoZoomer Virtual Microscopy, Hamamatsu Photonics, Hamamatsu, Japan).

Automatic scoring by image analysis. For quantification of immunostaining, scanned slides were first subjected to an automatic recognition image analysis system, the Definiens Developer XD 2.0 (Department of Pathology, Helmholtz Zentrum, München, Germany). This image process software is based on an object-oriented image analysis engine and characterized by improved classification and an enhanced segmentation process. Initially, regions of interests representing tumor cells or stromal cells, were identified by a pathologist. Further segmentation and classification were automatically performed via the established object-based software. Tumor cells and tumor stroma cells in each specimen were scored independently. Artifacts, including aberrant staining and air bubbles, were re-examined and excluded subsequently. Average staining intensity and percentage of immunostained areas were finally caculated based on the cellular analysis. In the end, multiplication of these two scores were denominated as the automatic tumor score (aTS) or automatic stromal score (aSS) for latter statistical analysis.

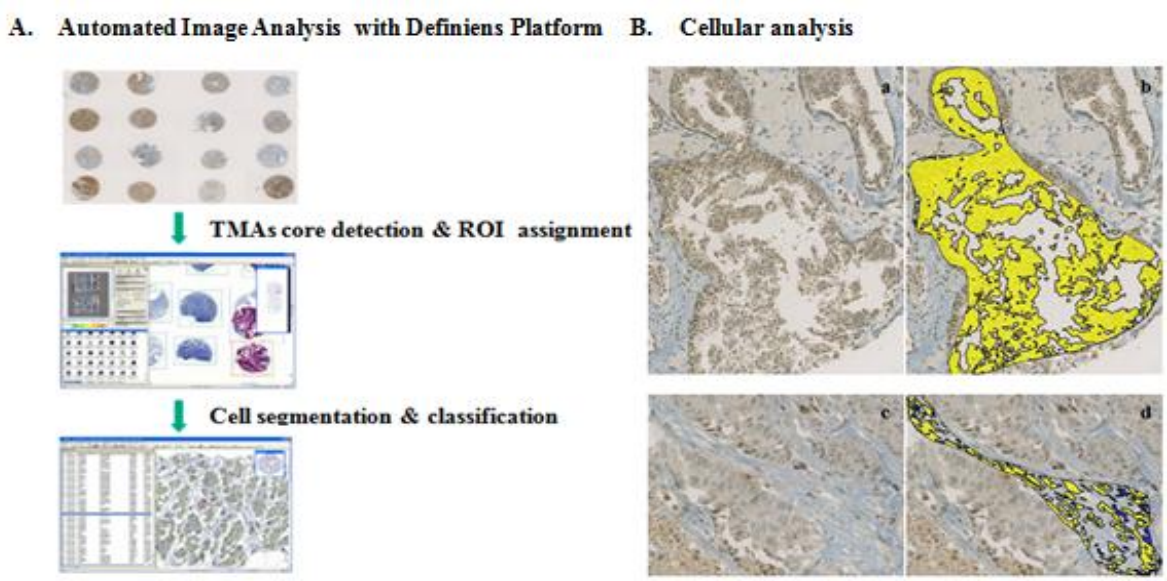

Figure 10. **(A)** Procedure of automated image analysis with Definiens Developer XD software. **(B)** Annotated images results: (a) original tumor cell image stained with brown color substracte (DAB+); (b) region of interest of tumor cell image enhanced with yellow color; (c) original stromal cell image; (d) region of interest of stromal cell image. Magnification x 200.

Manual immunostaining evaluation. For estimation of immunoreactivity, staining pattern and intensity was routinely evaluated by pathologists based on a semiquantitative immunoreactive score method (IRS, Remmele score). Staining intensity (0-3 scale) and percentage of stained cells (0-4 scale) of the relevant area were scored separetely for tumor cells, stromal cells, and the extracellular matrix. Staining intensity was classified on a scale of 0 to 3 (0 - no; 1 - weak; 2 - moderate; 3 - strong). Percentage of cells of the relevant area was scored by fraction (%) of positive cells in the relative areas with a scale of 1 (< 10 %), 2 (11~50 %), 3 (51~80 %), and 4 (> 80 %). Immunoreactivity scores (IRS) for tumor cells and stromal cells were obtained by multiplication of the intensity score values with positivity score values and then denominated as the manual-tumor-score (mTS) and manual-stroma-score (mSS), respectively. In addition, manual evaluation was applied for lymphocyte-score (mLS) and necrosis-score (mNS), independently.

Table 19. KLK4 immunoscores based on Remmele score

Intensity		Percentage		IRS	
	Score	**%**	**Score**		**Score**
no	0	≤ 10	1	negative	0-2
weak	1	11-50	2	weakly positive	3-4
moderate	2	51-80	3	moderately positive	6-8
strong	3	> 80	4	strongly positive	9-12

4.8 Statistical analyses

Statistical analyses were performed using the SPSS software (IBM SPSS StatisticsVersion 20, Armonk, NY). All statistical analyses were two-sided, and a p-value ≤ 0.05 was defined as statistically significant. Relationships of score values from manual and automatic evaluation systems were assessed by Spearman rank correlation coefficient (rho) and regarded as strong when R ≥ 0.5. Missing values were excluded pairwise; associations between hK4 protein expression status and clinical or pathological variables of triple-negative breast cancer patients were determined using Pearson Chi-square (χ^2) or Fisher's exact tests when expected count less than 5; Outcome variables are time to tumor progression (TTP) and overall survival (OS) time to tumor progression (TTP) is defined as the time elapsed between treatment initiation and tumor progression or death from tumor, OS is defined as the period between date of primary surgery and date of death. For survival analyses, OS and TTP of patients were used as long-term follow-up end points, respectively. The impact of different histopathological and clinical factors as well as hK4 protein status on OS and TTP were analyzed by univariate and multivariate Cox regression models. The multivariate Cox's regression model was adjusted for known clinical prognostic factors of the breast cancer patients: patient age, tumor size, nodal status, lymphatic invasion, nuclear grade, histological subtypes, and analyzed using forward selection. The resulting hazard ratio, its 95 % confidence interval (95 % CI) and the p-value reflect their

respective statistical significance. Survival curves were generated according to Kaplan-Meier reference and significance was assessed based on log-rank test.

5. Results

5.1 Cell microarrays (CMAs) for KLK4 assessment

In the very initial stage, two cell microarrays comprising fourteen transfected OV-MZ-6 cell lines and 31 different tumor cell lines, were constructed and available for immunoctyochemistry staining, in order to investigate the performance of antibody pAb 587 used in the present work to detect KLK4 protein exression. Additionally, our goal was to use cell lines as tumor cell models to evaluate KLK4 expression and localization in a single cell. Since cells in the constructed CMAs were simultaneously stained under similar conditions, relative quantitative immuoreaction intensities can be compared.

Antibody pAb587 showed higher staining intensity with KLK4 transfected OV-MZ-6 cells than other ones, implicating that it recognizes the correct epitopes.

Basically, the majority of staining concentrated in the cell but staining spot occured around the cell as well (see appendix Table 11.3 and 11.4). pAb587 obviously confirms its reliability by significant positive staining in the KLK4 overexpressing OV-MZ-6 cell line. It did not show any cross reaction with other cell lines.

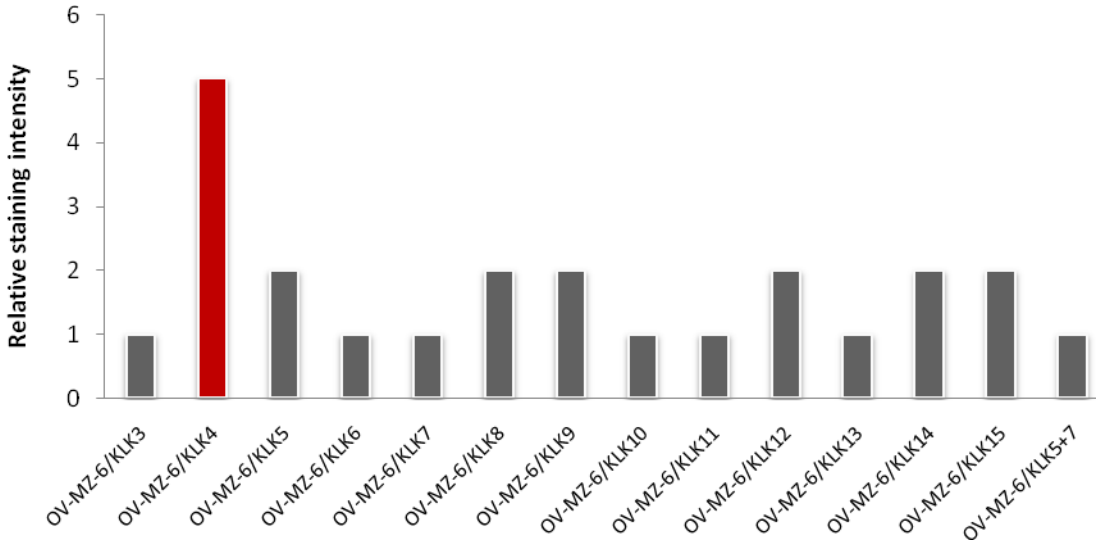

Figure 11. Relative KLK4 staining intensity by pAb587 in OV-MZ-6 cells transfected with different KLKs

Anther cell microarray, including 31 tumor cell lines and normal blood cells, was also examined for KLK4 expression using antibody pAb587. Results showed positivity for KLK4 overexpressing OV-MZ-6 cells. Besides that, LnCAP cells, as well as lymphocytes and trophoblasts were also recognized by strong (LnCAP) and moderate (lymphocytes and trophoblasts) reaction signal with the KLK4 antibody, which is consistent with a previous report[175]. However, breast cancer cell lines of interest, MDA-MB-231 and MCF-7, both did no show reaction with antibody pAb587. Another breast cancer cell line T47D express KLK4 as previously reported while it unfortunately was not incorporated in our CMAs[180].

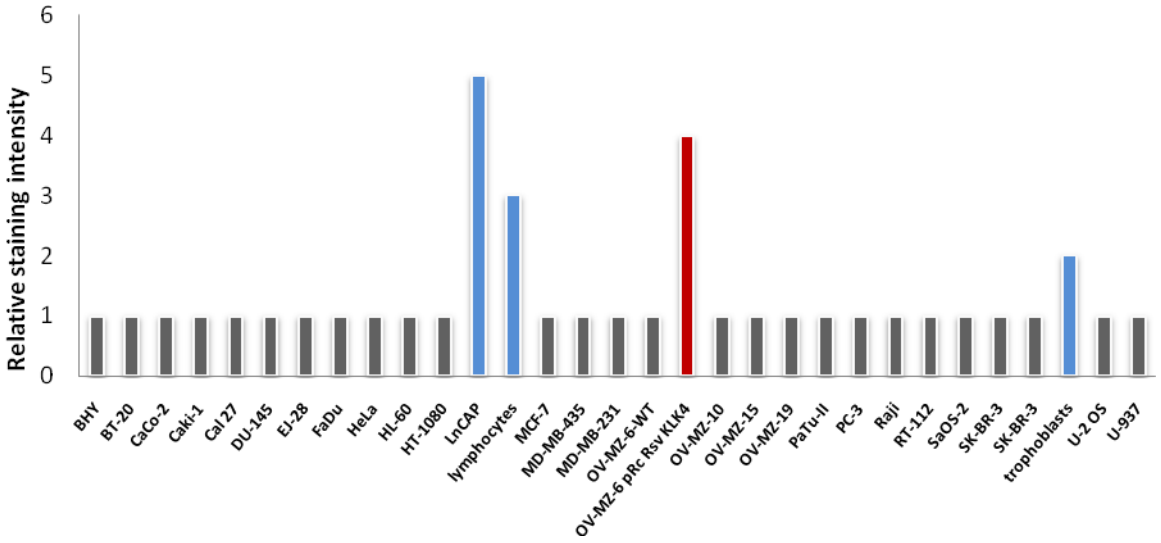

Figure 12. Relative KLK4 staining intensity by pAb587 in different tumor cells and blood cells

5.2 Cytospins for KLK4 assessment

In order to simulate tumor cells presenting tissue specimens, cytospins were prepared and subjected to immunocytochemistry staining before using valuable patient FFPE tissue sections. Optimized immunocytochemical protocol was the pilot test format and later applied for tissue section staining to investigate KLK4 expression and localization at the celluar and subcellular level. Compared with CMAs, cytospins provided us a monolayer of cells where cell morphology and structure is more distinct, also background staining casued by clotting reagents is avoided[196].

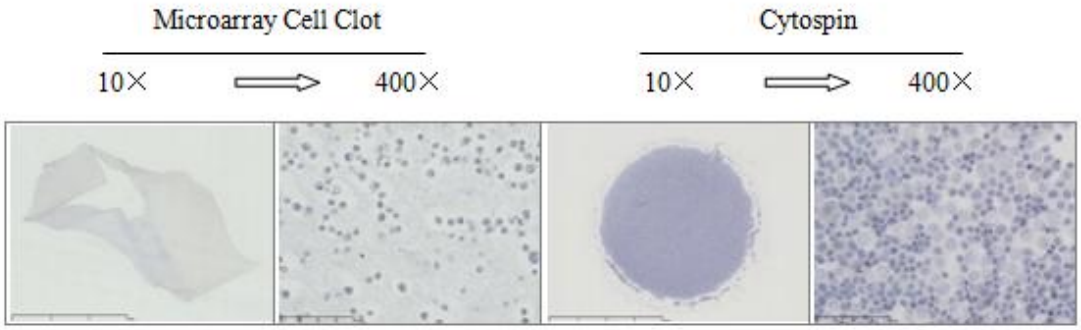

Figure 13. CMA clots vs cytospins consisting of MDA-MB-231 cells

For cytospin immunostaining, three main variables (a) fixation, (b) permeabilization, and (c) staining methodology were taken into account to achieve optimal working conditions for the antibodies directed to KLK4. The OV-MZ6 pRv RSV KLK4 cell line as the KLK4-overexpressing cell line, was tested under different conditions, while OV-MZ-6 RSV vector cell lines served as the negative control because of the absent KLK4 expression. MDA-MB-231 and MCF-7, as the representative of breast cancer cell lines, also were applied to identify expression pattern of KLK4 in breast cancer cells using antibody pAb587.

Fixation conditions. Fixation is crucial to guarantee cell morphology and maintain epitope architecture in the immunohistochemistry assay. Inappropriate fixation might impair antibody binding capability. Common fixatives such as ethanol, methanol, acetone, as well as paraformaldehyde (PFA) have been widely used in tissue research. Among them, 4 % PFA in PBS has served as an established fixative for cultured cells. However, as a cross-linking reagent, PFA action is effected by its concentration, fixation, and incubation temperature. Also, the PFA-fixative can form intermolecular bridges through interaction with free amino groups and thus establish a network of linked antigens.

Table 20. Fixative variables tested in the present study

Concentration [%]	Temperature [℃]	Incubation time [min]
Phosphate-buffered 1 % PFA	4 ℃	overnight
	Rt (21 ℃)	30 min
Phosphate-buffered 4 % PFA *	4 ℃	overnight
	Rt (21 ℃)	30 min

*

Generally speaking, high temperature can speed up the fixation process while fixation at low temperature seems to prevent cell structures from the damage. However, in the present study, temperature, incubation time, and PEA concentration affected cell morphology to a small extent, whereas prolonged incubation time (overnight) and high concentration (4 %) of PFA indeed enhanced the intensity of KLK4 staining. Furthermore, more cytoplasmic staining was observed using 4 % PFA fixation at 4 ℃ overnight. This might be caused by greater stability of polyclonal antibodies in higher salt concentrations and more contact possibility between antibody and antigens caused by enhanced cross-link network in cytoplasm[197].

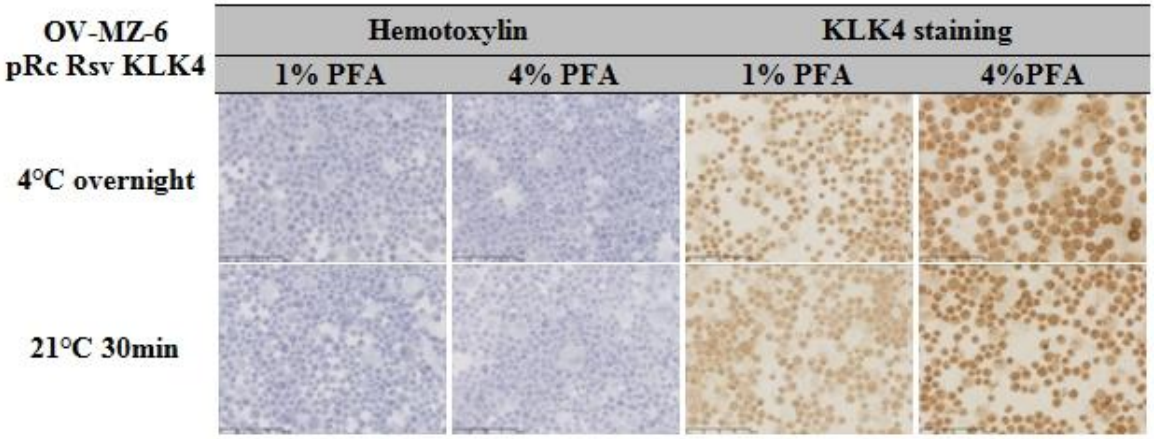

Figure 14. Cytospins fixed with 1 % or 4 % buffered PFA in PBS/0.1BSA for 30 min at RT or overnight at 4 ℃. Blue for nucleus (hematoxylin), brown for anti-KLK4 (pAb587, 3.5 µg/ml). LSAB method with avidin and biotin blocking, no antigen retrieval included. Magnification x 400.

Permeabilization

Following cross-linking fixation, essential reagents, including saponin and TritonX-100, were applied to extract the cell plasma membranes, allowing cell-impermeable antibodies to access intracellular structures through formed small holes in intact cells. Various experiments

demonstrated that saponin or TritonX100 addition facilitates antibody reactivity when a cross-linking reagent is used. Extensive permeabilization may result in damage of cell/antigen structure while insufficient permeability may produce negative results or high background staing. Saponin is a relatively mild detergent that dissolves cholesterol present in the plasma membrane, which is routinely used for labeling smaller molecules that exist in a soluble state within the cytoplasm. Low concentrations of 0.1-0.2 % were tested for 15 or 30min and 0.1 % for 30min was finally chosen; Triton X-100 can efficiently solvates cellular membranes without disturbing protein-protein interactions. Concentrations ranging from 0.05 to 0.1 % were applied for 5-15 min to test the optimal permeabilizing conditions and 0.05 % for 15min was chosed after several times test.

Table 21. Permeabilization variables tested in the present study

Reagents	Concentration [w/v]	Incubation time [min]
PBS/0.1 BSA	/	/
Saponin	0.1 %	15
	0.1 %	30
	0.2 %	15
	0.2 %	30
Triton X-100	0.05 %	5
	0.05 %	10
	0.05 %	15
	0.1 %	5
	0.1 %	10
	0.1 %	15

Our test results showed permeabilization enhanced the intracelluar staining pattern to certain extent compared with only fixed ones. Saponin is preferred by its less damage to cell morphology and more cytoplasm staining. On the other hand, due to its viscosity, diluted TritonX-100 seems to be difficultly controlled to be attached on the frozen cytospins and sometimes dispersed everywhere even vanished from certain part of section, leading to less satisfied contact with cells mounted on cytospins and falsified therefore negative staining results. In the meantime, obtained

expression patterns in other three cell lines, also support MDA-MB-231 and MCF-7 did not express KLK4, although few unspecific background sites have been observed. Compared with KLK4 negative control, OV-MZ-6 RSV vector, there was no significant increasement of staining intensity. More importantly, these background staining is not cell-cell heterogeneity and no distinct crisp cell membrane reactivity has been observed, which provided these stainings might come from fasle positive staining.

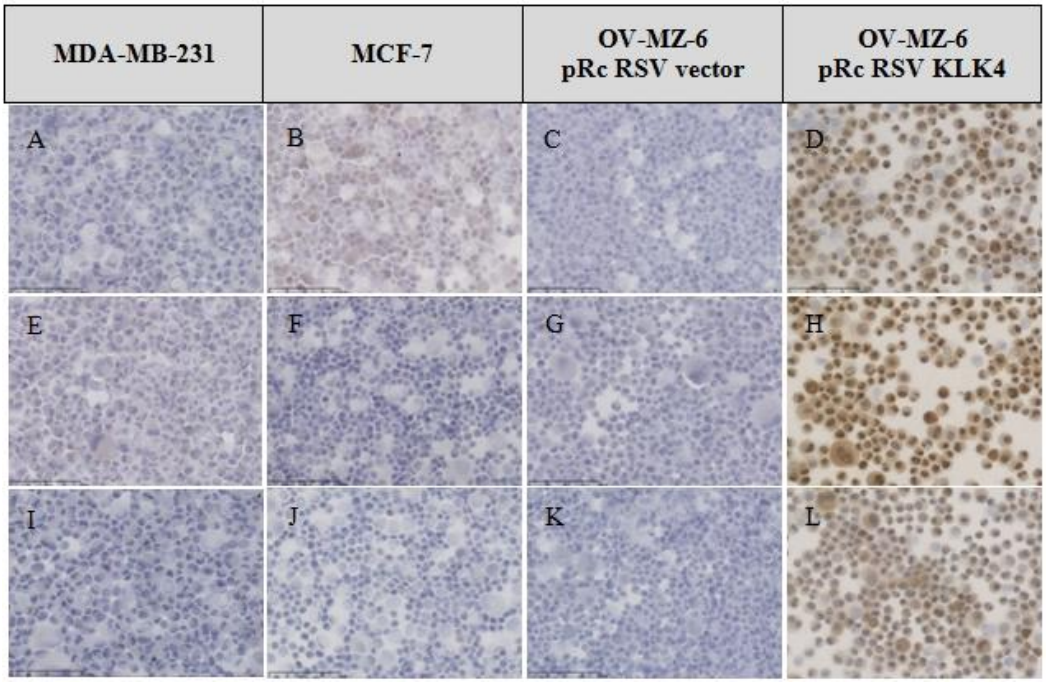

Figure 15. MDA-MB-231 (A,E,I), MCF-7 (B,F,J), OV-MZ-6 Rsv (C,G,K), OV-MZ-6 KLK4 (D,H,L) were treated without permeabilization (A-D), with 0.1 % saponin for 30 min (E-H) or 0.05 % Triton X-100 for 15 min (I-L). Cell cytospins stained with pAb587 (3.5 μg/mL). Brown for KLK4 (DAB+), blue for nuclei (hematoxylin). Magnification x 400.

Staining methodology

The most important issue concerning about the optimization of immunocytochemistry is the staining methodology. Significant variables including antigen retrieval, blocking procedures, as

well as the dilutions were observed and qualified in different immunohistochemical detection method, LSAB and Polymer method.

Table 22. Staining variables tested in the present study

Method	Antigen retrieval	Blocking	Dilutions
LSAB	+/- pressure cooking	+/- streptavidin-biotin block	1/200 (0.875 µg/ml) 1/100 (1.75 µg/ml) 1/50 (3.5 µg/ml)
Polymer		/	

The immunohistochemical detection method used for cytospins staining include DAKO LSAB system and Zytomed Polymer method with chromogen DAB^+ (mentioned in the previous chapter). The optimal primary antibody dilution 1:100 was set up after numerous tests with these qualified staining techniques.

The avidin and biotin blocking procedure was routinely used to block endogenous biotin or biotin-binding activity in tissue sections. Using cytospins as a model of tumor tissue, commercial avidin and biotin blocking kits (#K5003, Dako, Glostrup, Denmark) were still applied under LSAB method system, in order to observe difference between staining with avidin-biotin block and ones without blocking.

Heat induced epitope retrieval (HIER) developed by Dr. Shan-Rong Shi, was considered to expand the range of antigens that are detectable in paraffin sections. However, many aspects like heating time, temperature, pH of the solution might affect the final staining results. In the persent study, HIER in a 0.1M citrate buffer (pH 6) with a pressue cooker was tested to optimize the condition of staining.

According to our results, endogenous avidin-biotin blocking did not show the significant benifit of decreacing nonspecific background. However, HIER indeed strongly increased the staining intensity of cytoplasm, perinucleus as well as cellular edge with LSAB method. It has been

hypothesized that HIER breaked the molecular cross-links induced by PFA and thus unmasked blocked antigen sites, futhermore conduced to the return of native entigen structure. In contrast, HIER also possibly should be responsible for the recovery of endogenous biotin, which usually induce bothersome unwanted artifacts. Considering higher level endogenous biotin in frozen tissues than FFPE tissues, the method to block endogenous biotin are partially effective to certain extent, and might add another complexity to the already complex procedure.

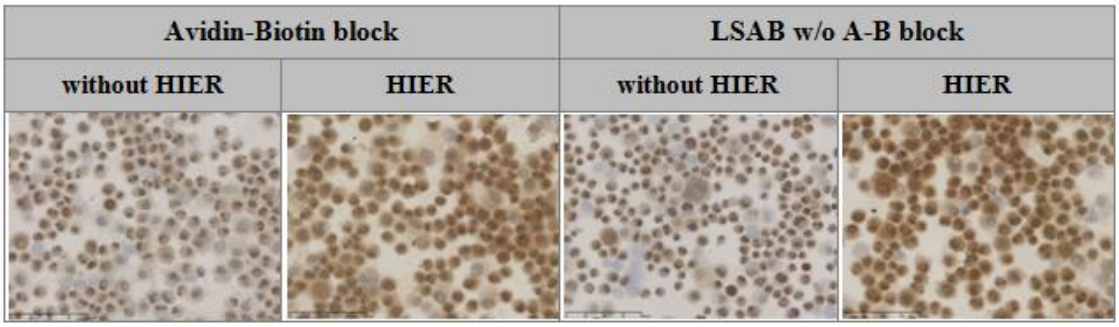

Figure 16. OV-MZ-6 KLK4 cytospins, tested with KLK4 antibody pAb587 (3.5 µg/mL) +/−HIER and +/- avidin-biotin block, LSAB method. Cytospins fixed at 21 ℃ for 30min, 0.1 % saponin 30 min. Brown KLK4 (DAB+), blue nuclei (hematoxylin). Magnification x 400.

On the other hand, HIER produced less difference of staining intensity with Polymer method, implicating that the enhancement of staining induced by HIER in LSAB system might result from excessive false positive artifects to a certain degree.

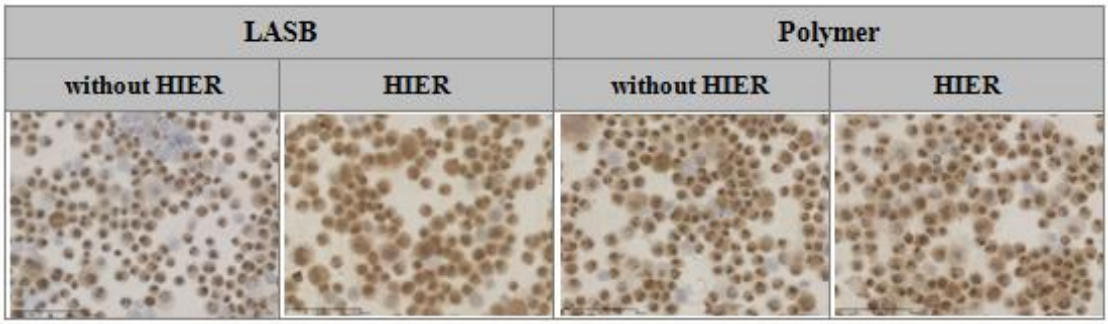

Figure 17. OVMZ-6 RSV-KLK4 stained for KLK4 with pAb587 (3.5 µg/mL) +/- pretreatment employing the LSAB or Zytomed Polymer Method. Brown KLK4 (DAB+), blue nuclei (hematoxylin). Magnification x 400.

In the end, besides OVMZ-6 RSV-KLK4, other three cell lines MDA-MB-231, MCF-7 as well as OVMZ-6 RSV-vector were also tested under aforementioned variables, including cross-linking fixative (1 % or 4 % buffered PFA, 4 ℃ overnight or 30 min at RT), permeabilization factor (yes or no, saponin 0.1-0.2 % for 15/30 min, Triton X-100 0.05-0.1 % for 5/10/15min), HIER (yes or no). Staining result was evaluated by pathologists though comparing relative staining intensity.

Table 23. Summarized intensities of staining with variables tested in the present study

4 % PFA fixed OV-MZ-6 pRc RSV KLK4						
Permeabilization	/		0.1 % saponin for 30 min		0.05 % Triton X-100 for 15 min	
Pretreatment	/	HIER	/	HIER	/	HIER
LSAB	+	++#	++*	++#	++	++#
Polymer	+	+	++*	++	++	++

#HIER+ revealed more background staining in LSAB system

*Saponin displayed more cytoplasmic staining than other fixation

Compared with the Polymer method, the LSAB method produced less crisper staining, no matter if saponin or Triton X-100 was employed. With the LSAB method, there was no significant difference between cell staining with streptavidin-biotin blocking and the ones without. Otherwise, the staining with LSAB system was highly affected by HIER, which might caused the adverse effect (increased background staining). On the other side, application of Saponin or TritonX-100 promoted distinct cytoplasmic staining using Polymer method. HIER was not a prerequisite for successful color product development and excluded from the final protocol. Taking all the factors into account, optimal condition and standard protocol for cytospins staining has been established. Subsequent to fixation with 4 % PFA for 30 min and permeabilization with 1 % sapoin for 30 min, cytospin cells were reccomanded to be stained for KLK4 protein with pAb587 (1:100, 3.5 µg/mL) employing the Zytomed Polymer method without HIER or avidin-biotin blocking treatment. OV-MZ-6 pRc RSV KLK4, as a KLK4

producing cell line, was stained using established protocol to give birth to a ideal clear image to manifest the expression pattern and locolization of KLK4 protein.

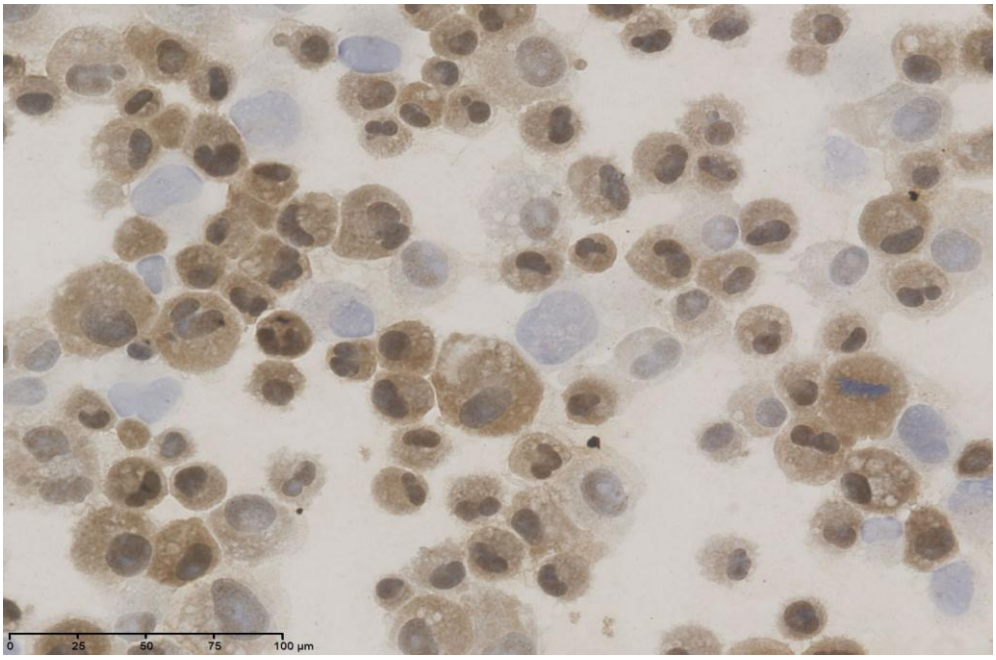

Figure 18. OV-MZ-6 pRc RSV KLK4 cytospins stained with KLK4 antibody pAb587 (3.5 µg/mL) employing Zytomed Polymer method. Cytospins were treated by fixation for 30 min and the 0.1 % saponin added for 30 min at 21 ℃. Brown: KLK4 (DAB+), blue: nuclei (hematoxylin). Magnification x 400.

5.3 Flow cytometry for KLK4 assessment

In order to trace and measure the intracellular KLK4 in single cells, flow cytofluorometry (FC) was applied to MDA-MB-231, MCF-7, and OV-MZ-6 RSV vector/KLK4 cell lines. Although FC cannot locate where a component is within the cell, it can detect the target in the cell or on its surface by appropriate permeabilization. Through comparing fluorescent signals from living cells and those in fixed cells +/− permeabilization, it can show whether the fluorescent component is distributed on the cell surface or located to intracellular compartments.

FC experiment on living cells. For living cells experiment, propidium iodide is used to assess cell viability and exclude dead cells from analysis. 1 µg/ml propidium iodide and 10 µg/ml RNase A was added to each 250 µl sample and incubated in the dark for 5 min. If the percentage of dead cells exceeds 50 %, the samples were discarded.

FC experiment on buffered PFA-fixed cells. 8 % PFA solution was prepared by dissolving 8 g PFA (#31268.01 Serva Electrophoresis, Heidelberg, Germany) in 85 ml 0.1M phosphate buffer (100 ml 0.1M Na_2HPO_4 was adjusted with 0.1M NaH_2PO_4 to pH 7.4, then adjusted with H_2Odist to 200 ml) in a fume hood on the heating plate (50-70 ℃). Then 2N NaOH (2-3 drops) was added to dissolve the turbidity, and adjusted with 2N HCl to pH 7.4 with pH test paper. This 8 % PFA solution was added to an equivalent volume of cell suspension to achieve a final work concentration of 4 % PFA. Cells were incubated overnight at 4 ℃, and then washed 3 times with TBS. Finally, fixed cells were resuspended in PBS/1 % BSA, and the cell number adjusted to 10^6/ml. 250 µl cell suspension contains approximately 25,000 cells.

pAb587 was diluted 1:100 in PBS/1 % BSA and incubated with the cells for 40 min at RT. Then the secondary antibody conjugated with Alexa-488 was diluted 1:1,000 and incubated for 30 min with cells at room temperature. The equivalent concentration of isotype control and autofluorescent control were tested in parallel (see chapter Material and Methods).

Living OV-MZ-6 RSV KLK4 cells did not react with KLK4 pAb587, the fluorescent signal (green) did not show any difference from the cells reacted with an irrelevant isotype control antibody (pink). This implicates that the KLK4 protein is not expressed on the cell membrane surface. Our experiments showed different degrees of fluorescent signal when fixation +/- permeabilization treatment was applied (Saponin/Triton X-100).

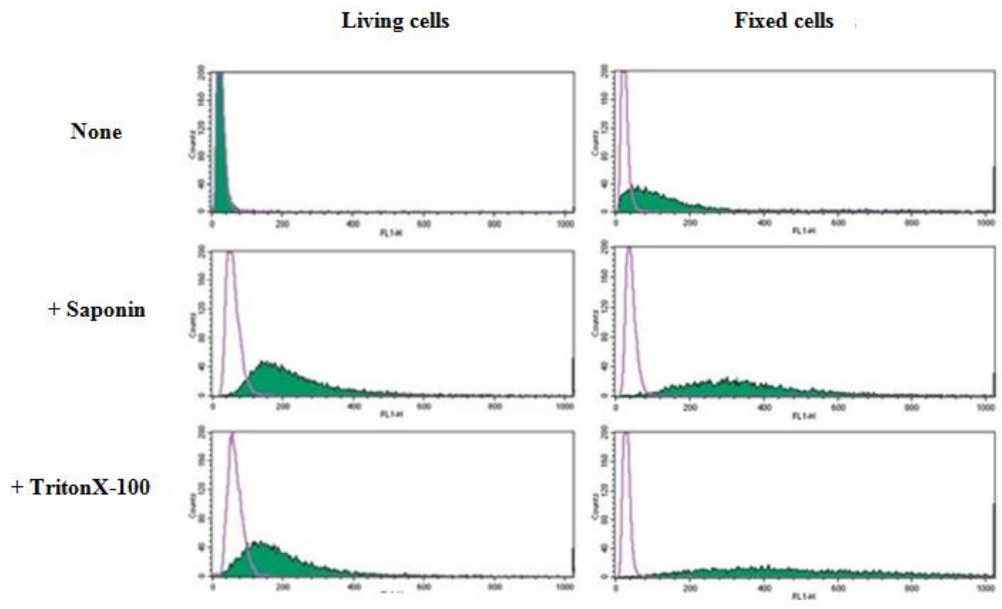

Figure 19. Living and 4 % PFA-fixed OV-MZ-6 pRc RSV KLK4 cells. Pink: IgG control (1:1,000, 3.5 µg/ml). Green: pAb587 1:100 (3.5 µg/ml)

Considering the fact that PFA fixation and saponin or Triton X-100 permeabilization induced different amplitides of fluorescent signal (Figure 19), the mean fluorescence channel values were calculated and determined as the relative expression level of KLK4 under various treatment conditions. Figure 20 displays a summary of the mean fluorescence values determined for OV-MZ-6 RSV KLK4 treated differently.

Cellular expression of KLK4 (FC mean values) in OV-MZ-6 KLK4

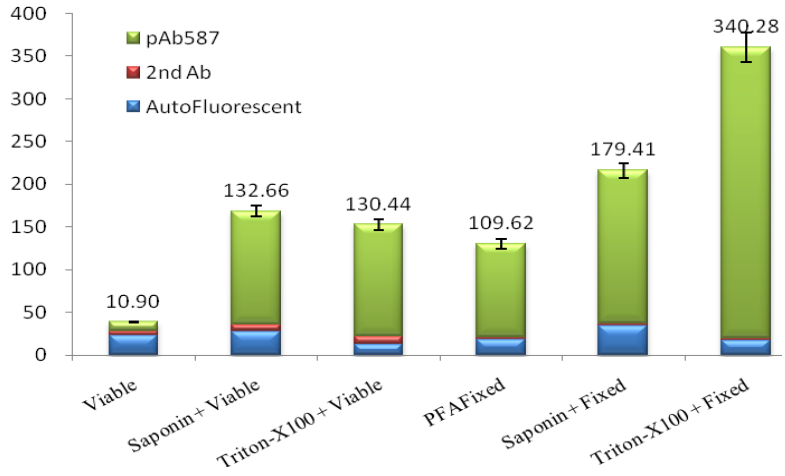

Figure 20. Fluorescence mean channel values of OV-MZ-6 pRc RSV KLK4 cells. Green: pAb587 (1:100, 3.5 µg/ml). Pink: 2nd Ab control 1:1,000. Blue: autofluorescence

The mean fluorescence values from other three cell lines were also collected, similar to the OV-MZ-6 RSV KLK4 cell line. pAb587 reacted poorly with these three cell lines, in contrast to the KLK4-transfected one(Figure 21). These results are comparable to cytospins data, confirming the absence of KLK4 expression in the breast cancer cell lines MDA-MB-231 and MCF-7.

Cellular Expression of KLK4 (FC mean values) in different cell line

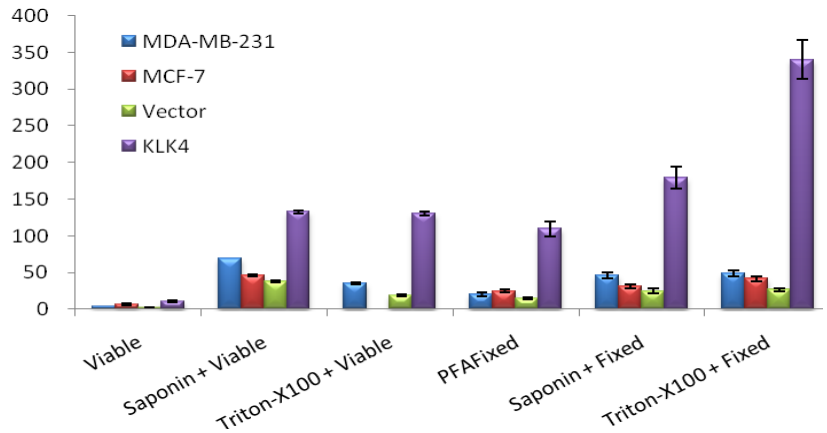

Figure 21. Mean fluorescence values from MDA-MB-231 (blue), MCF-7 (pink) and OV-MZ-6 pRc RSVvector (green)/ KLK4 (purple), stained with pAb587 1:100 (3.5 µg/ml) and 2nd Ab labeled with Alex488 (1:1,000)

5.4 CLSM for KLK4 assessment

As a complement to immunocytostaining and flow cytofluorometry, confocal laser microscopy (CLSM) provides us not only with precise cell morphology but also exact localization of the proteins in question[198]. As a pre-test assay, OV-MZ-6 pRc RSV KLK4 cytospins were stained with KLK4-directed antibody pAb587 and subsequently reacted with Alexa488-fluorescently labeled secondary antibody to rabbit IgG (#A-11008; goat anti-rabbit 1:1,000 stock: 2 mg/mL). The fluorescence image was visualized by CLSM. Evidently, the fluorescence signal was located in the cytoplasm of the tested KLK4-overexpressing ovarian cancer cell line OV-MZ-6 pRc RSV KLK4 (Figure 22).

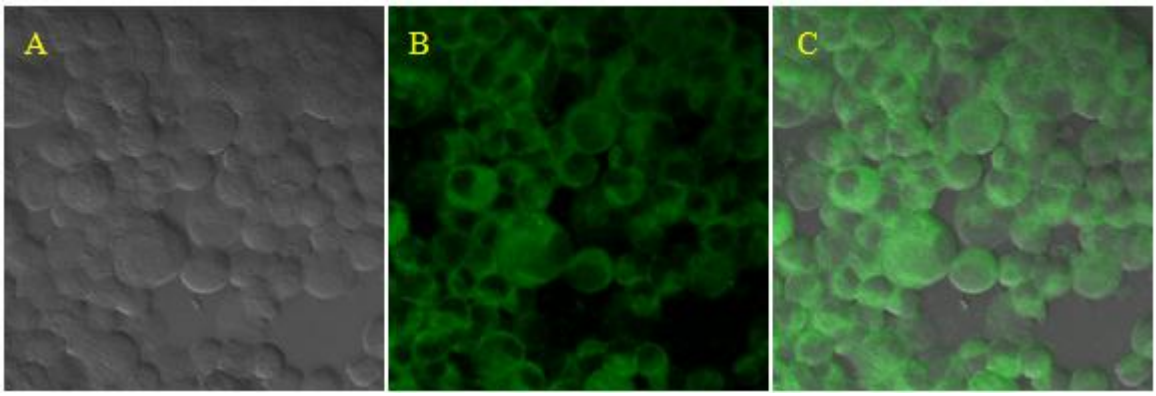

Figure 22. OV-MZ-6 pRc RSV KLK4 cytospin stained with KLK4-directed antibody pAb587 (3.5 µg/ml). After reaction with secondary antibody conjugated with Alexa488 (2 µg/ml), fluorescence was detected by CLSM. A: confocal image (grey). **B:** KLK4 detected with pAB587 to KL4 and visualized with anti-rabbit-IgG labeled with Alexa488 (green). **C:** merged overlay image.

Subsequently, MDA-MB-231, MCF-7, OV-MZ-6-*wt*, PC-3 pRc RSV KLK4, and vector only transfected cell lines were grown in an 8-well chamberslide forming a cell monolayer (# 946140802 non-pyrogenic, Sarstedt Nümbrecht, Germany). The adherent monolayer cells were subjected to KLK4-staining to be monitored by CLSM. In the adherent monolayer cells, when stained for KLK4 with pAb587 and reaction with Alexa488-labeled secondary antibody, KLK4 expression was located in the cytoplasmic compartment of the PC3 pRc RSV KLK4 cell line only, similar to OV-MZ-6 pRc RSV KLK4 (Figure 23). The MCF-7, MDA-MB-231, OV-MZ-6-*wt*, and the PC-3 pRc RSV vector cells did not show any significant KLK4 expression signal. No significant fluorescence signal (DAPI) was detected in the nuclei of any of the cells investigated. Phalloidin BODIPY650/665 (0.66 µM, Invitrogen Eugene Oregon, USA) was employed as a marker of F-actin filaments to illustrate the inner cellular part (Figure 24).

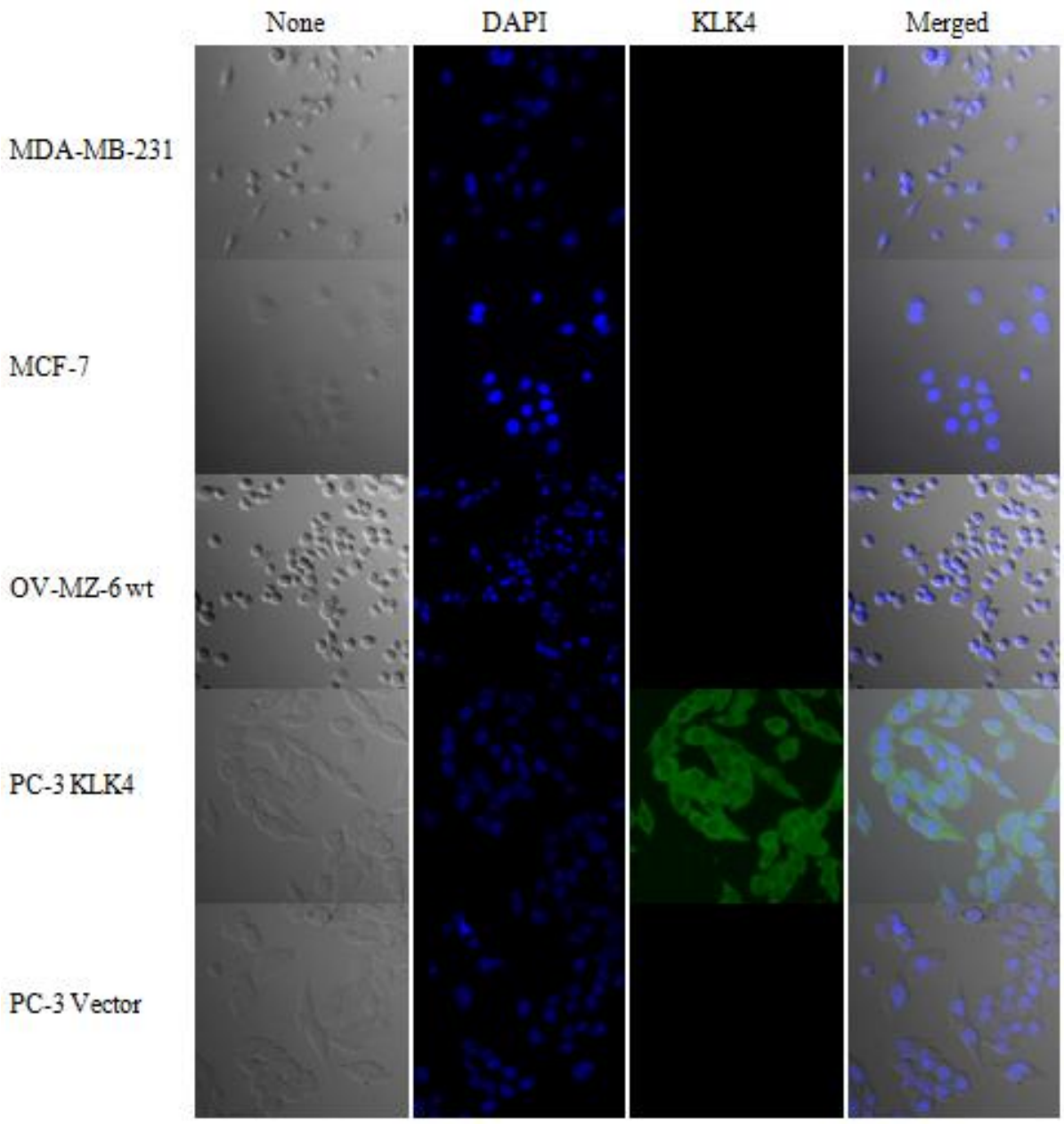

Figure 23. MDA-MB-231 MCF-7 OV-MZ-6-wt and PC-3 pRc RSV KLK4/vector cells stained for KLK4 protein with pAb587 (3.5 µg/mL). Secondary detection antibody Alexa488 (2 µg/mL). First of the left columns represents the confocal image for KLK4 staining, the second column nuclei stained with DAPI (Roche, 0.2 µg/ml), the third represents KLK4 staining. The right image represents the overlay of columns one to three. Magnification x 200.

Phalloidin BODIPY650/665 (0.66 µM, Invitrogen, Eugene, Oregon, USA) were used as a marker of F-actin filaments to display the cytoplasmic structures. The images show intracellular

and cytoplasmic localization of KLK4 in transfected cells, while no KLK4 staining was located to the nucleus or perinuclear region.

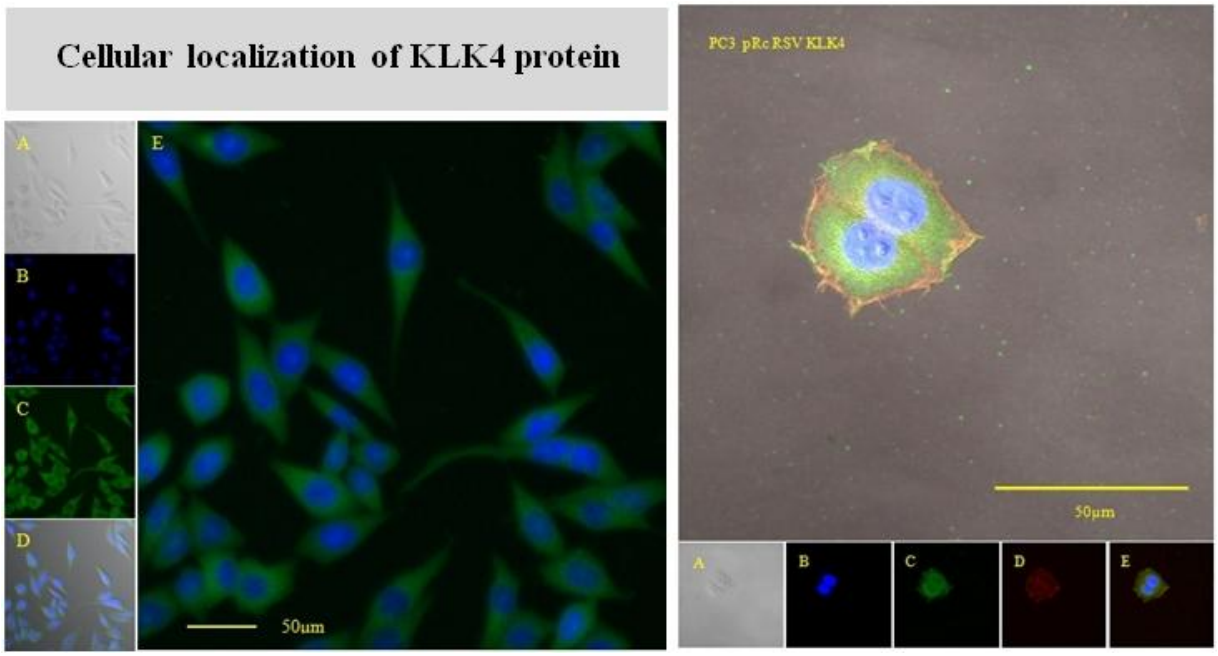

Figure 24. PC-3 pRc RSV KLK4 cells. **Left:** Magnification x 200. (A) confocal image, (B) Nucleus with DAPI (0.2 µg/ml), (C) stained for KLK4 with pAb587, (3.5 µg/mL), and (D) overlay image. **Right:** Magnification x 400 (Oil) (A) confocal image, (B) Nucleus stained with DAPI (0.2 ug/ml), (C) stained for KLK4 with pAb587 (D) cytoplasm stained with phalloidin BODIPY 650/665(0.66 µM). (E) overlay image.

5.5 Assessment of KLK4 mRNA expression by qPCR

Relative KLK4 mRNA expression levels in MCF-7, MDA-MB-231, OV-MZ-6-wt, OV-MZ-6 pRc RSV KLK4, PC-3 pRc RSV KLK4 cells, PC-3 pRc RSV vector, and PC-3 pRc RSV KLK4 cells were determined simutaneously and normalized to the housekeeping gene *HPRT1*-FAM Hs01003267. Using the Relative Quantitation (ΔΔCt) method, the different mRNA expression levels in these cell lines were compared and summarized (Figure 25). Only the transfected KLK4

overexpressing cell lines PC-3 pRc RSV KLK4 cells KLK4 and PC-3 pRc RSV KLK4 cells show significant KLK4 mRNA expression while the breast cancer cell lines MDA-MB-231 and MCF-7 as well as the ovarian cancer cell line OV-MZ-6-*wt,* OV-MZ-6 pRc RSV KLK4, and the PC-3 pRc RSV KLK4 cells did not express significant KLK4 mRNA. The control cell lines OV-MZ-6 pRc RSV vector and PC-3 pRc RSV vector cells were also negative for KLK4 expression.

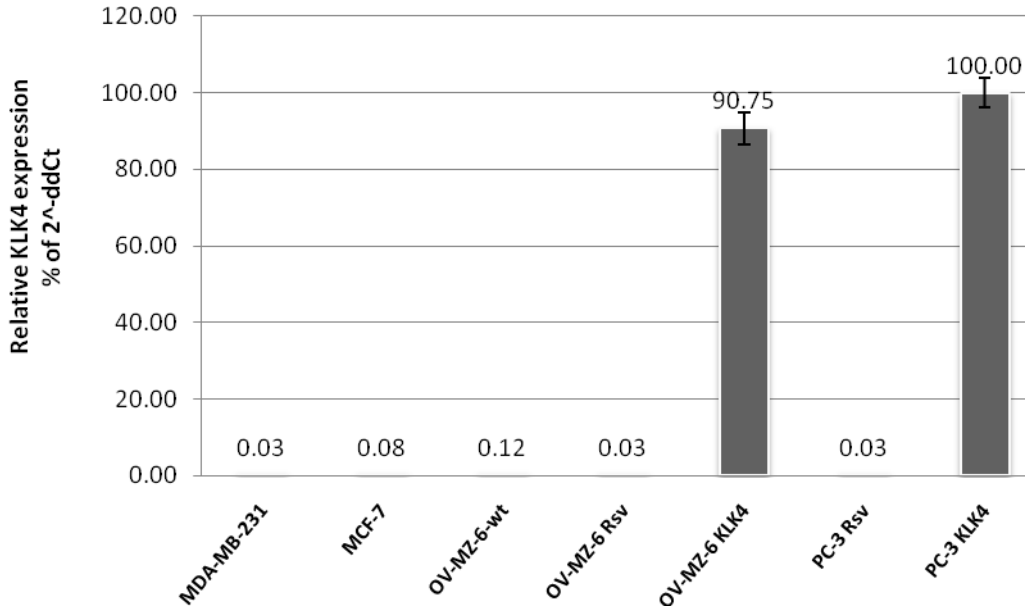

Figure 25. Relative KLK4 mRNA expression in cell lines MDA-MB-231, MCF-7 OV-MZ-6 wild type, OV-MZ-6 pRc RSV, OV-MZ-6 pRc RSV/KLK4, PC-3 pRc RSV, and PC-3 pRc RSV/KLK4, normalized to housekeeping gene HPRT-1 expression.

5.6 Assessment of KLK4 protein expression by western blotting

In order to study KLK4 protein expression, conditioned culture supernatants (30 µg/lane) of MDA-MB-231, MCF-7, OV-MZ-6-*wild type,* PC-3 pRc RSV vector, and PC-3 pRc RSV KLK4 cell lines were collected and whole cell extracts prepared (60 µg/lane). Cellular fractions (nuclei,

cytoplasm, cytoskeleton, prepared by the ProteoExtract® Subcellular Proteome Extraction Kit, S-PEK Merck, Darmstadt, Germany) and recombinant KLK4 (as the control protein, 0.3-3 U/lane) were also included. Protein concentrations were determined by the BCA protein assay (#23221 Pierce, Rockford IL, USA).

Table 24. Quantification of cellular fractions, whole cell lysates, and dialyzed culture media.

Cell type	Cell fraction	Protein concentration (µg/µl)	Protein (mg)	Proportion of total protein (%)	Deviation (%)
MDA-MB-231	F1 cytoplasm	1.40	8.40	75.55 %	0.40
	F2 nucleus	0.73	1.10	9.84 %	0.07
	F3 cytoskeleton	0.36	0.54	4.86 %	0.05
	F4 supernatant	1.10	1.10	9.86 %	0.07
	F5 whole cell lysate	1.71	3.42	100 %	0.03
MCF-7	F1 cytoplasm	3.25	19.52	72.87 %	0.12
	F2 nucleus	1.18	1.77	6.59 %	0.08
	F3 cytoskeleton	1.77	2.65	9.89 %	0.09
	F4 supernatant	2.86	2.86	10.66 %	0.07
	F5 whole cell lysate	3.74	7.48	100 %	0.04
OV-MZ-6-wt	F1 cytoplasm	2.75	13.24	77.05 %	0.11
	F2 nucleus	1.08	1.62	9.42 %	0.07
	F3 cytoskeleton	0.72	1.08	6.31 %	0.06
	F4 supernatant	1.24	1.24	7.21 %	0.06
	F5 whole cell lysate	2.18	4.36	100 %	0.08
PC-3 pRv RSv	F1 cytoplasm	2.13	12.77	81.76 %	0.03
	F2 nucleus	0.72	1.07	6.88 %	0.06
	F3 cytoskeleton	0.40	0.60	3.82 %	0.07
	F4 supernatant	1.18	1.18	7.54 %	0.02
	F5 whole cell lysate	2.70	5.40	100 %	0.10
PC-3 pRv KLK4	F1 cytoplasm	2.48	14.88	74.05 %	0.04
	F2 nucleus	0.95	1.42	7.09 %	0.06
	F3 cytoskeleton	0.40	0.59	2.96 %	0.20
	F4 supernatant	3.19	3.19	15.90 %	0.02
	F5 whole cell lysate	2.58	5.16	100 %	0.05

For each test, PC-3 pRc RSV KLK4 as the KLK4-positive cell line and PC-3 pRc RSV vector as the KLK4-negative control cell line plus in-house produced recombinant KLK4 (rec-KLK4) were subjected in parallel to western blot testing with KLK4-directed pAb587. rec-KLK4

optimum loading was determined first, ranging from 0.3 to 3 U rec-KLK4 with a protein band predominantely located at 25 kDa (Figure 26).

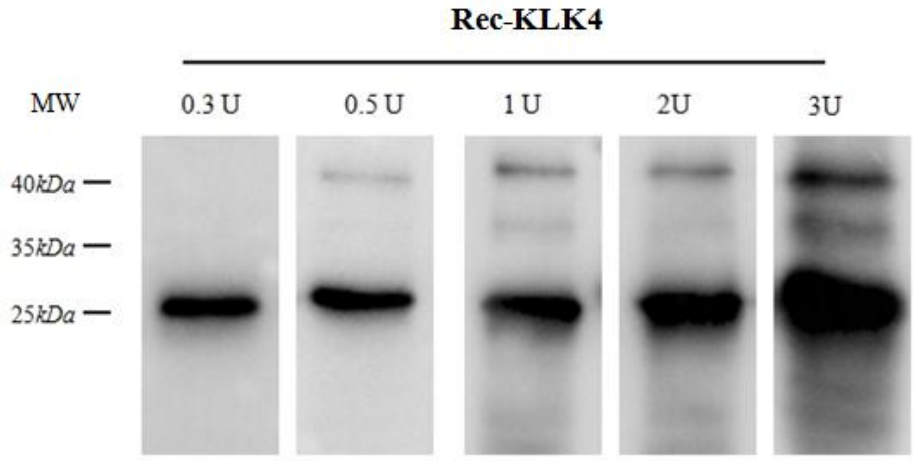

Figure 26. Different amounts of recombinant KLK4 (from 0.3 to 2 U/lane), stained with pAb587 (1:1,000, 0.35 µg/ml) under reducing conditions. Blocked with 5% skimmed milk. Detection by chemiluminescent ECL exposure, 3 min.

The second, minor 45 kDa KLK4 band detected is known as the nucleus form of KLK4[174, 175, 199–200]. In order to explore and identify this ~45 kDa band of KLK4 in conditioned medium (supernatants) collected from cultivated MDA-MB-231, MCF-7, OV-MZ-6-*wt*, and PC-3 pRc RSV vector/KLK4 cell lines were blotted and KLK4 content detected employing pAb587 under different conditions including reducing/non-reducing conditions, blocking with 5% skimmed milk/BSA, different incubation times and temperatures for primary pAb587. Although the KLK4 protein mainly deposited at around 25 kDa in conditioned culture medium under different test conditions, however, using 5% skimmed milk powder to block the blotted proteins, the 40 kDa KLK4 band was detected, even in the PC-3 pRc RSV vector cell line, which initially was determined as KLK4-negative or KLK4-low producing reference cell line (Figure 27). This additional 40 kDa KLK4 band did not appear when 5% BSA was used as the blocking agent instead of skimmed milk.

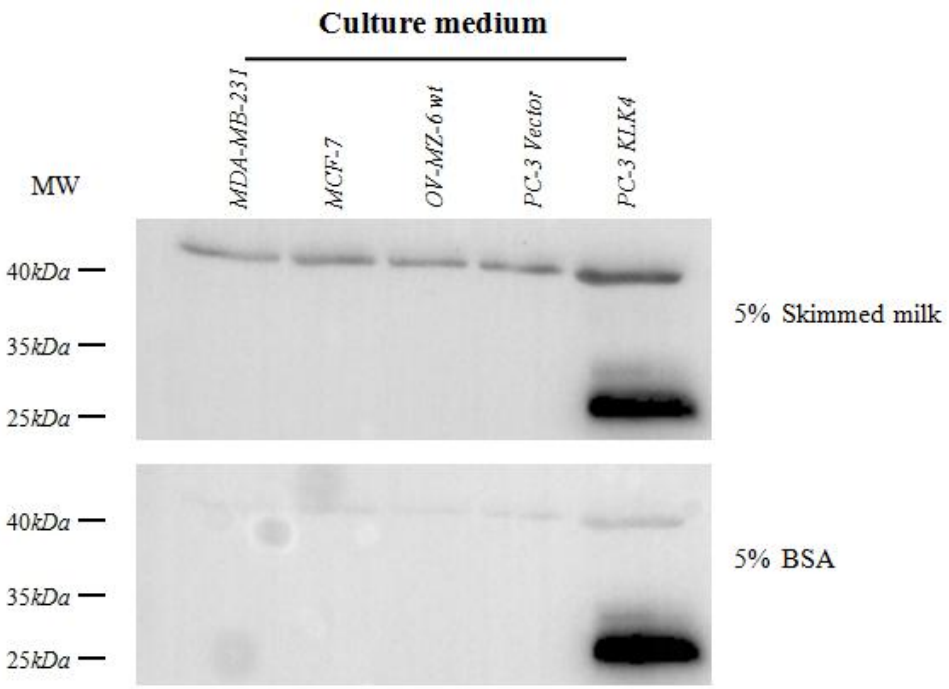

Figure 27. Samples of conditioned culture medium (30 µg/lane) obtained from different cell lines. Blotted under reducing conditions and stained with KLK4-directed antibody pAb587 (0. 35 µg/ml). Blocked with 5% skimmed milk and 5% BSA, respectively. Detection by chemilu minescent ECL exposure, 180 sec.

Whole cell lysates from different cell lines as well as rec-KLK4 were subjected to western blotting (Figure 28). Only the transfected KLK4 overexpressing PC-3 cell line shows a weak band at the molecular mass 25 kD, the 40 kD KLK4 band was not detected since blocked with BSA. After stripping, anti-GAPDH (0.1 µg/mL) was applied as the house-keeping protein.

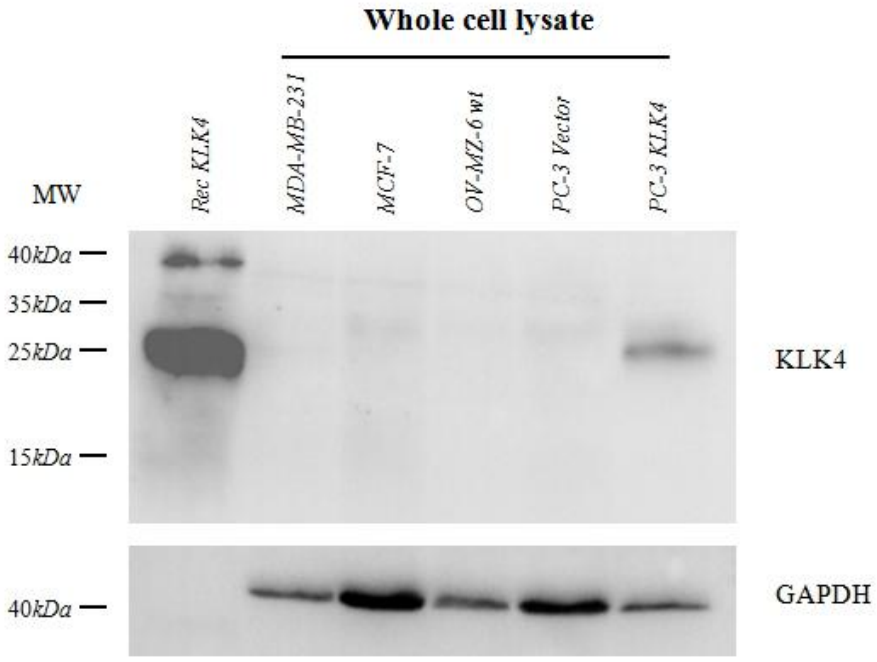

Figure 28. Samples from different cell lysates and rec-KLK4 immunoprecipitated with KLK4-directed antibody pAb587 (0. 35 µg/ml). Anti-GAPDH (0.1 µg/mL) served as the cytoplasm protein marker (40 kDa). Blot blocked with 5% BSA overnight. Detection by chemiluminescent ECL exposure, 180 sec.

In order to reveal origin, localization, and amount of KLK4 protein expression in spent medium and cellular subfractions of PC-3 pRc RSV KLK4 cells, whole cell lysate, cellular fractions, and culture medium were subjected to western blotting using KLK4-directed pAb587. rec-KLK4, the housekeeping cytoplasmic protein GAPDH, histone H3 as the nuclear marker, and cytokeratin CAM 5.2 as the cytoskeleton marker were included as controls (Figure 29). No contamination between different cell compartments was detected. Significant secretion of the 25 kDa KLK4 band was detected in the culture medium of PC-3 pRc RSV KLK4 cells, with weak representation of KLK4 protein in the whole cell lysate, preferentially in its cytoplasm.

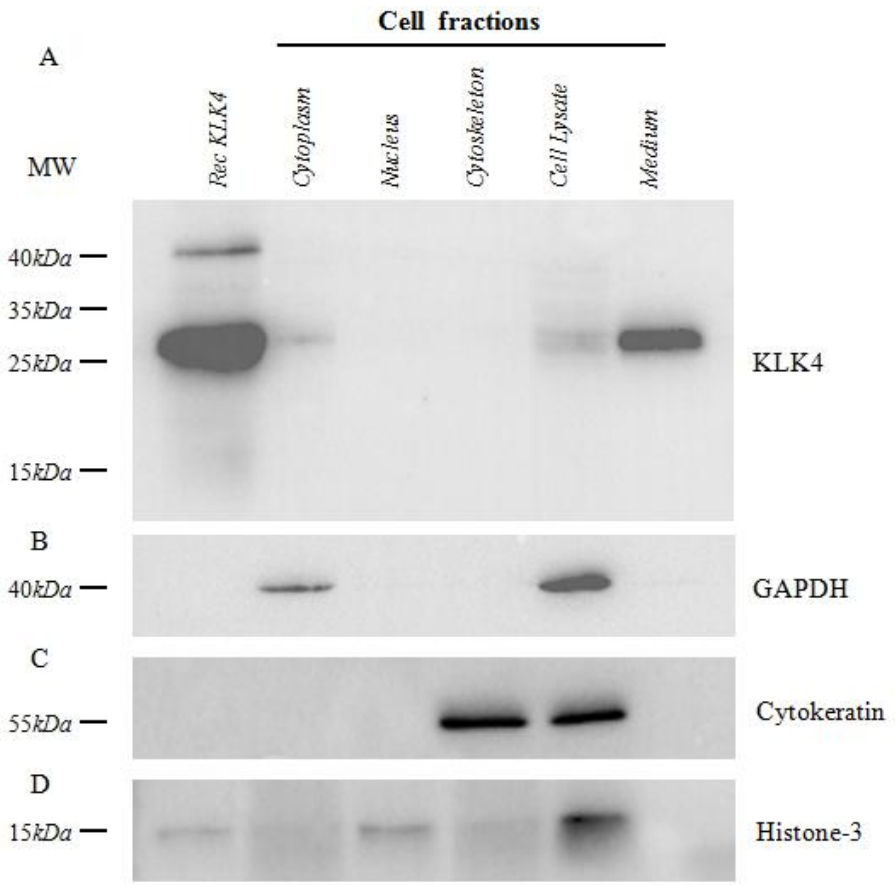

Figure 29. **(A)** rec-KLK4 (1 U), cytoplasm (30 µg/lane), nucleus (30 µg/lane), cytoskeleton (30 µg/lane), cell lysate (60 µg/lane), and conditioned medium (30 µg/lane) employing pAb587 (0.35 µg/mL). **(B)** GAPDH (anti-GAPDH 1:1,000). **(C)** Cytokeratin (anti-cytokeratin (CAM 5.2), 1:500). **(D)** Histone (anti-histone H3 1:500) blocked with 5% BSA overnight detected by chemiluminescent ECL exposure, 180 sec.

5.7 Assessment of KLK4 protein expression and localization in different TMAs by IHC

In order to optimize the immunostaining protocol (SOP, standard operating procedure) for KLK4 protein expression assessment in tumor tissues, SOPs were developed employing normal, benign and malignant prostate specimens, known for KLK4 expression[41]. Formalin fixation may generate large numbers of hydroxymethyl groups that link to protein groups to form strong

cross-link bonds between proteins and divalent cations resulting in “cage -like” complexes which may mask the antigen in question. Although the mechanism of HIER (heat-induced epitope retrieval) is not completely understood, the precipitation of tissue-bound divalent cations may be the reason to put the epitope back to a native-like state[201]. Unlike microwave ovens, pressure cookers do not have hot and cold spots so heating is more evenly distributed and reproducible. In addition to reversing epitope conformational changes induced by the cross-linking effects of formalin fixation, and futhermore enhancing the detectablility of epitopes, HIER has also been found to enhance the reactivity of endogenous biotin present in the tissue which subsequently will bind to streptavidin and thus produces unwanted artifacts[202]. Although formalin fixation and paraffin embedding has been shown to significantly reduce the expression of endogenous biotin, the residual activity can still be observed in tissues.

However, striking improvement has been observed when citrate buffer is used with HIER while addition of avidin-biotin was shown to reduce endogenous biotin artifacts, especially in benign prostatic hyperplasia (BPH) and prostate cancer cases. The increased staining mainly concentrated in cytoplasm and perinucleus part of glandular luminal cells which is similar to staining pattern observed in cytospins staining test.

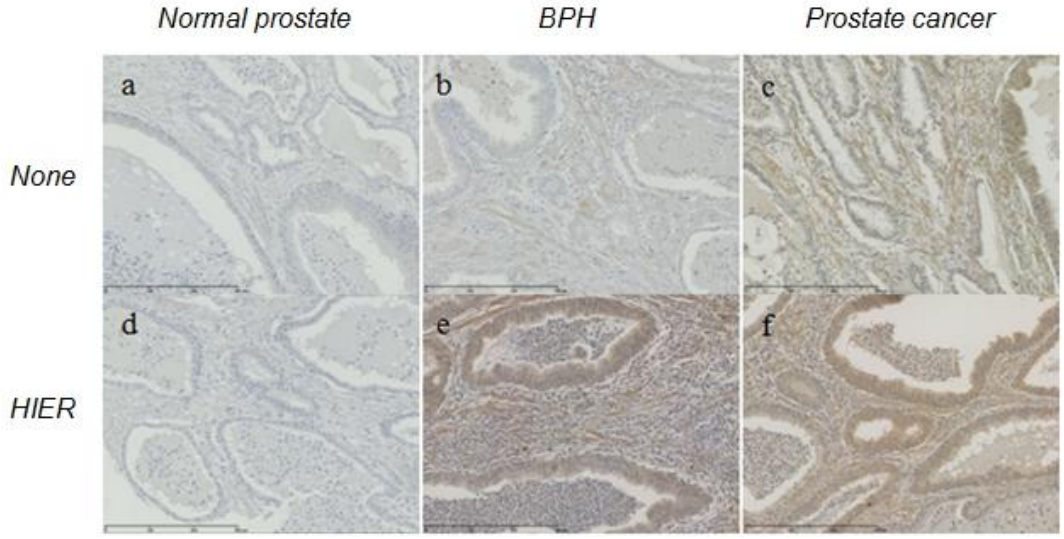

Figure 30. Prostate tissue stained for KLK4 employing pAb587 (3.5 μg/mL) and the LSAB method but no avidin/biotin blocking procedure. No HIER (heat pretreatment) (a, b, c). Antigen retrieval by HIER (d, e, f). KLK4 staining detected by DAB+ chromogenic reagent (brown). Blue for hematoxylin staining of the nucleus. Magnification: x 200. BPH: benign prostate hyperplasia.

Polymer based immunohistochemical method system which does not rely on the avidin-biotin signal amplification utilize a unique technology based on a polymer backbone to which multiple antibodies and enzyme molecules are conjugated allowing the entire staining procedure to be accomplished in a single step[203]. Pronounced staining for tumor cells and less staining for stroma cells in glandular epithelia have been viewed without the company of any background staining. Distinctive intracellular staining also vary from differen cell compartments including nucleus perinucleus cytoplasm and cell edge. This is in agreement with results produced by others[134].

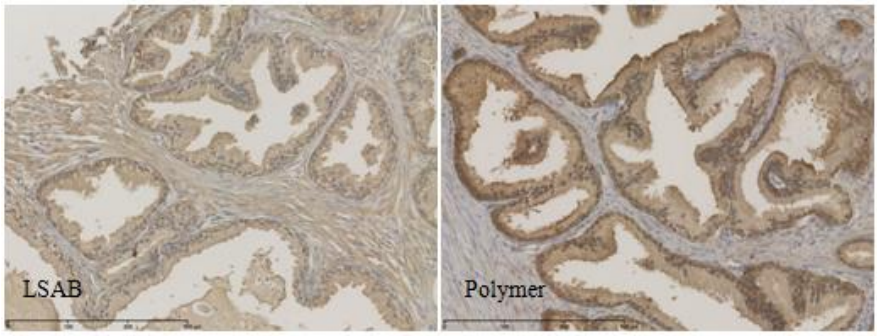

Figure 31. Prostate tissue stained for KLK4 (pAb587, 3.5 μg/mL) employing the LSAB method or the Zytomed Polymer system, detected by DAB+ chromogenic reagent (brown). Blue for hematoxylin staining of the nucleus. Magnification: x 200.

SOPs developed for manual immunohistochemical/immunocytochemical staining of KLK4 in tumor tissue sections

A) Staining for KLK4 with pAb587 using the DAKO LSAB/DAB system

1. **Deparaffinized and rehydrated tissue sections in descending row of graded ethanol.** 2 x 10 min xylene; then 2 x 100% isopropanol, 1 x 96% ethanol, 1 x 70% ethanol. Each step for 5 min followed by 5 min wash in TBS with intervening buffer change.
2. **Blocking of endogenous peroxidase activity.** 3% H_2O_2, 130 µl per tissue section, 20 min RT, followed by 5 min wash in TBS with intervening buffer change.
3. **Blocking of streptavidin/biotin activity.** Streptavidin/biotin blocking solution 130 µl per tissue section for 15 min, RT, followed by 5 min wash in TBS with intervening buffer change.
4. **Apply primary antibody.** Dilute antibody in green antibody diluent (DAKO S2022) at RT immediately before use. Negative controls use antibody diluent only. Apply 130 µL/slide of this dilution; incubate for 2 h at RT. Subsequently wash for 5 min with TBS with intervening buffer change. Recommended dilution: pAb587 1:100 (stock: 0. 35 mg/mL) → 3. 5 µg/mL
5. **Apply Reagent A.** 130 µl per tissue section (DAKO LSAB kit #K5003), 30 min at RT. Subsequently wash for 5 min with TBS with intervening buffer change.
6. **Apply Reagent B.** 130 µl per tissue section (DAKO LSAB kit #K5003) ,30 min at RT. Subsequently wash for 5 min with TBS with intervening buffer change.
7. **Apply DAB substrate from DAKO LSAB-kit (K5003).** 1 ml HRP substrate buffer (D) + 20 µL DAB+ chromogen (C). For 10 slides apply 130 µL per tissue section, 8 min, RT. Subsequently wash for 5 min with TBS with intervening buffer change.
8. **Counterstain** with hematoxylin for 50 sec. Rinse under tap water for 3 min, then transfer slide into $H_2O_{dist,}$ 1 min.
9. **Dehydrate in ascending row of graded ethanol.** 70% ethanol, 96% ethanol, 2 x 100% isopropanol, 2 x xylene, 5 min each.
10. **Mounting.** Mount slides with Pertex mounting medium.

B) Staining for KLK4 with pAb587 using the *Zytomed HRP one-step Polymer system*

1. **Deparaffinized and rehydrated tissue sections in descending row of graded ethanol.** 2 x 10 min xylene; then 2 x 100% isopropanol, 1 x 96% ethanol, 1 x 70% ethanol. Each step for 5 min followed by 5 min wash in TBS with intervening buffer change.
2. **Blocking of endogenous peroxidase activity.** 3% H_2O_2, 130 µl per tissue section, 20 min RT, followed by 5 min wash in TBS with intervening buffer change.
3. **Apply primary antibody.** Dilute antibody in green antibody diluent (Zytomed #ZUC025-500) at RT immediately before use. Negative controls use antibody diluent only. Apply 130 µL/slide of this dilution; incubate for 2 h at RT. Subsequently wash for 5 min with TBS with intervening buffer change. Recommended dilution: pAb587 1:100 (stock: 0. 35 mg/mL) → 3. 5 µg/mL.
4. **Apply Zytochem Plus HRP One-step Polymer anti-mouse/rabbit/rat** 130 µl per tissue section (Zytomed # ZUC053-100), 30 min at RT. Subsequently wash for 5 min with TBS with intervening

buffer change.

5. **Apply DAB substrate from Zytomed (ZUC053-100). S**ubstrate buffer solution, pH 7. 5, containing <0. 1% H_2O_2, stabilizer enhancer, and an antimicrobial agent. Chromogen solution: 5% 3,3'-diaminobenzidine tetrahydrochloride, 1 ml HRP substrate buffer (D) + 50 µL DAB+ chromogen (C) for 10 slides, 8 min, RT. Apply 130 µL per tissue section, 10 min at RT. Subsequently wash for 5 min with TBS with intervening buffer change.
6. **Counterstain** with hematoxylin for 50 sec. Rinse under tap water for 3 min, then transfer slide into $H_2O_{dist,}$ 1 min.
7. **Dehydrate in ascending row of graded ethanol.** 70% ethanol, 96% ethanol, 2 x 100% isopropanol, 2 x xylene, 5 min each.
8. **Mounting.** Mount slides with Pertex mounting medium.

In the end, the manual staining procedure employing HIER and the LSAB method were abandoned and instead, TMAs representing the triple-negative breast cancer cohort, were stained using KLK4-directed pAb587 by the VENTANA Benchmark® XT automatic staining system. Automatic staining for KLK4 was characterized by neglectible interindividual variance, thus allowing parallel examination of several TMAs at once. In some cases, for TNBC specimens, the nuclei of the tumor cells were stained whereas different degree of cytoplasmic staining of glandular epithelial cells were observed and partly in tumor stroma cells as well (Figure 32).

C) Staining for KLK4 with pAb587 using the Ventana system ultraView®

1. Deparaffinization and rehydration.
2. Associate printed barcode on slides with corresponding antibody name, date, and accession number.
3. Load the reaction buffer detection kit dispenser and other required reagents onto the reagent tray.
4. Install the reagent tray on the automated slide stainer and validate the bulk fluids and waste.
5. Load the slides onto the automated slide stainer and start the staining run.
6. Heat the slides and deparaffinize with heat and detergents.
7. Apply UV inhibitor (1 drop) for 4 min.
8. Dilute primary antibody pAb587 (1:100, 100 µl per slide) in DAKO REALTM antibody diluent (code S2022), 1 h.
9. Apply UV HRP UNIV MULT (1 drop) for 8 min.

10. Apply UV DAB (1 drop), UV DAB H_2O_2 (1 drop), and LCS for 8 min.

11. Apply UV COPPER (1 drop) for 4 min.

12. Apply COUNTERSTAIN 1 (1 drop) and LCS for 8 min.

13. Apply BLUING REAGENT (1 drop) and LCS for 4 min.

14. Remove slides and wash in mild dishwash detergent to remove the coverslip solution.

15. Dehydrate and mount slides with permanent mounting media.

Automatic staining, characterized by less interindividual variance by allowing examination of numbers of samples under the same conditions, also demonstrated comparable heterogeneous distribution patterns in tested triple-negative breast cancer samples. The staining results of nine tissue microarray are quite similar. The nucleus of the tumor cells present only weak staining in some cases, whereas different degrees of cytoplasmic staining of glandular epithelial cells have been revealed. The automatic stained brown product was mainly deposited into the tumor cells and partly in tumor stroma cells in glandular epithelial cells, both revealing a weak to moderate staining from patient to patient.

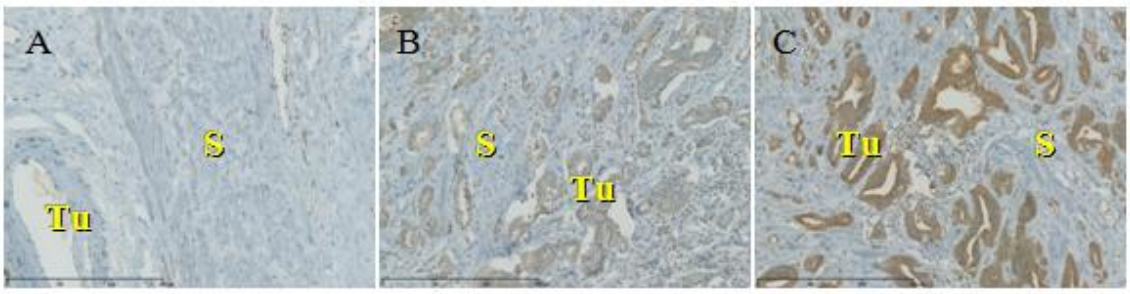

Figure 32. Expression of KLK4 antigen in breast cancer tissues. TMAs were stained with pAb587 employing the Ventana ultraView® method. (A) Displays almost no KLK4 antigen. (B) Faint cytoplasmic staining of tumor cells but no stromal cell staining. (C) Pronounced cytoplasmic staining within tumor cells plus moderate stromal cell staining. (Tu: tumor cells S: stroma cells). Magnification x 200.

Of interest, our staining results also show that smooth muscle cells are positive for KLK4 expression (Figure 33) which is in agreement with previously published data[131]. In some cases,

secrection (milk ?) exhibited strong reaction with KLK4-directed pAb587. Another important finding is that staining of non-tumor cells was observed in stromal cell-infiltrated and necrotic regions implicating that KLK4 may be involved in immunofunctional tumor cell reactions. In fact, KLK4-specific cytotoxic T-lymphocyte responses have been reported [204, 205].

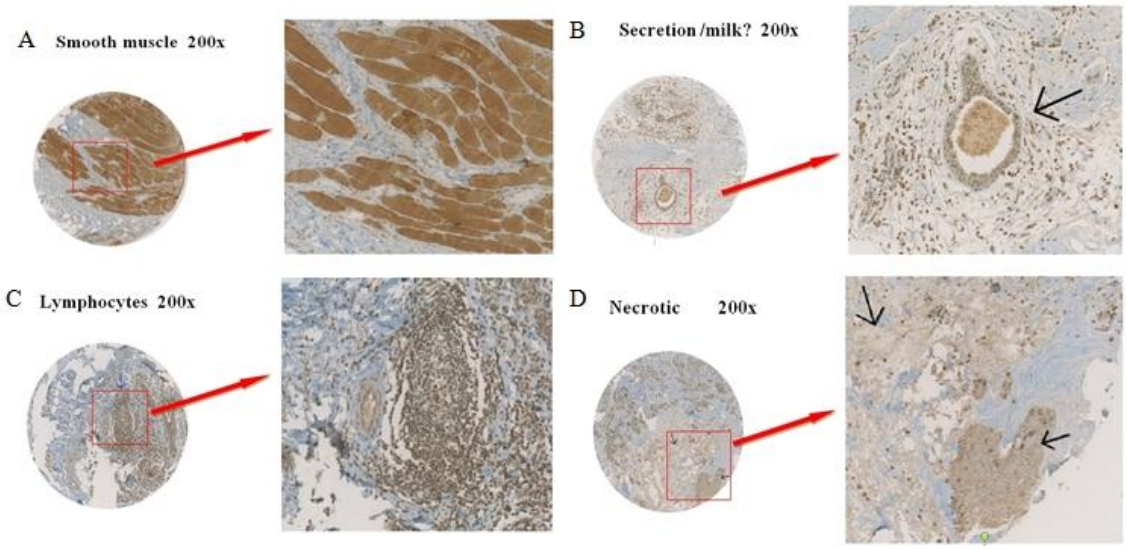

Figure 33. Expression of KLK4 antigen in breast cancer tissues. TMA sections were stained with pAb587 employing the Ventana ultraView® method. (A) Smooth muscle cells display intense staining. (B) Breast duct secretion (milk ?) with significant staining intensity. (C) Pronounced staining within lymphocyte-infiltrated regions. (D) Pronounced staining within necrotic regions. Magnification x 200.

5.8 Statistical analysis of KLK4 expression in the triple-negative breast cancer collective

For the assessment of the clinical value of KLK4 expression in triple-negative breast cancer, 188 TNBC specimens were stained immunohistochemically with pAb587 using the Ventana Benchmark® XT system. KLK4 immunoscores derived from tumor cells (KLK4-mTS), tumor stroma cells (KLK4-mSS) as well as lymphocyte-infiltrated (KLK4-mLS) and necrotic regions

(KLK4-mNS) were aquired through manual scoring by experienced pathologists based on the immunoreactive scoring system. In parallel, automatic-tumor-scoring (KLK4-aTS) and stromal-scoring (KLK4-aSS) were produced with the help of an automated image recognition analysis software (Definiens DeveloperXD 2. 0) All tumor staining scoring values obtained automatic or manual system were categorized into two groups (low versus high) using the median or 3/4 percentile (75 %) as the optimized cut-off point (Table 25).

Table 25. Manual and automatic scoring values of KLK4 immunostaining of TNBC TMA specimens

Parameter	Median	Range	Cutoff	Low/high (% high)
KLK4-mTS	0	0-6	> ***0***	96/92 (48.9 % high)
KLK4-mSS	1	0-6	> ***1***	99/89 (47.3 % high)
KLK4-mLS	1	0-6	> ***1***	99/89 (47.3 % high)
KLK4-mNS	0	0-3	> ***0***	136/52 (27.7 % high)
KLK4-aTS	0.2800	0-0.5750	> ***0.5050***	97/91 (48.4 % high)
KLK4-aSS	0.2200	0-0.4200	> ***0.2200***	96/92 (48.9 % high)

Association of KLK4 expression with clinical and histopathological parameters

Prior to correlating KLK4 antigen levels with the clinical and pathological factors, the relationship among KLK4 immunoscores is analyzed using the Spearman rank correlation coefficient (*rho*) calculation. Statistical significance is defined when *rho*>0.5. No significant correlation between the various KLK4-immunoscores was observed. Also, comparing two different scoring systems, the automated analysis scores did not show any significant correlation with any one of the manual immunoscores (Table 26).

Table 26. KLK4 staining scoring values: Spearman correlations (rho)

	KLK4-mTS	KLK4-mSS	KLK4-aTS	KLK4-aSS	KLK4-mLS
KLK4-mSS	-0.076				
KLK4-aTS	0.265**	0.041			

KLK4-aSS	-0.022	0.073	0.500**		
KLK4-mLS	-0.076	0.232**	0.275**	0.372**	
KLK4-mNS	0.108	0.128	-0.099	-0.201*	-0.039

*$P < 0.05$;** $P < 0.01$

The relationship between KLK4 immunoscore values with clinical and pathological parameters of TNBC patients was calculated using the Pearson Chi-square (χ^2) test. All results and respective *P*-values are summarized in Table 27. Elevated manual KLK4 immunostaining scores in tumor stroma cells (KLK4-mSS) is significantly associated with the presence of disease recurrence (p=0.022). Advanced histological grade is found to be strongly associated with high automatical scoring values of tumor stroma cells (KLK4-aSS, p=0.003) and manual immunoscores in lymphocyte-infiltrated regions (KLK4-mLS, p=0.024). In addition, menopausal status (pre/perimenopausal) is associated with elevated manual immunoscores of tumor cells (KLK4-mTS, p=0.014) and lymphocyte-infiltrated regions (KLK4-mLS, p =0.014). High automatic immunoscore is associated with age (KLK4-aTS, p=0.020). Besides these, no other KLK4 immunoscores demonstrated any significant correlation with the mentioned clinical or histomorphological variables.

Table 27. Association of clinical/histomorphologic factors with KLK4 immunoscores

Parameters	N	High mTS (>0)	High mSS (>1)	High aTS (>0.2800)	High aSS (>0.2250)	High mLS (>1)	High mNS (>0)
Age (years)	*P*	0.196	0.110	**0.020**	0.109	0.056	0.695
≤ 50	61	34(55.7 %)	34(55.7 %)	**37(60.7 %)**	35(57.4 %)	35(57.4 %)	18(29.5 %)
> 50	127	58(45.7 %)	55(43.3 %)	54(42.5 %)	57(44.9 %)	54(42.5 %)	34(26.8 %)
Menopause	*P*	**0.014**	0.133	0.053	0.067	**0.014**	0.859
Pre/peri	59	**37(62.7 %)**	33(55.9 %)	35(59.3 %)	35(59.3 %)	**36(61.0 %)**	17(28.8 %)
Post	127	55(43.3 %)	56(44.1 %)	56(44.1 %)	57(44.9 %)	53(41.7 %)	35(27.6 %)
Tumor Size	*P*	0.225	0.098	0.687	0.970	0.224	0.377
pT1+pT2	149	77(51.7 %)	66(44.3 %)	71(47.7 %)	73(49.0 %)	73(49.0 %)	43(28.9 %)

pT3+pT4	37	15(40.5 %)	22(59.5 %)	19(51.4 %)	18(48.6 %)	14(37.8 %)	8(21.6 %)
Nodal status	*P*	0.397	0.856	0.397	0.672	0.332	0.736
pN0+pN1	156	86(51.3 %)	75(48.1 %)	76(48.7 %)	77(49.4 %)	76(48.7 %)	43(27.6 %)
pN2+pN3	26	11(42.3 %)	12(46.2 %)	15(57.7 %)	14(53.8 %)	10(38.5 %)	8(30.8 %)
Nuclear Grade	*P*	0.075	0.814	0.521	**0.003**	**0.024**	0.359
G1/2	24	16(66.7 %)	11(45.8 %)	13(54.2 %)	5(20.8 %)	6(25.0 %)	5(20.8 %)
G3	157	79(47.1 %)	76(48.4 %)	74(47.1 %)	**83(52.9 %)**	**78(49.7 %)**	47(29.9 %)
Disease Recurrence	*P*	0.513	**0.022**	0.530	0.839	0.658	0.484
No	149	75(50.3 %)	64(43.0 %)	70(47.0 %)	73(49.0 %)	72(48.3 %)	44(29.5 %)
Yes	34	15(44.1 %)	**22(64.7 %)**	18(52.9 %)	16(47.1 %)	15(44.1 %)	8(23.5 %)

Chi^2 test cut-off: median or 75% percentile (KLK4-mNS). pN0: no regional lymph nodes affected with tumor load. pN1: 1 to 3 lymph nodes affected. pN2: 4 to 9 lymph nodes affected. 10 and >10 lymph nodes affected.

Association of clinical and histomorphological factors plus KLK4 expression with TNBC patient's disease-free and overall survival

Univariate and multivariate Cox regression analyses were performed to evaluate association of clinical and histomorphological factors plus KLK4 protein expression with time-to-progression (TTP, disease-free survival) or overall survival (OS) of adjuvantly treated (chemotherapy and/or endocrine therapy) TNBC (triple-negative breast cancer) patients. For survival analyses, at first, established clinicopathological factors (age, tumor size, nuclear grade, menopausal status, type of surgery, disease recurrence) plus KLK4 immunoscores were assessed by univariate analyses. Factors with statistical significance (p <0.05) were then subjected to multivariate Cox regression analysis.

Several of the clinical and histomorphological factors plus KLK4 immunoscores as listed in Table 28 were evaluated as statistically significant for disease-free (time-to-progression) survival of TNBC patients. In univariate analysis, tumor size, nodal status, and type of surgery were of statistical significance for disease-free survival. In addition, elevated KLK4 manual immunoscore present in tumor stroma cells (KLK4-mSS) is significantly associated with

increased risk of disease progression (HR=2.261, p <0.001). KLK4-mSS immunoscore is also an independent statistically significant factor for disease-free survival of TNBC patients (HR=2.122, p =0.007) as shown by multivariate analysis. Of the relevant clinical parameters, lymph node involvement (HR=2.881, p =0.007) and type of surgery (HR=2.108, p =0-029) were also of statistical significance by multivariate analysis.

Table 28. Uni- and multivariate Cox regression analysis for time-to-progression (TTP, disease-free survival) in TNBC patients

Variable	No.	Univariate		Multivariate	
		HR [95 % CI]	*P*	HR [95 % CI]	*P*
Tumor size	**170**				
pT1/2	135	**3.761 (2.315-6.109)**	***< 0.001***	1.557 (0.718-3.379)	*0.262*
pT3/4	35				
Nodal status	**168**				
pN0/1	143	**2.949 (1.669-5.211)**	***< 0.001***	**2.811 (1.327-5.954)**	***0.007***
pN2/3	25				
Surgery	**167**				
Breast Conservation	99	**2.619 (1.638-4.186)**	***< 0.001***	**2.108 (1.078-4.124)**	***0.029***
Mastectomy	68				
Age (years)	**172**				
≦50 years	55	1.340 (0.807-2.225)	*0.258*	na	na
> 50 years	117				
Nuclear Grade	**167**				
G1/2	24	1.205 (0.617-2.353)	*0.585*	na	na
G3	143				
Menopause	**171**				
Pre/peri	55	1.143 (0.698-1.872)	*0.596*	na	na
Post	116				
KLK4-mSS	**172**				
Low	91	**2.261 (1.407-3.632)**	***< 0.001***	**2.122 (1.229-3.665)**	***0.007***
High	81				
KLK4-mNS	**172**				
Low	121	1.203 (0.743-1.947)	*0.453*	na	na
High	51				
KLK4-mTS	**172**				
Low	86	0.925 (0.586-1.462)	*0.739*	na	na
High	86				
KLK4-aTS	**172**				
Low	87	0.899 (0.569-1.421)	*0.648*	na	na

High	85				
KLK4-mLS	**172**				
Low High	87 85	0.833 (0.527-1.318)	*0.436*	na	na
KLK4-aSS	**172**				
Low High	87 85	0.792 (0.500-1.253)	*0.318*	na	na

HR[95% CI]: hazard ratio [95% confidence interval] of Cox regression analysis. Statistical significance defined as P<0.05 in black bold type. na: not assessed since not significant by univariate analysis. pN0: no regional lymph nodes affected with tumor load. pN1: 1 to 3 lymph nodes affected. pN2: 4 to 9 lymph nodes affected. 10 and >10 lymph nodes affected.

Next, the association of clinical and histomorphological factors plus KLK4 expression with TNBC patients' overall survival (OS) was assessed. By univariate analysis, the clinical/histomorphological parameters nodal status, tumor size, type of surgery, patient age, and menopausal status were shown to be of statistical significance to predict survival probability of TNBC patients (Table 29). None of the KLK4 immunoscores evaluated were of statistical significance, however, KLK4-mSS as a marker of KLK4 expression in tumor stroma cells was shown to approach statistical significance, which is in line with its statistical significance demonstrated for disease-free survival (HR=1.586, p =0.059). Univariate results are also plotted in Figure 34 (disease-free survival) and Figure 35 (overall survival).

Table 29. Uni- and multivariate Cox regression analysis for overall survival (OS) in TNBC patients

Variable	No.	Univariate		Multivariate	
		HR [95 % CI]	*P*	HR [95 % CI]	*P*
Nodal status	**163**				
pN0/1 pN2/3	138 25	**5.404 (23.148-9.279)**	***<0.001***	**4.415 (1.966-9.917)**	***<0.001***
Tumor size	**165**				
pT1/2 pT3/4	131 34	**4.319 (2.597-7.185)**	***<0.001***	1.247 (0.553-2.813)	*0.594*
Surgery	**162**				
Breast conservation Mastectomy	95 67	**3.451 (2.077-5.734)**	***<0.001***	**2.317 (1.073-5.001)**	***0.032***
Age (years)	**167**				

≦50	54	**2.290 (1.250-4.198)**	***0.007***	2.336 (0.648-8.417)	*0.194*
> 50	113				
Menopause	**166**				
Pre/peri	54	**1.853 (1.043-3.291)**	***0.035***	0.516 (0.150-1.781)	*0.295*
Post	112				
Nuclear grade	**162**				
G1/2	24	1.424 (0.703-2.884)	*0.327*	na	na
G3	138				
KLK4-mSS	**167**				
Low	88	1.586 (0.983-2.558)	*0.059*	na	na
High	79				
KLK4-mNS	**167**				
Low	117	1.517 (0.930-2.475)	*0.095*	na	na
High	50				
KLK4-aTS	**167**				
Low	86	0.844 (0.523-1.361)	*0.486*	na	na
High	81				
KLK4-aSS	**167**				
Low	85	0.824 (0.511-1.330)	*0.428*	na	na
High	82				
KLK4-mTS	**167**				
Low	83	0.798 (0.494-1.289)	*0.356*	na	na
High	84				
KLK4-mLS	**167**				
Low	85	0.764 (0.470-1.241)	*0.276*	na	na
High	85				

HR [95% CI]: hazard ratio [95% confidence interval] of Cox regression analysis. Statistical significance defined as $P<0.05$ in black bold type. na: not assessed since not significant by univariate analysis. pN0: no regional lymph nodes affected with tumor load. pN1: 1 to 3 lymph nodes affected. pN2: 4 to 9 lymph nodes affected. 10 and >10 lymph nodes affected.

Figure 34. Kaplan-Meier curves (time-to-progression (disease-free) probability) concerning KLK4 protein expression in TMAs of TNBC patients. **(A)** KLK4-mTS **(B)** KLK4-mSS **(C)** KLK4-aTS **(D)** KLK4-aSS **(E)** KLK4-mLS **(F)** KLK4-mNS. (n=number of patients, e=number of events).

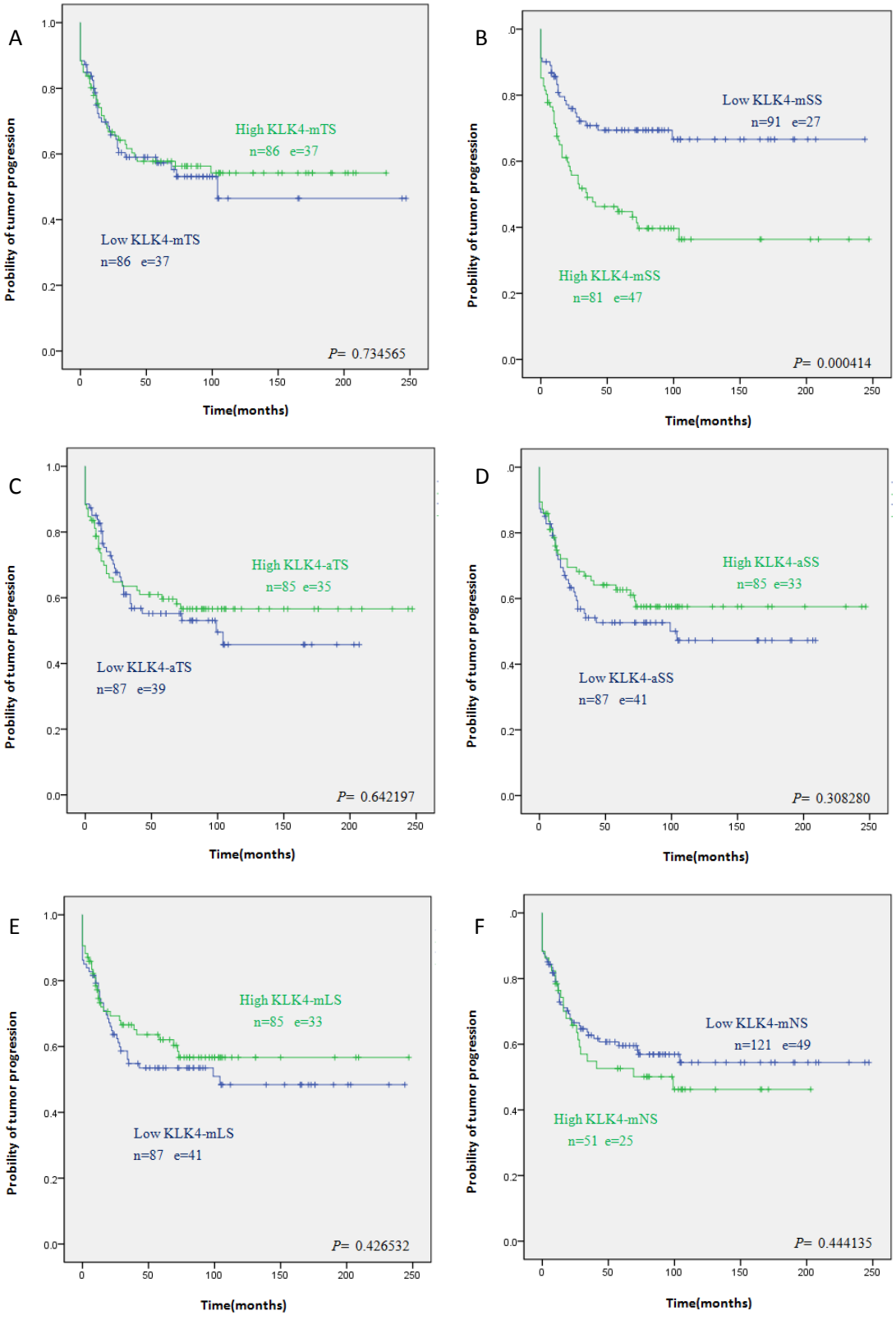

Figure 35. Kaplan-Meier curves (overall survival probability) concerning KLK4 protein expression in TMAs of TNBC patients. **(A)** KLK4-mTS **(B)** KLK4-mSS **(C)** KLK4-aTS **(D)** KLK4-aSS **(E)** KLK4-mLS **(F)** KLK4-mNS. (n=number of patients, e=number of events).

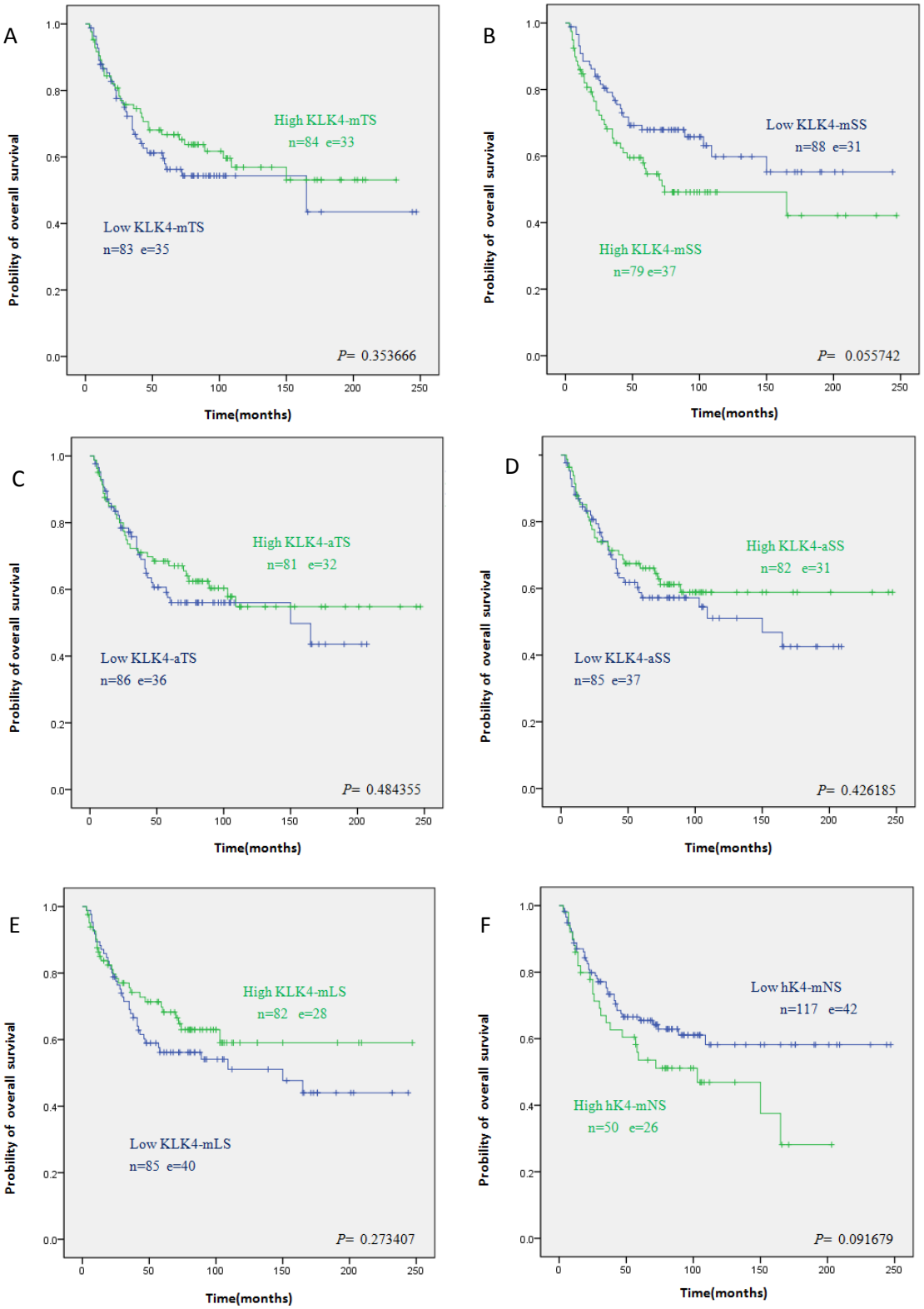

6. Discussion

Since breast cancer is considered a group of heterogeneous diseases, the previous “one size fits all” or "trial and error" concept should be abandoned in breast cancer treatment. Yet, in cancer treatment regimens, individualized therapy concepts do require specific biomarkers which can be applied to different cancer subgroups to predict the course of the disease or response to systemic therapy.

KLKs, a family of fifteen different serine proteases expressed in steroid hormone-dependent organs, are expressed in the breast as well, with KLK4 being the only one overexpressed in the malignant state of the breast. So far, no data were available correlating KLK4 protein overexpression with breast cancer disease-free or overall survival in the clinically important subgroup of triple-negative breast cancer (TNBC) patients, lacking expression of the surface receptors ER, PR, and HER2. Therefore, for the first time, this study was conducted to evaluate the clinical impact of KLK4 expression in a treated TNBC cohort completely lacking ER, PR, and HER2 expression.

Initially, expression of KLK4 and its localization at the cellular and subcellular level were analyzed employing different cell lines and different technologies such as qRCR, flow cytofluoremetry, immunocytostaining, western blotting, and CLSM technology. Proof was presented that KLK4 is a secreted protein, originally located in the cell’s cytoplasm, including tumor and non-tumor cells, but not being localized to the nucleus.

KLK4 expression in triple-negative breast cancers was assessed by immunohistichemistry using the proprietary selective antibody pAb587. Optimal working conditions to set up standard-operating-procedures (SOPs) for KLK4 immunostaining were established and protocoled in this study. Results show that manual assessment of immunostaining is superior

over automated scoring methodology. With that protocol, it was shown for 188 TNBC patients that KLK4 expression in stromal cells present in the tumor bed of TNBC specimens is indicative for disease-free and overall survival of TNBC patients, mainly treated with adjuvant polychemotherapy.

It has long been established that hormones play an important role in the pathogenesis of breast cancer. However, its hormone receptor-negative subgroup TNBC urgently needs the identification of novel biomarkers that can illustrate with ease tumor progression and dissemination. Although KLK4 has been reported to be upregulated in breast cancer[170], its pathologic and transcriptional role is still ill-defined. Especially, its expression, and thus clinical impact, in steroid hormone receptor-negative breast cancer (TNBC) has not been investigated yet. Thus, the first analysis of expression of KLK4 in triple-negative breast cancer cell lines was conducted in this study (Table 30). For this, expression and/or localization of KLK4 protein was assessed in numerous cell lines employing various techniques including immunocytochemistry (ICC), flow cytofluorometry (FACS), confocal laser scanning microscopy (CLSM), quantitative RT-PCR (qPCR) as well as western bloting (WB).

Table 30. Summary of cell lines and techniques used to investigate cellular KLK4 expression

Method	MCF-7	MDA-MB-231	OV-MZ-6-*wt*	Vector	KLK4 transfected
ICC*	-	-	na	-	+
FACS*	-	-	na	-	+
CLSM*	-	-	-	-	+
q-RT-PCR[#]	-	-	-	-	+
WB[#]	-	-	-	-	+

* Data from OV-MZ-6 pRc RSV vector/KLK4 cell line. # Data from PC-3 pRc RSV vector/KLK4 cell line. na=not available. ICC: immunocytochemistry. FACS: fluorescence activated cell sorting. CLSM: confocal laser scan microscopy. q-RT-PCR: quantitative RT-PCR. WB: western blotting. – means expression is negative. + means expression is positive.

Table 31. Summary of cell lines and techniques used to investigate localization of KLK4 on cellualar level.

Method	Intracellular	Extracellular	Cytoplasm	Nucleus
ICC*	+	-	na	na
FC*	+	na	na	na
CLSM[#]	+	na	+	-
Q-RT-PCR[#]	na	na	na	na
WB[#]	+	+++	+	-

* Data from OV-MZ-6 pRc RSV vector/KLK4 cell line. # Data from PC-3 pRc RSV vector/KLK4 cell line. na=not available. ICC: immunocytochemistry. FACS: fluorescence activated cell sorting. CLSM: confocal laser scan microscopy. q-RT-PCR: quantitative RT-PCR. WB: western blotting. – means expression is negative. + means expression is positive.

The summarized data indicate applicability of the proprietary antibody pAb587 for the detection and quantification KLK4 protein in human tumor cells, including triple-negative breast cancer cells. Our results demonstrate the lack of KLK4 expression in breast cancer cell lines MDA-MB-231 and MCF-7 as well of the ovarian cancer cell line OV-MZ-6-*wt*. Until today, no literature has been published describing the expression of KLK4 in hormone-negative breast cancer cell lines. Consequently, this is the first time of identifying lack of KLK4 expression in triple-negative breast cancer cell lines MCF7 and MDA-MB-231.

Previous reports on KLK4 expression in MCF-7 cells were either incomplete or showed contradictory results. The commercially available antibody HPA051839 (Sigma-Aldrich) to KLK4 demonstrated a negative reaction with MCF-7 cells. Antibody H-50: sc-20622 (Santa Cruz) to KLK4 showed a positive reaction in MCF-7 cells. Our findings, employing the monospecific, selective antibody pAB587 confirmed absence of KLK4 expression the MCF-7 and MDA-MB-231 cell line, data supported by lack of expression of KLK4 at the mRNA level. Yet, previous studies reported expression of KLK4 in hormone receptor-positive breast cancer

cell lines[180]. Our data demonstrated that KLK4 was well detected in transfected KLK4 overexpressing cell lines. Furthermore, contrary to a previous report[174] regarding prostate cancer, our experiments provided supporting evidence for the absence of a nuclear KLK4 form (Table 31).

KLK4 is synthesized as an inactive precursor with a 26-aa signal peptide followed by a 4-aa activation peptide and a 224-aa catalytic domain of the mature chain. A protease with a signal peptide may have extracellular substrates as is the case for the KLKs that have been biochemically characterized so far[176]. After cleavage of the signal peptide the proenzyme is activated extracellularly[40, 146]. Similar to other KLKs, KLK4 is secreted extracellularly and remains inactive until the prodomain is removed. We therefore anticipate that the antibody pAb587 is also direct to the activated form of the KLK4 protein.

Major discrepancy with reports in the literature[170, 174, 175] is description of a protein of a 40 kDa KLK4 protein as the nuclear form of KLK4. Although pAb587 detected the 40 kDa KLK4 band by western blotting of recKLK4 as well, its reduction by 5% BSA in conditioned culture medium revealed that it might not be a real KLK4 protein but rather a false-positive reaction with another cross-reacting antigen. As a histological proof, in our studies, pAb587 did not stain KLK4 in the nucleus of TNBC specimens.

In the triple-negative breast cancer collective investigated, weak to moderate KLK4 staining in tumor cells and tumor stromal cells was observed by immunohistochemistry employing pAb587. Interestingly, KLK4 immunoscores (KLK4-mSS) in tumor stroma cells evaluated by a manual scoring system is significantly associated with the presence of disease-free and overall survival. Automatic scoring of tumor stroma cells (KLK4-aSS) was found to be insufficient for potential clinical application. The studies also validated the relationship between KLK4 expression in the tumor stroma and elevated tumor grade of breast cancer patients[134, 151].

Both univariate and multivariate Cox regression analyses showed that besides the known cancer biomarkers age, tumor size, nuclear grade, nodal status, and KLK4 antigen levels expressed in tumor stroma cells might be potential predictors for disease-free and overall survival of TNBC patients. High KLK4 immunoscores in tumor stroma cells (KLK4-mSS) were found to be significantly associated with a high risk for tumor progression and early death of TNBC patients. Thus, KLK4 overexpression in tumor stroma cells is considered an unfavorable prognostic biomarker for TNBC patients treated with systemic cancer therapy.

Although the molecular mechanism of KLK4 regulating extracellular stroma remodeling is still in its infancy, one has to consider the following. It has been reported that enzymatically active KLK4 can convert enzymatically inactive pro-uPA into its active counterpart uPA (a serine protease) which in turn will bind to its specific transmembrane receptor (uPAR) resulting in the activation of inactive plasmin into the broad-specific serine protease plasmin, thus facilitating extracellular matrix remodeling and thereby promoting and supporting metastasis[58, 59, 179]. Besides that, KLK4 is also an endogenous activator of protease-activated receptor 1 and 2 (PAR1 PAR2) stimulating the proteolytic cleavage of PAR1 and 2 and subsequently promoting ERK1/2 activation in the surrounding stroma[61, 72]. Ultimately, its induction of interleukin-6 and other cytokines leads to the initiation of tumor–stroma interactions[73]. Thus, it is reasonable to conclude that KLK4 might be part of an enzymatic cascade pathway directly or indirectly regulating and modifying the tumor microenvironment through PAR1/2 signaling or uPA-plasminogen axis. In conclusion, we propose that KLK4 protein assessment may serve as a novel biomarker to predict disease progression and overall survival in the very aggressive TNBC subgroup. Such markers are scarce and urgently needed to aid with clinical decision making regarding adjuvant systemic therapy for this important breast cancer subgroup.

7. Summary

Triple-negative breast cancer (TNBC) is characterized by its aggressive pattern and resistance to endocrine therapies. Owing to the absence of specific molecular targets, still today, no effective therapies, except chemotherapy, are available for TNBC patients. In this respect, human kallikrein-related peptidases (KLKs) do provide a rich source of biomarkers instrumental for tumor cell dissemination and tumor progression. Considering its exclusively elevated overexpression in breast cancer at the mRNA and protein level, KLK4 draws focal attention among the other fourteen KLKs, not being overexpressed, to be a potential biomarker for describing the course of disease of the TNBC patients, also having received systemic adjuvant therapy.

So far, detailed research regarding the clinical utility of KLK4 as a disease-forecast biomarker in breast cancer is scarce. In studies published so far, quantitative assessment of KLK4 expression relied on the description of KLK4 mRNA expression or KLK4 protein expression determined by enzymometric assays (ELISA), only. Quantitative evaluation of KLK4 protein expression by immunohistochemistry method did not exist, thus, standard operating procedures (SOP) for KLK4 immunostaining were not available. As a result, the clinical impact of KLK4 for disease-free or overall survival in the clinically important breast cancer subgroup of TNBC patients was not assessed by immunohistochemistry yet.

Thus, the aim and objective of the present study was to explore at the by immunohistochemistry the potential role of the cancer biomarker human kallikrein-related peptidase 4 (KLK4) in triple-negative breast cancer specimens. For this, the KLK4-directed monospecific propriatory antibody pAb587 was first tested on different cell lines lacking KLK4 or overexpressing KLK4 by different technologies, including qRT-PCR, flow cytofluorometry (FACS), confocal laser

scanning microscopy (CLSM), and and immunocytochemistry. Results demonstrated expression of KLK4 mRNA, secretion of KLK4 into the culture medium, and localization of the KLK4 protein to the cytoplasm of KLK4 expressing tumor cell lines.

Standard operating procedures (SOP) for immunohistochemical staining and measures of quantification of KLK4 in tissue microarrays (TMAs) derived from primary tumor tissues of triple-negative breast cancer patients were established for manual and automatic scoring. Statistical analyses employing univariate and multivariate analyses, revealed the importance of elevated KLK4 expression in tumor stroma cells assessed by manual scoring (KLK4-mSS) to be associated with both disease-free and overall survival.

Evidently, KLK4, a serine protease secreted into the breast cancer tumor bed by tumor stromal cells may impact on the integrity of the breast extracellular matrix and thus may facilitate tumor cell dissemination, also in TNBC. Hence, quantitative assessment of KLK4 by immunohistochemistry in formalin-fixed paraffin-embedded TNBC specimens is a novel way of determining the fate of the TNBC patient, both for disease-free and overall survival.

8. Appendix

8.1 TNM-stage, description taken from American Joint Committee on Cancer (AJCC)

T Classifications (Primary tumor size)

Category	Definition
TX	Primary tumor cannot be assessed.
T0	No evidence of primary tumor.
Tis	Carcinoma *in situ*.
Tis (DCIS)	DCIS ductal carcinoma *in situ*.
Tis (LCIS)	LCIS lobular carcinoma *in situ*.
Tis (Paget)	Paget disease of the nipple NOT associated with invasive carcinoma and/or carcinoma *in situ* (DCIS and/or LCIS) in the underlying breast parenchyma. Carcinomas in the breast parenchyma associated with Paget disease are categorized based on the size and characteristics of the

	parenchymal disease although the presence of Paget disease should still be noted.
T1	Tumor ≤20 mm in greatest dimension.
T1mi	Tumor ≤1 mm in greatest dimension.
T1a	Tumor >1 mm but ≤ 5 mm in greatest dimension.
T1b	Tumor >5 mm but ≤ 10 mm in greatest dimension.
T1c	Tumor >10 mm but ≤ 20 mm in greatest dimension.
T2	Tumor >20 mm but ≤ 50 mm in greatest dimension.
T3	Tumor >50 mm in greatest dimension.
T4	Tumor of any size with direct extension to the chest wall and/or to the skin (ulceration or skin nodules)
T4a	Extension to the chest wall not including only pectoralis muscle adherence/invasion.
T4b	Ulceration and/or ipsilateral satellite nodules and/or edema (including peau d'orange) of the skin which do not meet the criteria for inflammatory carcinoma.
T4c	Both T4a and T4b.
T4d	Inflammatory carcinoma.

N Classifications (Nodal status)

Category	Definition
NX	Regional lymph nodes cannot be assessed (e. g. previously removed)
NX	Regional lymph nodes cannot be assessed (e. g. previously removed)
N0	No regional lymph node metastases.
N1	Metastases to movable ipsilateral level I II axillary lymph node(s)
N2	Metastases in ipsilateral level I II axillary lymph nodes that are clinically fixed or matted. OR Metastases in clinically detectedb ipsilateral internal mammary nodes in the absence of clinically evident axillary lymph node metastases.
N2a	Metastases in ipsilateral level I II axillary lymph nodes fixed to one another (matted) or to other structures.
N2b	Metastases only in clinically detectedb ipsilateral internal mammary nodes and in the absence of clinically evident level I II axillary lymph node metastases.
N3	Metastases in ipsilateral infraclavicular (level III axillary) lymph node (s) with or without level I II axillary lymph node involvement. OR Metastases in clinically detectedb ipsilateral internal mammary lymph node (s) with clinically evident level I II axillary lymph node metastases. OR Metastases in ipsilateral supraclavicular lymph node (s) with or without axillary or internal mammary lymph node involvement.
N3a	Metastases in ipsilateral infraclavicular lymph node(s)
N3b	Metastases in ipsilateral internal mammary lymph node(s) and axillary lymph node(s)
N3c	Metastases in ipsilateral supraclavicular lymph node(s)

M Classifications (Metastases)

Category	Definition
M0	No clinical or radiographic evidence of distant metastases.
cM0 (i+)	No clinical or radiographic evidence of distant metastases but deposits of molecularly or microscopically detected tumor cells in circulating blood bone marrow or other nonregional nodal tissue that are ≤0.2 mm in a patient without symptoms or signs of metastases.
M1	Distant detectable metastases as determined by classic clinical and radiographic means and/or histologically proven >0.2 mm.

TNM stage

Stage	T	N	M
0	Tis	N0	M0
IA	T1b	N0	M0
IB	T0	N1mi	M0
	T1b	N1mi	M0
IIA	T0	N1c	M0
	T1b	N1c	M0
	T2	N0	M0
IIB	T2	N1	M0
	T3	N0	M0
IIIA	T0	N2	M0
	T1b	N2	M0
	T2	N2	M0
	T3	N1	M0
	T3	N2	M0
IIIB	T4	N0	M0
	T4	N1	M0
	T4	N2	M0
IIIC	Any T	N3	M0
IV	Any T	Any N	M1

8.2 Nottingham grading system

Tubule formation	Majority of tumor (>75%)	1
	Moderate degree (10-75%)	2
	Little or none (<10%)	3
Mitotic count	0-9 mitoses/10 hpf	1
	10-19 mitoses/10 hpf	2
	20 or >mitoses/10 hpf	3
Nuclear pleomorphism	Small regular uniform cells	1

	Moderate nuclear size and variation	2
	Marked nuclear variation	2
Combined histologic grade	Low grade (I)	3-5
	Intermediate grade (II)	6-7
	High grade (III)	8-9

8.3 Different expression of KLK4 protein in KLK4-transfected OV-MZ-6 cell line detected with antibody pAb587 to KLK4

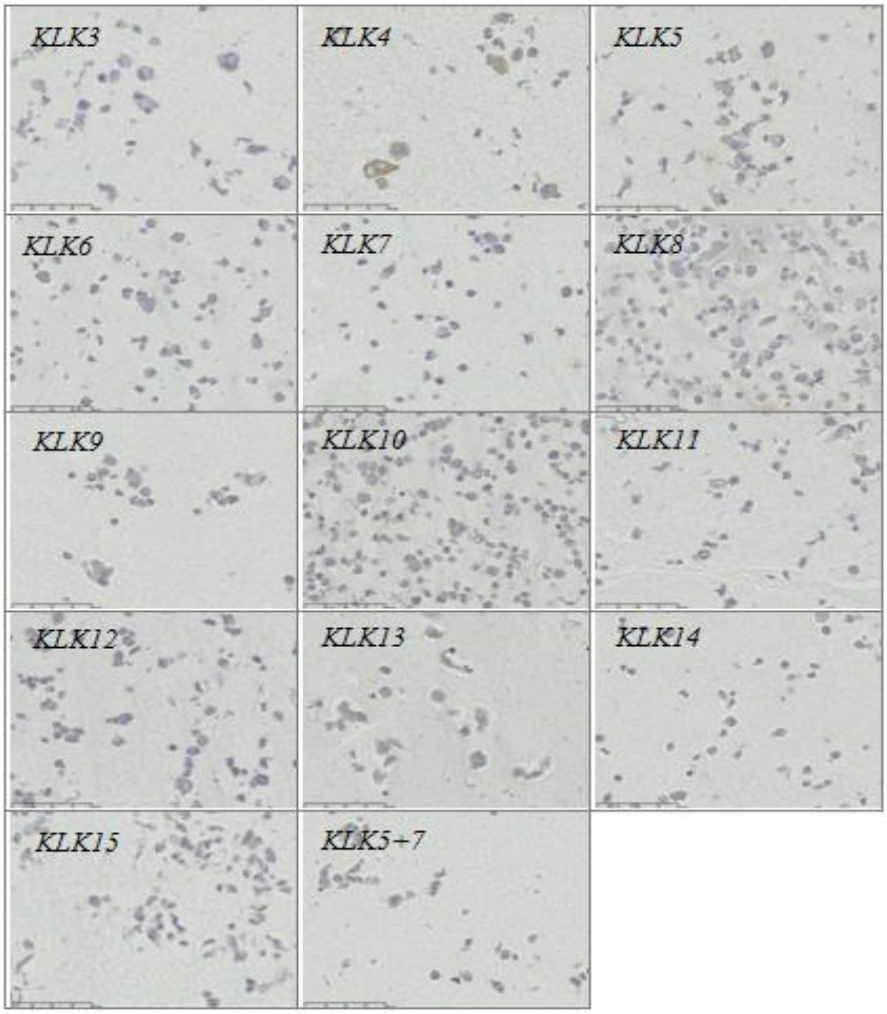

Figure 36. OV-MZ-6 cell line transfected with different KLKs (cell microarray): OV-MZ-6 pRc Rsv transfected with KLK3-15 each and combination of KLK5+7. Nuclei (blue, stained with hematoxylin). KLK4: brown (DAB Zytomed Polymer method). Magnification 400 x.

8.4 Different cell lines tested for KLK4 protein expression with KLK4-directed antibody pAb587

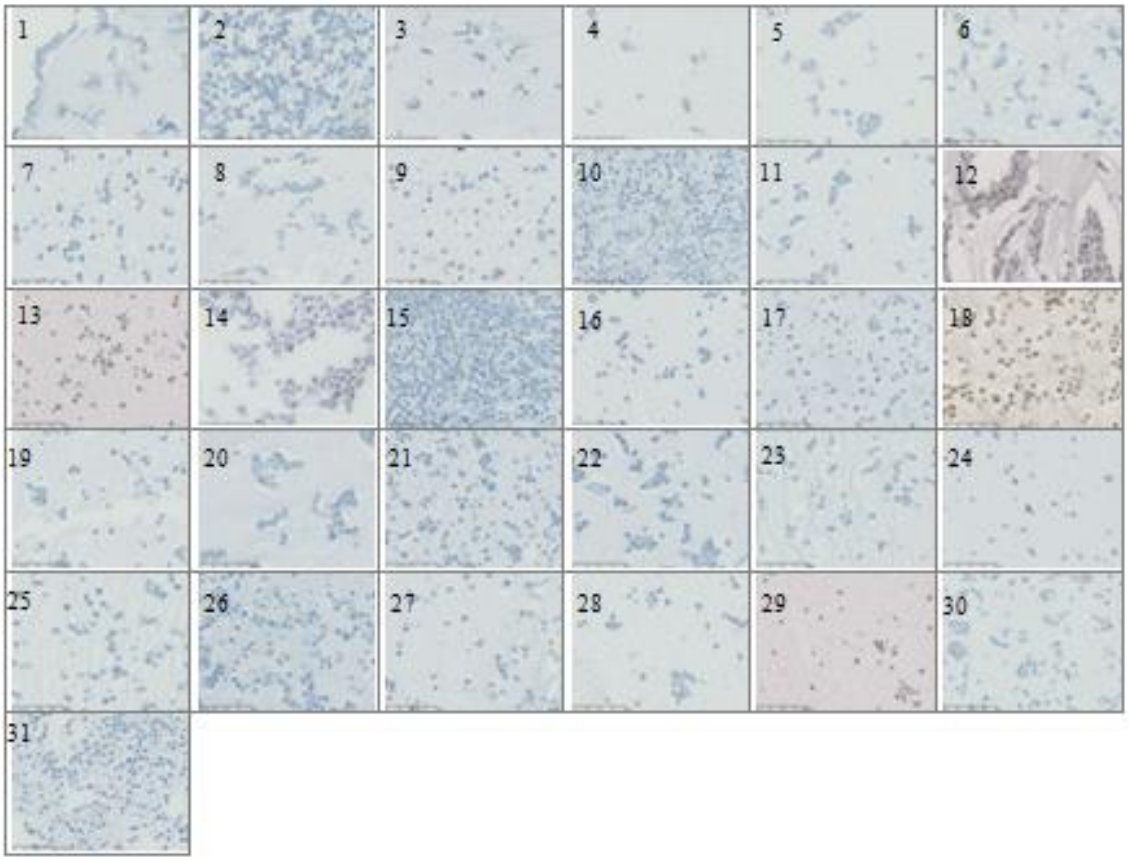

Figure 37. 31 different cell types as part of a cell microarray, stained with pAb587 to KLK4 (3.5 µg/mL) (1) BHY (2) BT-20 (3) CaCo-2 (4) Caki-1 (5) Cal 27 (6) DU-145 (7) EJ-28 (8) FaDu (9) HeLa (10) HL-60 (11) HT-1080 (12) LnCAP (13) lymphocytes (14) MCF-7 (15) MD-MB-435 (16) MD-MB-231 (17) OV-MZ-6-WT (18) OV-MZ-6 pRc Rsv KLK4 (19) OV-MZ-10 (20) OV-MZ-15 (21) OV-MZ-19 (22) PaTu-II (23) PC-3 (24) Raji (25) RT-112 (26) SaOS-2 (27) SK-BR-3 (28) SNB-19 (29) trophoblasts cells (30) U-2 OS (31) U-937. LnCAP OV-MZ-6 pRc Rsv KLK4 as the positive control; PC-3 U-2 OS as the negative control. KLK4 brown (DAB+), Nuclei blue (hematoxylin). Ventana Polymer method employed. Magnification 400 x.

8.5 Total RNA amounts measured by the NanoDrop apparatus

Cell line	Concentration (ng/µl)	$A_{260/280}$	$A_{260/230}$
MDA-MB-231	3,888.1	2.05	2.01
MCF-7	4,760.2	1.84	1.80
OV-MZ-6 WT	4,678.2	1.95	2.06
OV-MZ-6 RSV	4,310.5	1.84	1.89
OV-MZ-6 KLK4	4,681.5	1.94	1.95
PC-3 RSV	3,853.0	2.06	2.06
PC-3 KLK4	3,423.5	2.11	2.17

8.6 Set-up table for cytofluorometric assays (CLSM)

	DAPI	**Alexa Fluor® 488** Goat anti-rabbit IgG (H+L)	**Propidium iodide (PI)**	**Phalloidin** BODIPY650/665
Receptor	DNA/RNA	Fc portion of IgG	DNA /RNA	F-actin
Concentration	100 ng/ml	2 µg/ml	1 µg/ml	0.66 nM
Excitation	358 nm	496 nm	535 nm	647 nm
Emission	461 nm	519 nm	617 nm	661 nm
Filter	BP420-500	/	/	LP640
Scale	420-516	-556	640-	640-
Intensity	405 nm+2.6 %	488 nm+2.5 %	555 nm+2.7 %	639 nm+2.6 %
Pinhole	7 µm	4 µm	6.1 µm	4.2 µm
Gain setting	900	900	869	913

9. List of own publications

1. *Schmitt M, Magdolen V, **Yang F**, Kiechle M, Bayani J, Yousef GM, Scorilas A, Diamandis EP, Dorn J. Emerging clinical importance of the cancer biomarkers kallikrein-related peptidases (KLK) in female and male reproductive organ malignancies. Radiol Oncol. 2013; 47:319-329.*
2. *Dorn J, Bayani J, Yousef GM, **Yang F**, Magdolen V, Kiechle M, Diamandis EP, Schmitt M. Clinical utility of kallikrein-related peptidases (KLK) in urogenital malignancies. Thromb Haemost. 2013; 110:408-422.*

10. Acknowledgements

First of all, I would like to thank my doctoral father, my supervisor Prof. Dr. rer. nat. Dr. med. habil. Manfred Schmitt, who offered me the chance to work with him and allowed me to conduct this thesis. I could never have finished this project and learned systematic research methods without his consistent support and guidance, and this from the very beginning. I am so grateful that I could be part of his research team and work on such an interesting scientific topic. If this project is a ship, he is definitely the captain. I would also like to express my deep gratitude to Prof. Dr. rer. nat. habil. Viktor Magdolen who helped me a lot in introducing to me the research background of KLKs and sharing with me his inspiring thoughts. I am indebted to him for lots of constructive suggestions and valuable advice. There are also many other colleagues I would like to thank: Prof. Dr. rer. nat. Dr. med. habil. Ute Reuning, who gave me numerous valuable advice and showed me how to use the CLSM; Prof. Dr. med. Axel Walch who helped me with the evaluation of immunohistochemical staining; Dr. rer. nat. Eva Gross, Anita Welk (MTA) who

provided meaningful suggestions for patient data collection and statistical analyses; Elisabeth Schüren (MTA), Daniela Hellmann (VTA), Sabine Creutzburg (MTA), Dr. rer. nat. Rudolf Napieralski who all taught me basic experiments necessary for this thesis and also offered me their kind advice and assistance. I would also like to express my gratitude to some other colleagues who work in the Clinical Research Unit of the Department of Obstetrics and Gynecology of the Technical University of Munich, including Sandra Baur (VTA), Anke Benge (MTA), Alex Stöckel (MTA), and Alex Sturmheit (MTA). The space is just too little to mention all of them who assisted me; their assistance in realizing my project means a lot to me. Special thanks go to Claudia Beutner, the personal assistant to Prof. Schmitt, she is very kind and was always there whenever I needed help and assistance. My collaborators and doctoral fellows Dr. med. Nikolay Malyshev, Claudia Cerny, Dominik Alterauge, and Dr. med. Caixia Zhu, they all gave me lots of personal ideas on my research and also on my future career as a medical doctor back home. My Chinese professor, Prof. Dr. Tong, who gave me the chance of studying abroad and collaborating with such a wonderful team in such an amazing lab, he has given me unconditional support and help. Last but not least, my parents and my wife Xiaohui Liu. It was them who encouraged me to move forward whenever I found it was hard to persist and needed mental support.

11.References

1) GLOBOCAN 2012 v1. 0 Cancer Incidence and Mortality Worldwide: IARC CancerBase No. 11 [Internet]. Lyon France: International Agency for Research on Cancer; 2013.

2) American Cancer Society. Breast Cancer Facts & Figures 2013-2014. Atlanta: American Cancer Sociey. Inc. 2013.

3) Kim T, Giuliano AE, and Lyman GH. Lymphatic mapping and sentinel lymph node biopsy in early-stage breast carcinoma: a metaanalysis. Cancer. 2006; 106:4-16.

4) Giuliano AE, Hunt KK, Ballman KV, Beitsch PD, Whitworth PW, Blumencranz PW, Leitch AM, Saha S, McCall LM, and Morrow M. Axillary dissection vs no axillary dissection in women with invasive breast cancer and sentinel node metastasis: a randomized clinical trial. JAMA. 2011; 305:569-75.

5) Early Breast Cancer Trialists' Collaborative Group (EBCTCG). Effect of radiotherapy after breast-conserving surgery on 10-year recurrence and 15-year breast cancer death: meta-analysis of individual patient data for 10 801 women in 17 randomised trials. Lancet. 2011; 378 (9804):1707-16.

6) Mauri D, Pavlidis N, and Ioannidis JP. Neoadjuvant versus adjuvant systemic treatment in breast cancer: a meta-analysis. J Natl Cancer Inst. 2005 Feb 2; 97 (3):188-94.

7) Perou CM, Sørlie T, Eisen MB, van de Rijn M, Jeffrey SS, Rees CA, Pollack JR, Ross DT, Johnsen H, Akslen LA, Fluge O, Pergamenschikov A, Williams C, Zhu SX, Lønning PE, Børresen-Dale AL, Brown PO, and Botstein D. Molecular portraits of human breast tumours. Nature. 2000; 406 (6797):747-52.

8) Geyer FC, Marchio C, and Reis-Filho JS. The role of molecular analysis in breast cancer. Pathology. 2009; 41:77-88.

9) Edge SB, Byrd DR, and Compton CC. AJCC Cancer Staging Manual. 7th ed. New York NY: Springer 2010; 347-76

10) Simpson JF, Gray R, Dressler LG, Cobau CD, Falkson CI, Gilchrist KW, Pandya KJ, Page DL, and Robert NJ. Prognostic value of histologic grade and proliferative activity in axillary node-positive breast cancer: results from the Eastern Cooperative Oncology Group Companion Study EST4189. J Clin Oncol. 2000; 18:2059-69.

11) Krishnamurthy S, Poornima R, Challa VR, and Goud YG. Triple negative breast cancer - our experience and review. Indian J Surg Oncol. 2012; 3:12-6.

12) von Minckwitz G, Untch M, Blohmer JU, Costa SD, Eidtmann H, Fasching PA, Gerber B, Eiermann W, Hilfrich J, Huober J, Jackisch C, Kaufmann M, Konecny GE, Denkert C, Nekljudova V, Mehta K, and Loibl S. Definition and impact of pathologic complete response on prognosis after neoadjuvant chemotherapy in various intrinsic breast cancer subtypes. J Clin Oncol. 2012; 30:1796-804.

13) Early Breast Cancer Trialists' Collaborative Group (EBCTCG). Relevance of breast cancer hormone receptors and other factors to the efficacy of adjuvant tamoxifen: patient-level meta-analysis of randomised trials. Lancet. 2011; 378 (9793):771-84.

14) Dowsett M, Cuzick J, Ingle J, Coates A, Forbes J, Bliss J, Buyse M, Baum M, Buzdar A, Colleoni M, Coombes C, Snowdon C, Gnant M, Jakesz R, Kaufmann M, Boccardo F, Godwin J, Davies C, and Peto R. Meta-analysis of breast cancer outcomes in adjuvant trials of aromatase inhibitors versus tamoxifen. J Clin Oncol. 2010; 28:509-18.

15) Romond EH, Perez EA, Bryant J, Suman VJ, Geyer CE Jr, Davidson NE, Tan-Chiu E, Martino S, Paik S, Kaufman PA, Swain SM, Pisansky TM, Fehrenbacher L, Kutteh LA, Vogel VG, Visscher DW, Yothers G, Jenkins RB, Brown AM, Dakhil SR, Mamounas EP, Lingle WL, Klein PM, Ingle JN, and Wolmark N. Trastuzumab plus adjuvant chemotherapy for operable HER2-positive breast cancer. N Engl J Med. 2005; 353:1673-84.

16) Cameron D, Casey M, Oliva C, Newstat B, Imwalle B, and Geyer CE. Lapatinib plus capecitabine in women with HER-2-positive advanced breast cancer: final survival analysis of a phase III randomized trial. Oncologist. 2010; 15:924-34

17) Harbeck N, Kates RE, Look MP, Meijer-Van Gelder ME, Klijn JG, Krüger A, Kiechle M, Jänicke F, Schmitt M, and Foekens JA. Enhanced benefit from adjuvant chemotherapy in breast cancer patients classified high-risk according to urokinase-type plas minogen activator (uPA) and plasminogen activator inhibitor type 1. Cancer Res. 2002; 62:4617-22.

18) van de Rijn M, Perou CM, Tibshirani R, Haas P, Kallioniemi O, Kononen J, Torhorst J, Sauter G, Zuber M, Köchli OR, Mross F, Dieterich H, Seitz R, Ross D, Botstein D, and Brown P. Expression of cytokeratins 17 and 5 identifies a group of breast carcinomas with poor clinical outcome. Am J Pathol. 2002; 161:1991-6.

19) Rakha EA, Putti TC, Abd El-Rehim DM, Paish C, Green AR, Powe DG, Lee AH, Robertson JF, and Ellis IO. Morphological and immunophenotypic analysis of breast carcinomas with basal and myoepithelial differentiation. J Pathol. 2006; 208:495-506.

20) Bertucci F, Finetti P, Cervera N, Esterni B, Hermitte F, Viens P, and Birnbaum D. How basal are triple-negative breast cancers? Int J Cancer. 2008; 123:236-40.

21) Haffty BG, Yang Q, Reiss M, Kearney T, Higgins SA, Weidhaas J, Harris L, Hait W, and Toppmeyer D. Locoregional relapse and distant metastasis in conservatively managed triple negative early-stage breast cancer. J Clin Oncol. 2006; 24:5652-7.

22) Carey LA, Perou CM, Livasy CA, Dressler LG, Cowan D, Conway K, Karaca G, Troester MA, Tse CK, Edmiston S, Deming SL, Geradts J, Cheang MC, Nielsen TO, Moorman PG, Earp HS, and Millikan RC. Race breast cancer subtypes and survival in the Carolina Breast Cancer Study. JAMA. 2006; 295:2492-502.

23) Foulkes WD, Smith IE, and Reis-Filho JS. Triple-negative breast cancer. N Engl J Med. 2010; 363:1938-48.

24) Bonzanini M, Morelli L, Bonandini EM, Leonardi E, Pertile R, and Dalla Palma P. Cytologic features of triple-negative breast carcinoma. Cancer Cytopa. 2012; 120:401-9.

25) Foulkes WD, Brunet JS, Stefansson IM, Straume O, Chappuis PO, Bégin LR, Hamel N, Goffin JR, Wong N, Trudel M, Kapusta L, Porter P, and Akslen LA. The prognostic implication of the basal-like (cyclin E high/p27 low/p53+/glomeruloid-microvascular-proliferation+) phenotype of BRCA1-related breast cancer. Cancer Res. 2004; 64:830-5.

26) Rodríguez-Pinilla SM, Sarrió D, Honrado E, Moreno-Bueno G, Hardisson D, Calero F, Benítez J, and Palacios J. Vimentin and la minin expression is associated with basal-like phenotype in both sporadic and BRCA1-associated breast carcinomas. J Clin Pathol. 2007; 60:1006-12.

27) Dawood S, Broglio K, Esteva FJ, Yang W, Kau SW, Islam R, Albarracin C, Yu TK, Green M, Hortobagyi GN, and Gonzalez-Angulo AM. Survival among women with triple receptor-negative breast cancer and brain metastases. Ann Oncol. 2009; 20:621-7.

28) Pal SK, Childs BH, and Pegram M. Triple negative breast cancer: unmet medical needs. Breast Cancer Res Treat. 2011; 125:627-36.

29) Bayraktar S, and Glück S. Molecularly targeted therapies for metastatic triple-negative breast cancer. Breast Cancer Res Treat. 2013; 138:21-35.

30) Harris L, Fritsche H, Mennel R, Norton L, Ravdin P, Taube S, Somerfield MR, Hayes DF, and Bast RC Jr; American Society of Clinical Oncology 2007 update of recommendations for the use of tumor markers in breast cancer. J Clin Oncol. 2007; 25:5287-312.

31) Hayes DF, Bast RC, Desch CE, Fritsche H Jr, Kemeny NE, Jessup JM, Locker GY, Macdonald JS, Mennel RG, Norton L, Ravdin P, Taube S, and Winn RJ. Tumor marker utility grading system: a framework to evaluate clinical utility of tumor markers. J Nat Cancer Inst. 1996; 88:1456-66.

32) Foekens JA, Peters HA, Look MP, Portengen H, Schmitt M, Kramer MD, Brünner N, Jänicke F, Meijer-van Gelder ME, Henzen-Logmans SC, van Putten WL, and Klijn JG. The urokinase system of plas minogen activation and prognosis in 2780 breast cancer patients. Cancer Res. 2000; 60:636-43.

33) Dowsett M, and Dunbier AK. Emerging biomarkers and new understanding of traditional markers in personalized therapy for breast cancer. Clin Cancer Res. 2008; 14:8019-26.

34) Schmitt M, Mengele K, Napieralski R, Magdolen V, Reuning U, Gkazepis A, Sweep F, Brünner N, Foekens J, and Harbeck N. Clinical utility of level-of-evidence-1 disease forecast cancer biomarkers uPA and its inhibitor PAI-1. Expert Rev Mol Diagn. 2010; 10:1051-67

35) Kraut H, Frey EK, and Werle E. Der Nachweis eines Kreislaufhormons in der Pankreasdrüse. Hoppe-Seyler's Z Physiol Chem 189; 97–106.

36) Lundwall A, Band V, Blaber M, Clements JA, Courty Y, Diamandis EP, Fritz H, Lilja H, Malm J, Maltais LJ, Olsson AY, Petraki C, Scorilas A, Sotiropoulou G, Stenman UH, Stephan C, Talieri M, and Yousef GM. A comprehensive nomenclature for serine proteases with homology to tissue kallikreins. Biol Chem. 2006; 387:637-41.

37) Diamandis EP, Yousef GM, Soosaipillai AR, and Bunting P. Human kallikrein 6 (zyme/protease M/neurosin): a new serum biomarker of ovarian carcinoma. Clin Biochem. 2000; 33:579-83.

38) Obiezu CV, and Diamandis EP. Human tissue kallikrein gene family: applications in cancer. Cancer Lett. 2005; 224:1-22.

39) Goettig P, Magdolen V, and Brandstetter H. Natural and synthetic inhibitors of kallikrein-related peptidases (KLKs) Biochimie. 2010; 92:1546-67.

40) Borgoño CA, Michael IP, and Diamandis EP. Human tissue kallikreins: physiologic roles and applications in cancer. Mol Cancer Res. 2004; 2:257-80.

41) Yousef GM, and Diamandis EP. The new human tissue kallikrein gene family: structure function and association to disease. Endocr Rev. 2001; 22:184-204.

42) Clements JA, Willemsen NM, Myers SA, and Dong Y. The tissue kallikrein family of serine proteases: functional roles in human disease and potential as clinical biomarkers. Crit Rev Clin Lab Sci. 2004; 41:265-312.

43) Yousef GM, and Diamandis EP. Human tissue kallikreins: a new enzymatic cascade pathway ? Biol Chem. 2002; 383:1045-57.

44) Bhoola KD, Figueroa CD , and Worthy K. Bioregulation of kinins: kallikreins kininogens and kininases. Pharmacol Rev. 1992; 44:1-80.

45) Lilja H. A kallikrein-like serine protease in prostatic fluid cleaves the predo minant se minal vesicle protein. J Clin Invest. 1985; 76:1899-903.

46) Deperthes D, Frenette G, Brillard-Bourdet M, Bourgeois L, Gauthier F, Tremblay RR, and Dubé JY. Potential involvement of kallikrein hK2 in the hydrolysis of the human seminal vesicle proteins after ejaculation. J Androl. 1996; 17:659-65.

47) Charlesworth MC, Young CY, Miller VM, and Tindall DJ. Kininogenase activity of prostate-derived human glandular kallikrein (hK2) purified from seminal fluid. J Androl. 1999; 20:220-9.

48) Diamandis EP. New diagnostic applications and physiological functions of prostate specific antigen. Scand J Clin Lab Invest Suppl. 1995; 221:105-12.

49) Sauter ER, Daly M, Linahan K, Ehya H, Engstrom PF, Bonney G, Ross EA, Yu H, and Diamandis E. Prostate-specific antigen levels in nipple aspirate fluid correlate with breast cancer risk. Cancer Epidemiol Biomarkers Prev. 1996; 5:967-70.

50) Simmer JP, and Hu JC. Expression structure and function of enamel proteinases. Connect Tissue Res 2002; 43:441-9.

51) Michael IP, Sotiropoulou G, Pampalakis G, Magklara A, Ghosh M, Wasney G, and Diamandis EP. Biochemical and enzymatic characterization of human kallikrein 5 (hK5) a novel serine protease potentially involved in cancer progression. J Biol Chem. 2005; 280:14628-35.

52) Shan SJ, Scorilas A, Katsaros D, and Diamandis EP. Transcriptional upregulation of human tissue kallikrein 6 in ovarian cancer: clinical and mechanistic aspects. Br J Cancer. 2007; 96:362-72.

53) Little SP, Dixon EP, Norris F, Buckley W, Becker GW, Johnson M, Dobbins JR, Wyrick T, Miller JR, MacKellar W, Hepburn D, Corvalan J, McClure D, Liu X, Stephenson D, Clemens J, and Johnstone EM. Zyme a novel and potentially amyloidogenic enzyme cDNA isolated from Alzheimer's disease brain. J Biol Chem. 1997; 272:25135-42.

54) Sondell B, Jonsson M, Dyberg P, and Egelrud T. In situ evidence that the population of Langerhans cells in normal human epidermis may be heterogeneous. Br J Dermatol. 1997; 136:687-93.

55) Ekholm E, Sondell B, Strandén P, Brattsand M, and Egelrud T. Expression of stratum corneum chymotryptic enzyme in human sebaceous follicles. Acta Derm Venereol. 1998; 78:343-7.

56) Johnson SK, Ramani VC, Hennings L, and Haun RS. Kallikrein 7 enhances pancreatic cancer cell invasion by shedding E-cadherin. Cancer. 2007; 109:1811-20.

57) Stamenkovic I. Extracellular matrix remodelling: the role of matrix metalloproteinases. J Pathol. 2003; 200:448-64.

58) Frenette G, Tremblay RR, Lazure C, and Dube JY. Prostatic kallikrein hK2 but not prostate-specific antigen (hK3) activates single-chain urokinase-type pn activator. Int J Cancer 1997; 71:897-9.

59) Takayama TK, McMullen BA, Nelson PS, Matsumura M, and Fujikawa K. Characterization of hK4 (prostase) a prostate-specificserine protease: activation of the precursor of prostate specific antigen (pro-PSA) and single-chain urokinase type plasminogen activator and degradation of prostatic acidphosphatase. Biochemistry. 2001; 40:15341-8.

60) Egeblad M, and Werb Z. New functions for the matrix metalloproteinases in cancer progression. Nat Rev Cancer 2002; 2:161-74.

61) Mize GJ, Wang W, and Takayama TK. Prostate-specific kallikreins-2 and -4 enhance the proliferation of DU-145 prostate cancer cells through protease-activated receptors-1 and -2. Mol Cancer Res. 2008 Jun; 6:1043-51.

62) Bayés A, Tsetsenis T, Ventura S, Vendrell J, Aviles FX, and Sotiropoulou G. Humankallikrein 6 activityis regulated via an auto proteolytic mechanism of activation/inactivation. Biol Chem. 2004; 385:517-24

63) Rénhault S, Monget P, Mazerbourg S, Tremblay R, Gutman N, Gauthier F, and Moreau T. Insulin-like growth factor binding proteins (IGFBPs) aspotential physiological substrates for human kallikreins hK2and hK3. EurJ Biochem. 2001; 268:2960-8.

64) Koistinen H, Paju A, Koistinen R, Finne P, Lövgren J, Wu P, Seppälä M, and Stenman UH. Prostate-specific antigen and other prostate-derived proteases cleave IGFBP-3 but prostate cancer is not associated with proteolytically cleaved circulating IGFBP-3. Prostate. 2002; 50:112-8.

65) Matsumura M, Bhatt AS, Andress D, Clegg N, Takayama TK, Craik CS, and Nelson PS. Substrates of the prostate-specific serine protease prostase/KLK4 defined by positional-scanning peptide libraries. Prostate. 2005; 62:1-13.

66) Sano A, Sangai T, Maeda H, Nakamura M, Hasebe T, and Ochiai A. Kallikrein 11 expressed in human breast cancer cells releases insulin-like growth factor through degradation of IGFBP-3. Int J Oncol. 2007; 30:1493-8.

67) Borgoño CA, Michael IP, Shaw JL, Luo LY, Ghosh MC, Soosaipillai A, Grass L, Katsaros D, and Diamandis EP. Expression and functional characterization of the cancer-related serine protease human tissue kallikrein 14. J Biol Chem. 2007; 282:2405-22.

68) Samani AA, Yakar S, LeRoith D, and Brodt P. The role of the IGF system in cancer growth and metastasis: overview and recent insights. Endocr Rev. 2007; 28:20-47.

69) Emami N, and Diamandis EP. Utility of kallikrein-related peptidases (KLKs) as cancer biomarkers. Clin Chem. 2008; 54:1600-7.

70) Oikonomopoulou K, Hansen KK, Saifeddine M, Tea I, Blaber M, Blaber SI, Scarisbrick I, Andrade-Gordon P, Cottrell GS, Bunnett NW, Diamandis EP, and Hollenberg MD. Proteinase-activated receptors targets for kallikrein signaling. J Biol Chem. 2006; 281:32095-112.

71) Chung H, Hamza M, Oikonomopoulou K, Gratio V, Saifeddine M, Virca GD, Diamandis EP, Hollenberg MD, and Darmoul D. Kallikrein-related peptidase signaling in colon carcinoma cells: targeting proteinase-activated receptors. Biol Chem. 2012; 393:413-20.

72) Ramsay AJ, Dong Y, Hunt ML, Linn M, Samaratunga H, Clements JA, and Hooper JD. Kallikrein-related peptidase 4 (KLK4) initiates intracellular signaling via protease-activated receptors (PARs) KLK4 and PAR-2 are co-expressed during prostate cancer progression. J Biol Chem. 2008; 283:12293-304.

73) Wang W, Mize GJ, Zhang X, and Takayama TK. Kallikrein-related peptidase-4 initiates tumor-stroma interactions in prostate cancer through protease-activated receptor-1. Int J Cancer. 2010; 126:599-610.

74) Mason SD, and Joyce JA. Proteolytic networks in cancer. Trends Cell Biol. 201121:228-37.

75) Magklara A, Mellati AA, Wasney GA, Little SP, Sotiropoulou G, Becker GW, and Diamandis EP. Characterization of the enzymatic activity of human kallikrein 6: Autoactivation substrate specificity and regulation by inhibitors. Biochem Biophys Res Commun. 2003; 307:948-55.

76) Tschesche H, Michaelis J, Kohnert U, Fedrowitz J, and Oberhoff R. Tissue kallikrein effectively activates latent matrix degrading metalloenzymes. Adv Exp Med Biol. 1989; 247A:545-8.

77) Menashi S, Fridman R, Desrivieres S, Lu H, Legrand Y, and Soria C. Regulation of 92-kD gelatinase B activity in the extracellular matrix by tissue kallikrein. Ann N Y Acad Sci. 994; 732:466-8.

78) Mikolajczyk SD, Millar LS, Marker KM, Grauer LS, Goel A, Cass MM, Kumar A, and Saedi MS. Ala217 is important for the catalytic function and autoactivation of prostate-specific human kallikrein 2. Eur J Biochem. 1997; 246:440-6.

79) Kapadia C, Ghosh MC, Grass L, and Diamandis EP. Human kallikrein 13 involvement in extracellular matrix degradation. Biochem Biophys Res Commun. 2004; 323:1084-90.

80) Yoon H, Blaber SI, Debela M, Goettig P, Scarisbrick IA, and Blaber M. A completed KLK activome profile: investigation of activation profiles of KLK9 10 and 15. Biol Chem. 2009; 390:373-7.

81) Thiery JP, Acloque H, Huang RY, and Nieto MA. Epithelial-mesenchymal transitions in development and disease. Cell. 2009; 139:871-90.

82) Gao L, Chao L, and Chao J. A novel signaling pathway of tissue kallikrein in promoting keratinocyte migration: activation of proteinase-activated receptor 1 and epidermal growth factor receptor. Exp Cell Res. 2010; 316:376-89

83) Veveris-Lowe TL, Lawrence MG, Collard RL, Bui L, Herington AC, Nicol DL, and Clements JA. Kallikrein 4 (hK4) and prostate-specific antigen (PSA) are associated with the loss of E-cadherin and an epithelial-mesenchymal transition (EMT) -like effect in prostate cancer cells. Endocr Relat Cancer. 2005; 12:631-43.

84) Derynck R, Akhurst RJ, and Balmain A. TGF-beta signaling in tumor suppression and cancer progression. Nat Genet. 2001; 29:117-29.

85) Pampalakis G, Prosnikli E, Agalioti T, Vlahou A, Zoumpourlis V, and Sotiropoulou G. A tumor-protective role for human kallikrein-related peptidase 6 in breast cancer mediated by inhibition of epithelial-to-mesenchymal transition. Cancer Res. 2009; 69:3779-87.

86) Mo L, Zhang J, and Shi J. Human kallikrein 7 induces epithelial-mesenchymaltransition like changes In prostate carcinoma cells: a role inprostate cancer invasion and progression. Anticancer Res. 2010; 30:3413-20.

87) Dallas SL, Zhao S, Cramer SD, Chen Z, Peehl DM, and Bonewald LF. Preferential production of latent transforming growth factor beta-2 by primary prostatic epithelial cells and its activation by prostate-specific antigen. J Cell Physiol. 2005; 202:361-70.

88) Emanueli C, Minasi A, Zacheo A, Chao J, Chao L, Salis MB, Straino S, Tozzi MG, Smith R, Gaspa L, Bianchini G, Stillo F, Capogrossi MC, and Madeddu P. Local delivery of human tissue kallikrein gene accelerates spontaneous angiogenesis in mouse model of hindlimb ischemia. Circulation. 2001; 103:125-32.

89) Heidtmann HH, Nettelbeck DM, Mingels A, Jäger R, Welker HG, and Kontermann RE. Generation of angiostatin-like fragments from plasminogen by prostate-specific antigen. Br J Cancer. 1999; 81:1269-73.

90) Sotiropoulou G, Rogakos V, Tsetsenis T, Pampalakis G, Zafiropoulos N, Simillides G, Yiotakis A, and Diamandis EP. Emerging interest in the kallikrein gene family for understanding and diagnosing cancer. Oncol Res 2003; 13:381-91.

91) Guillon-Munos A, Oikonomopoulou K, Michel N, Smith CR, Petit-Courty A, Canepa S, Reverdiau P, Heuzé-Vourc'h N, Diamandis EP, and Courty Y. Kallikrein-related peptidase 12 hydrolyzes matricellular proteins of the CCN family and modifies interactions of CCN1 and CCN5 with growth factors. J Biol Chem. 2011; 286:25505-18.

92) Henrikson KP, Salazar SL, Fenton JW 2nd, and Pentecost BT. Role of thrombin receptor in breast cancer invasiveness. Br J Cancer. 1999; 79:401-6.

93) Kamath L, Meydani A, Foss F, and Kuliopulos A. Signaling from protease-activated receptor-1 inhibits migration and invasion of breast cancer cells. Cancer Res. 2001; 61:5933-40.

94) Cramer SD, Chen Z, and Peehl DM. Prostate specific antigen cleaves parathyroid hormone-related protein in the PTH-like domain: inactivation of PTHrP-stimulated cAMP accumulation in mouse osteoblasts. J Urol. 1996; 156:526-31.

95) Gao J, Collard RL, Bui L, Herington AC, Nicol DL, and Clements JA. Kallikrein 4 is a potential mediator of cellular interactions between cancer cells and osteoblasts in metastatic prostate cancer. Prostate. 2007; 67:348-60.

96) Magklara A, Scorilas A, and Stephan C. Decreased concentrations of prostate-specific antigen and human glandular kallikrein 2 in malignant versus non malignant prostatic tissue. Urology. 2000; 56:527-32.

97) Steuber T, Vickers AJ, Serio AM, Vaisanen V, Haese A, Pettersson K, Eastham JA, Scardino PT, Huland H, and Lilja H. Comparison of free and total forms of serum human kallikrein 2 and prostate-specific antigen for prediction of locally advanced and recurrent prostate cancer. Clin Chem. 2007; 53:233-40.

98) Avgeris M, Mavridis K, and Scorilas A. Kallikrein-related peptidase genes as promising biomarkers for prognosis and monitoring of human malignancies. Biol Chem. 2010; 391:505-11.

99) Lilja H, Ulmert D, and Vickers AJ. Prostate-specific antigen and prostate cancer: prediction detection and monitoring. Nat Rev Cancer. 2008; 8:268-78.

100) Klokk TI, Kilander A, Xi Z, Waehre H, Risberg B, Danielsen HE, and Saatcioglu F. Kallikrein 4 is a proliferative factor that is overexpressed in prostate cancer. Cancer Res. 2007; 67:5221-30.

101) Xi Z, Kaern J, Davidson B, Klokk TI, Risberg B, Tropé C, and Saatcioglu F. Kallikrein 4 is associated with paclitaxel resistance in ovarian cancer. Gynecol Oncol. 2004; 94:80-5.

102) Korbakis D, Gregorakis AK, and Scorilas A. Quantitative analysis of human kallikrein 5 (KLK5) expression in prostate needle biopsies: an independent cancer biomarker. Clin Chem. 2009; 55 :904-13

103) Nakamura T, Scorilas A, Stephan C, Jung K, Soosaipillai AR, and Diamandis EP. The usefulness of serum human kallikrein 11 for discriminating between prostate cancer and benign prostatic hyperplasia. Cancer Res. 2003; 63:6543-6.

104) Bi X, He H, Ye Y, Dai Q, Han Z, Liang Y, and Zhong W. Association of TMPRSS2 and KLK11 gene expression levels with clinical progression of human prostate cancer. Med Oncol. 2010; 27:145-51.

105) Rabien A, Fritzsche F, Jung M, Diamandis EP, Loening SA, Dietel M, Jung K, Stephan C, and Kristiansen G. High expression of KLK14 in prostatic adenocarcinoma is associated with elevated risk of prostate-specific antigen relapse. Tumour Biol. 2008; 29 (1):1-8.

106) Stephan C, Yousef GM, Scorilas A, Jung K, Jung M, Kristiansen G, Hauptmann S, Bharaj BS, Nakamura T, Loening SA, and Diamandis E. Quantitative analysis of kallikrein 15 gene expression in prostate tissue. J Urol. 2003 Jan; 169 (1):361-4.

107) Paliouras M, and Diamandis EP. The kallikrein world: an update on the human tissue kallikreins. Biol Chem. 2006; 387:643-52.

108) Dong Y, Kaushal A, Bui L, Chu S, Fuller PJ, Nicklin J, Samaratunga H, and Clements JA. Human kallikrein 4 (KLK4) is highly expressed in serous ovarian carcinomas. Clin Cancer Res. 2001; 7:2363-71.

109) Obiezu CV, Scorilas A, Katsaros D, Massobrio M, Yousef GM, Fracchioli S, Rigault de la Longrais IA, Arisio R, and Diamandis EP. Higher human kallikrein gene 4 (KLK4) expression indicates poor prognosis of ovarian cancer patients. Clin Cancer Res. 2001 Aug; 7 (8):2380-6.

110) Mavridis K, and Scorilas A. Prognostic value and biological role of the kallikrein-related peptidases in human malignancies. Future Oncol. 2010; 6:269-85.

111) Kim H, Scorilas A, Katsaros D, Yousef GM, Massobrio M, Fracchioli S, Piccinno R, Gordini G, and Diamandis EP. Human kallikrein gene 5 (KLK5) expression is an indicator of poor prognosis in ovarian cancer. Br J Cancer. 2001; 84:643-50.

112) Dorn J, Harbeck N, Kates R, Gkazepis A, Scorilas A, Soosaipillai A, Diamandis E, Kiechle M, Schmalfeldt B, and Schmitt M. Impact of expression differences of kallikrein-related peptidases and of uPA and PAI-1 between primary tumor and omentum metastasis in advanced ovarian cancer. Ann Oncol. 2011; 22:877-83.

113) Diamandis EP, Yousef GM, Soosaipillai AR, and Bunting P. Human kallikrein 6 (zyme/protease M/neurosin): a new serum biomarker of ovarian carcinoma. Clin Biochem. 2000; 33:579-83.

114) Luo LY, Grass L, and Diamandis EP. Steroid hormone regulation of the human kallikrein 10 (KLK10) gene in cancer cell lines and functional characterization of the KLK10 gene promoter. Clin Chim Acta. 2003; 337:115-26.

115) Yousef GM, and Diamandis EP. The human kallikrein gene family: new biomarkers for ovarian cancer. Cancer Treat Res. 2009; 149:165-87.

116) White NM, Mathews M, Yousef GM, Prizada A, Fontaine D, Ghatage P, Popadiuk C, Dawson L, and Dor é JJ. Human kallikrein related peptidases 6 and 13 in combination withCA125 is a more sensitive test for ovarian cancer than CA125 alone. Cancer Biomark. 2009; 5:279-87.

117) Diamandis EP, Yousef GM, Luo LY, Magklara A, and Obiezu CV. The new human kallikrein gene family: implications in carcinogenesis. Trends Endocrinol Metab. 2000; 11:54-60.

118) Hoffman BR, Katsaros D, Scorilas A, Diamandis P, Fracchioli S, Rigault de la Longrais IA, Colgan T, Puopolo M, Giardina G, Massobrio M, and Diamandis EP. Immunofluorometric quantitation and histochemical localisation of kallikrein 6 protein in ovarian cancer tissue: a new independent unfavourable prognostic biomarker. Br J Cancer. 2002; 87:763-71.

119) Koh SC, Razvi K, Chan YH, Narasimhan K, Ilancheran A, Low JJ, and Choolani M. The association with age human tissue kallikreins 6 and 10 and hemostatic markers for survival outcome from epithelial ovarian cancer. Arch Gynecol Obstet. 2011; 284:183-90.

120) Kyriakopoulou LG, Yousef GM, Scorilas A, Katsaros D, Massobrio M, Fracchioli S, and Diamandis EP. Prognostic value of quantitatively assessed KLK7 expression in ovarian cancer. Clin Biochem. 2003; 36:135-43.

121) Dong Y, Tan OL, Loessner D, Stephens C, Walpole C, Boyle GM, Parsons PG, and Clements JA. Kallikrein-related peptidase 7 promotes multicellular aggregation via the alpha (5) beta (1) integrin pathway and paclitaxel chemoresistance in serous epithelial ovarian carcinoma. Cancer Res. 2010; 70:2624-33.

122) Shigemasa K, Tian X, Gu L, Tanimoto H, Underwood LJ, O'Brien TJ, and Ohama K. Human Kallikrein 8 (hK8/TADG-14) expression is associated with an early clinical stage and favorable prognosis in ovarian cancer. Oncol Rep. 2004; 11: 1153-9.

123) Borgoño CA, Kishi T, Scorilas A, Harbeck N, Dorn J, Schmalfeldt B, Schmitt M, and Diamandis EP. Human kallikrein 8 protein is a favorable prognostic marker in ovarian cancer. Clin Cancer Res. 2006; 12:1487-93.

124) Kountourakis P, Psyrri A, Scorilas A, Markakis S, Kowalski D, Camp RL, Diamandis EP, and Dimopoulos MA. Expression and prognostic significance of kallikrein-related peptidase 8 protein levels in advanced ovarian cancer by using automated quantitative analysis. Thromb Haemost. 2009; 101:541-6.

125) Yousef GM, Kyriakopoulou LG, Scorilas A, Fracchioli S, Ghiringhello B, Zarghooni M, Chang A, Diamandis M, Giardina G, Hartwick WJ, Richiardi G, Massobrio M, Diamandis EP, and Katsaros

D. Quantitative expression of the human Kallikrein gene 9 (KLK9) in ovarian cancer: a new independent and favorable prognostic marker. Cancer Res. 2001; 61:7811-8.

126) Sidiropoulos M, Pampalakis G, Sotiropoulou G, Katsaros D, and Diamandis EP. Downregulation of human kallikrein 10 (KLK10/NES1) by CpG island hypermethylation in breast ovarian and prostate cancers. Tumour Biol. 2005; 26:324-36.

127) Borgoño CA, Fracchioli S, Yousef GM, Rigault de la Longrais IA, Luo LY, Soosaipillai A, Puopolo M, Grass L, Scorilas A, Diamandis EP, and Katsaros D. Favorable prognostic value of tissue human kallikrein 11 (hK11) in patients with ovarian carcinoma. Int J Cancer. 2003; 106:605-10.

128) White NM, Mathews M, Yousef GM, Prizada A, Popadiuk C, and Doré JJ. KLK6 and KLK13 predict tumor recurrence in epithelial ovarian carcinoma. Br J Cancer. 2009; 101:1107-13.

129) Yousef GM, Stephan C, Scorilas A, Ellatif MA, Jung K, Kristiansen G, Jung M, Polymeris ME, Diamandis EP. Differential expression of the human kallikrein gene 14 (KLK14) in normal and cancerous prostatic tissues. Prostate. 2003; 56:287-92.

130) Yousef GM, Scorilas A, Katsaros D, Fracchioli S, Iskander L, Borgono C, Rigault de la Longrais IA, Puopolo M, Massobrio M, and Diamandis EP. Prognostic value of the human kallikrein gene 15 expression in ovarian cancer. J Clin Oncol. 2003; 21:3119-26.

131) Shaw JL, and Diamandis EP. Distribution of 15 human kallikreins in tissues and biological fluids. Clin Chem. 2007; 53:1423-32

132) Schmitt M, Magdolen V, Yang F, Kiechle M, Bayani J, Yousef GM, Scorilas A, Diamandis EP, and Dorn J. Emerging clinical importance of the cancer biomarkers kallikrein-related peptidases (KLK) in female and male reproductive organ malignancies. Radiol Oncol. 2013; 47:319-29.

133) Yousef GM, Yacoub GM, Polymeris ME, Popalis C, Soosaipillai A, and Diamandis EP. Kallikrein gene downregulation in breast cancer. Br J Cancer. 2004; 90:167-72.

134) Mangé A, Desmetz C, Berthes ML, Maudelonde T, and Solassol J. Specific increase of human kallikrein 4 mRNA and protein levels in breast cancer stromal cells. Biochem Biophys Res Commun. 2008; 375:107-12

135) Avgeris M, Mavridis K, and Scorilas A. Kallikrein-related peptidases in prostate breast and ovarian cancers: from pathobiology to clinical relevance. Biol Chem. 2012; 393:301-17.

136) Anisowicz A, Sotiropoulou G, Stenman G, Mok SC, and Sager R. A novel protease homolog differentially expressed in breast and ovarian cancer. Mol Med. 1996; 2:624-36.

137) Yousef GM, Borgoño CA, White NM, Robb JD, Michael IP, Oikonomopoulou K, Khan S, and Diamandis EP. In silico analysis of the human kallikrein gene 6. Tumour Biol. 2004; 25:282-9.

138) Yousef GM, Magklara A, Chang A, Jung K, Katsaros D, and Diamandis EP. Cloning of a new member of the human kallikrein gene family KLK14 which is down-regulated in different malignancies. Cancer Res. 2001; 61:3425-31.

139) Fritzsche F, Gansukh T, Borgoño CA, Burkhardt M, Pahl S, Mayordomo E, Winzer KJ, Weichert W, Denkert C, Jung K, Stephan C, Dietel M, Diamandis EP, Dahl E, and Kristiansen G. Expression of human Kallikrein 14 (KLK14) in breast cancer is associated with higher tumour grades and positive nodal status. Br J Cancer. 2006; 94:540-7.

140) Papachristopoulou G, Avgeris M, Charlaftis A, and Scorilas A. Quantitative expression analysis and study of the novel human kallikrein-related peptidase 14 gene (KLK14) in malignant and benign breast tissues. Thromb Haemost. 2011; 105:131-7.

141) Sauter ER, Lininger J, Magklara A, Hewett JE, and Diamandis EP. Association of kallikrein expression in nipple aspirate fluid with breast cancer risk. Int J Cancer. 2004; 108:588-91.

142) Black MH, and Diamandis EP. The diagnostic and prognostic utility of prostate-specific antigen for diseases of the breast. Breast Cancer Res Treat. 2000; 59:1-14.

143) Yousef GM, Polymeris ME, Grass L, Soosaipillai A, Chan PC, Scorilas A, Borgoño C, Harbeck N, Schmalfeldt B, Dorn J, Schmitt M, and Diamandis EP. Human kallikrein 5: a potential novel serum biomarker for breast and ovarian cancer. Cancer Res. 2003; 63:3958-65.

144) Ewan King L, Li X, Cheikh Saad Bouh K, Pedneault M, and Chu CW. Human kallikrein 10 ELISA development and validation in breast cancer sera. Clin Biochem. 2007; 40:1057-62.

145) Borgoño CA, Grass L, Soosaipillai A, Yousef GM, Petraki CD, Howarth DH, Fracchioli S, Katsaros D, and Diamandis EP. Human kallikrein 14: a new potential biomarker for ovarian and breast cancer. Cancer Res. 2003; 63:9032-41.

146) Borgoño CA, and Diamandis EP. The emerging roles of human tissue kallikreins in cancer. Nat Rev Cancer. 2004; 4:876-90.

147) Emami N, and Diamandis EP. Utility of kallikrein-related peptidases (KLKs) as cancer biomarkers. Clin Chem. 2008; 54:1600-7.

148) Wolf WC, Evans DM, Chao L, and Chao J. A synthetic tissue kallikrein inhibitor suppresses cancer cell invasiveness. Am J Pathol. 2001; 159:1797-805.

149) Yu H, Levesque MA, Clark GM, and Diamandis EP. Prognostic value of prostate-specific antigen for women with breast cancer: a large United States cohort study. Clin Cancer Res. 1998; 4:1489-97.

150) Foekens JA, Diamandis EP, Yu H, Look MP, Meijer-van Gelder ME, van Putten WL, and Klijn JG. Expression of prostate-specific antigen (PSA) correlates with poor response to tamoxifen therapy in recurrent breast cancer. Br J Cancer. 1999; 79:888-94.

151) Papachristopoulou G, Avgeris M, and Scorilas A. Expression analysis and study of KLK4 in benign and malignant breast tumours. Thromb Haemost. 2009 Feb; 1 01 (2):381-7.

152) Avgeris M, Papachristopoulou G, and Polychronis A. Down-regulation of kallikrein-related peptidase 5 (KLK5) expression in breast cancer patients: a biomarker for the differential diagnosis of breast lesions. Clin Proteomics. 2011 May; 31;8 (1):5

153) Yousef GM, Scorilas A, Kyriakopoulou LG, Rendl L, Diamandis M, Ponzone R, Biglia N, Giai M, Roagna R, Sismondi P, and Diamandis EP. Human kallikrein gene 5 (KLK5) expression by quantitative PCR: an independent indicator of poor prognosis in breast cancer. Clin Chem. 2002 Aug; 48 (8):1241-50.

154) Talieri M, Devetzi M, Scorilas A, Prezas P, Ardavanis A, Apostolaki A, and Karameris A. Evaluation of kallikrein-related peptidase 5 expression and its significance for breast cancer patients: association with kallikrein-related peptidase 7 expression. Anticancer Res. 2011 Sep; 31 (9):3093-100.

155) Li X, Liu J, Wang Y, Zhang L, Ning L, and Feng Y. Parallel underexpression of kallikrein 5 and kallikrein 7 mRNA in breast malignancies. Cancer Sci. 2009 Apr; 100 (4):601-7.

156) Talieri M, Diamandis EP, Gourgiotis D, Mathioudaki K, and Scorilas A. Expression analysis of the human kallikrein 7 (KLK7) in breast tumors: a new potential biomarker for prognosis of breast carcinoma. Thromb Haemost. 2004 Jan; 91 (1):180-6.

157) Holzscheiter L, Biermann JC, Kotzsch M, Prezas P, Farthmann J, Baretton G, Luther T, Tjan-Heijnen VC, Talieri M, Schmitt M, Sweep FC, Span PN, and Magdolen V. Quantitative reverse transcription-PCR assay for detection of mRNA encoding full-length human tissue kallikrein 7: prognostic relevance of KLK7 mRNA expression in breast cancer. Clin Chem. 2006 Jun; 52 (6):1070-9.

158) Yousef GM, Scorilas A, Nakamura T, Ellatif MA, Ponzone R, Biglia N, Maggiorotto F, Roagna R, Sismondi P, and Diamandis EP. The prognostic value of the human kallikrein gene 9 (KLK9) in breast cancer. Breast Cancer Res Treat. 2003 Mar; 78 (2):149-58.

159) Yousef GM, White NM, and Michael IP. Identification of new splice variants and differential expression of the human kallikrein 10 gene, a candidate cancer biomarker. Tumour Biol. 2005 Sep-Oct; 26 (5):227-35.

160) Kioulafa M, Kaklamanis L, Stathopoulos E, Mavroudis D, Georgoulias V, and Lianidou ES. Kallikrein 10 (KLK10) methylation as a novel prognostic biomarker in early breast cancer. Ann Oncol. 2009 Jun;20 (6):1020-5.

161) Luo LY, Diamandis EP, and Look MP. Higher expression of human kallikrein 10 in breast cancer tissue predicts tamoxifen resistance. Br J Cancer. 2002 Jun 5; 86 (11):1790-6.

162) Chang A, Yousef GM, Scorilas A, Grass L, Sismondi P, Ponzone R, and Diamandis EP. Human kallikrein gene 13 (KLK13) expression by quantitative RT-PCR: an independent indicator of favourable prognosis in breast cancer. Br J Cancer. 2002 May 6; 86 (9):1457-64.

163) Yousef GM, Borgoño CA, and Scorilas A. Quantitative analysis of human kallikrein gene 14 expression in breast tumours indicates association with poor prognosis. Br J Cancer. 2002 Nov 18;87 (11):1287-93.

164) Yousef GM, Scorilas A, Magklara A, Memari N, Ponzone R, Sismondi P, Biglia N, Abd Ellatif M, and Diamandis EP. The androgen-regulated gene human kallikrein 15 (KLK15) is an independent and favourable prognostic marker for breast cancer. Br J Cancer. 2002 Nov 18; 87 (11):1294-300.

165) Nelson PS, Gan L, and Ferguson C. Molecular cloning and characterization of prostase, an androgen-regulated serine protease with prostate-restricted expression. Proc Natl Acad Sci U S A. 1999 Mar 16; 96 (6):3114-9.

166) Simmer JP, Hu Y, Lertlam R, Yamakoshi Y, and Hu JC. Hypomaturation enamel defects in KLK4 knockout/LacZ knockin mice. J Biol Chem. 2009 Jul 10; 284 (28): 19110-21.

167) Davidson B, Xi Z, and Saatcioglu F. Kallikrein 4 is expressed in malignant mesothelioma-further evidence for the histogenetic link between mesothelial and epithelial cells. Diagn Cytopathol. 2007 Feb;35 (2):80-4.

168) Obiezu CV, and Diamandis EP. An alternatively spliced variant of KLK4 expressed in prostatic tissue. Clin Biochem. 2000 Oct; 33 (7):599-600.

169) Dong Y, Kaushal A, Bui L, Chu S, Fuller PJ, Nicklin J, Samaratunga H, and Clements JA. Human kallikrein 4 (KLK4) is highly expressed in serous ovarian carcinomas. Clin Cancer Res. 2001 Aug; 7 (8):2363-71.

170) Korkmaz KS, Korkmaz CG, Pretlow TG, and Saatcioglu F. Distinctly different gene structure of KLK4/KLK-L1/prostase/ARM1 compared with other members of the kallikrein family: intracellular localization, alternative cDNA forms, and Regulation by multiple hormones. DNA Cell Biol. 2001 Jul; 20 (7):435-45.

171) Myers SA, and Clements JA. Kallikrein 4 (KLK4), a new member of the human kallikrein gene family is up-regulated by estrogen and progesterone in the human endometrial cancer cell line. J Clin Endocrinol Metab. 2001 May; 86 (5):2323-6.

172) Day CH, Fanger GR, Retter MW, Hylander BL, Penetrante RB, Houghton RL, Zhang X, McNeill PD, Filho AM, Nolasco M, Badaro R, Cheever MA, Reed SG, Dillon DC, and Watanabe Y. Characterization of KLK4 expression and detection of KLK4-specific antibody in prostate cancer patient sera.Oncogene. 2002 Oct 10; 21 (46):7114-20.

173) Obiezu CV, Soosaipillai A, Jung K, Stephan C, Scorilas A, Howarth DH, and Diamandis EP. Detection of human kallikrein 4 in healthy and cancerous prostatic tissues by immunofluorometry and immunohistochemistry. Clin Chem. 2002 Aug; 48 (8):1232-40.

174) Xi Z, Klokk TI, Korkmaz K, Kurys P, Elbi C, Risberg B, Danielsen H, Loda M, and Saatcioglu F. Kallikrein 4 is a predominantly nuclear protein and is overexpressed in prostate cancer. Cancer Res. 2004 Apr; 64 (7):2365-70.

175) Dong Y, Bui LT, Odorico DM, Tan OL, Myers SA, Samaratunga H, Gardiner RA, and Clements JA. Compartmentalized expression of kallikrein 4 (KLK4/hK4) isoforms in prostate cancer: nuclear, cytoplasmic and secreted forms. Endocr Relat Cancer.2005 Dec; 12 (4):875-89.

176) Simmer JP, and Bartlett JD. Kallikrein 4 is a secreted protein. Cancer Res. 2004 Nov 15;64 (22):8481-2.

177) Harvey TJ, Dong Y, Bui L, Jarrott R, Walsh T, and Clements JA. Production and characterization of antipeptidekallikrein 4 antibodies. Use of computer modeling to design peptides specific to Kallikrein 4. Methods Mol Med. 2003;81: 241-54.

178) Debela M, Magdolen V, Grimminger V, Sommerhoff C, Messerschmidt A, Huber R, Friedrich R, Bode W, and Goettig P. Crystal structures of human tissue kallikrein 4: activity modulation by a specific zinc binding site. J Mol Biol. 2006 Oct 6; 362 (5):1094-107.

179) Beaufort N, Debela M, Creutzburg S, Kellermann J, Bode W, Schmitt M, Pidard D, and Magdolen V. Interplay of human tissue kallikrein 4 (hK4) with the plasminogen activation system: hK4 regulates the structure and functions of the urokinase-type plasminogen activator receptor (uPAR). Biol Chem. 2006 Feb; 387 (2):217-22.

180) Lai J, Myers SA, Lawrence MG, Odorico DM, and Clements JA. Direct progesterone receptor and indirect androgen receptor interactions with the kallikrein-related peptidase 4 gene promoter in breast and prostate cancer. Mol Cancer Res. 2009 Jan; 7 (1):129-41.

181) Angelopoulou K, and Karagiannis GS. Structural characterization and expression of five novel canine kallikrein-related peptidases in mammary cancer. Mamm Genome. 2010 Oct; 21 (9-10):516-24.

182) Papachristopoulou G, Talieri M, and Scorilas A. Significant alterations in the expression pattern of kallikrein-related peptidase genes KLK4, KLK5 and KLK14 after treatment of breast cancer cells with the chemotherapeutic agents epirubicin, docetaxel and methotrexate. Tumour Biol. 2013 Feb; 34 (1):369-78.

183) Neve RM, Chin K, Fridlyand J, Yeh J, Baehner FL, Fevr T, Clark L, Bayani N, Coppe JP, Tong F, Speed T, Spellman PT, DeVries S, Lapuk A, Wang NJ, Kuo WL, Stilwell JL, Pinkel D, Albertson DG, Waldman FM, McCormick F, Dickson RB, Johnson MD, Lippman M, Ethier S, Gazdar A, and

Gray JW. A collection of breast cancer cell lines for the study of functionally distinct cancer subtypes. Cancer Cell. 2006 Dec; 10 (6):515-27.

184) Prat A, Parker JS, Karginova O, Fan C, Livasy C, Herschkowitz JI, He X, and Perou CM. Phenotypic and molecular characterization of the claudin-low intrinsic subtype of breast cancer. Breast Cancer Res. 2010; 12 (5):R68.

185) Seiz L, Kotzsch M, Grebenchtchikov NI, Geurts-Moespot AJ, Fuessel S, Goettig P, Gkazepis A, Wirth MP, Schmitt M, Lossnitzer A, Sweep FC, and Magdolen V. Polyclonal antibodies against kallikrein-related peptidase 4 (KLK4): immunohistochemical assessment of KLK4 expression in healthy tissues and prostate cancer. Biol Chem. 2010 Apr; 391 (4):391-401.

186) McKiernan E, O'Brien K, Grebenchtchikov N, Geurts-Moespot A, Sieuwerts AM, Martens JW, Magdolen V, Evoy D, McDermott E, Crown J, Sweep FC, and Duffy MJ. Protein kinase Cdelta expression in breast cancer as measured by real-time PCR, western blotting and ELISA. Br J Cancer. 2008 Nov 18; 99 (10):1644-50.

187) Leung SW, and Bedard YC. Immunocytochemical staining on ThinPrep processed smears. Mod Pathol. 1996;9: 301-6.

188) Kaplan MA, Segura AM, and Wang HH. Evaluation of CytoLyt and PreservCyt as preservatives for immunocytochemistry for cytokeratin in fine needle aspiration. Applied Immunohistochem. 1998; 6: 23-9.

189) Livak KJ, and Schmittgen TD. Analysis of relative gene expression data using real-time quantitative PCR and the 2 (-Delta Delta C (T)) Method. Methods. 2001 Dec; 25 (4):402-8.

190) Błachnio K. Efficient extraction of transmembrane proteins using ProteoExtract Transmembrane Protein Extraction Kit. Postepy Biochem. 2010; 56 (4):463-6. Polish.

191) Skacel M, Skilton B, Pettay JD, and Tubbs RR. Tissue microarrays: a powerful tool for high-throughput analysis of clinical specimens: a review of the method with validation data. Appl Immunohistochem Mol Morphol.2002 Mar; 10 (1):1-6.

192) Simon R, Mirlacher M, and Sauter G. Tissue microarrays in cancer diagnosis. Expert Rev Mol Diagn.2003 Jul; 3(4):421-30.

193) Conway C, Dobson L, O'Grady A, Kay E, Costello S, and O'Shea D. Virtual microscopy as an enabler of automated /quantitative assessment of protein expression in TMAs. Histochem Cell Biol. 2008 Sep; 130 (3):447-63.

194) Dorn J, Schmitt M, Kates R, Schmalfeldt B, Kiechle M, Scorilas A, Diamandis EP, and Harbeck N. Primary tumor levels of human tissue kallikreins affect surgical success and survival in ovarian cancer patients. Clin Cancer Res. 2007 Mar 15; 13 (6):1742-8.

195) Miller RT, and Estran CE. Heat-Induced Epitope Retrieval with a Pressure Cooker: Suggestions for Optimal Use. Applied Immunohistochemistry 3 (3): 190–193, 1995.

196) Oertel J, and Huhn D. Immunocytochemical methods in haematology and oncology. J Cancer Res Clin Oncol. 2000 Aug; 126(8):425-40.

197) Hayat MA. Microscopy, immunohistochemistry and antigen retrieval methods. Kluwer Academic. 2002

198) Noack F, Schmitt M, Bauer J, Helmecke D, Krüger W, Thorban S, Sandherr M, Kuhn W, Graeff H, and Harbeck N. A new approach to phenotyping disseminated tumor cells: methodological advances and clinical implications. Int J Biol Markers. 2000 Jan-Mar; 15 (1):100-4.

199) Mikolajczyk SD, Millar LS, Marker KM, Rittenhouse HG, Wolfert RL, Marks LS, Charlesworth MC, and Tindall DJ. Identification of a novel complex between human kallikrein 2 and protease inhibitor-6 in prostate cancer tissue. Cancer Res.1999 Aug 15; 59(16):3927-30.

200) Sood AK, Fletcher MS, Gruman LM, Coffin JE, Jabbari S, Khalkhali-Ellis Z, Arbour N, Seftor EA, and Hendrix MJ. The paradoxical expression of maspin in ovarian carcinoma. Clin Cancer Res.2002 Sep; 8 (9):2924-32.

201) Shi SR, Cote RJ, and Taylor CR. Standardization of immunohistochemistry based on antigen retrieval technique for routine formalin-fixed tissue sections. Appl Immunohistochem Mol Morphol. 1998; 6:89-96.

202) Miller RT, Kubier P, and Reynolds B. Blocking of Endogenous Avidin-Binding Activity in Immunohistochemistry: The Use of Skim Milk as an Economical and Effective Substitute for Commercial Biotin. Applied Immunohistochemistry and Molecular Morphology 7 (1): 63–65, 1999.

203) Bacallao R, Sohrab S, and Phillips C. Guiding principles of specimen preservation for confocal fluorescence microscopy. In J.B. Pawley (Ed.) Handbook of Biological Confocal Microscopy, 3rd e. Springer, New York: 2006 368-380.

204) Wilkinson R, Woods K, D'Rozario R, Prue R, Vari F, Hardy MY, Dong Y, Clements JA, Hart DN, and Radford KJ. Human kallikrein 4 signal peptide induces cytotoxic T cell responses in healthy donors and prostate cancer patients. Cancer Immunol Immunother. 2012Feb; 61 (2):169-79.

205) Kreike B, van Kouwenhove M, Horlings H, Weigelt B, Peterse H, Bartelink H, and van de Vijver MJ. Gene expression profiling and histopathological characterization of triple-negative/basal-like breast carcinomas. Breast Cancer Res. 2007; 9 (5):R65.